The Impact of the 1989 Exxon Valdez Oil Spill on Phytoplankton as Seen Through the Dinoflagellate Cyst Record

by

Maximilien Genest
B.Sc., University of Ottawa, 2014

A Thesis Submitted in Partial Fulfillment
of the Requirements for the Degree of

Master of Science

in the School of Earth and Ocean Sciences

Supervisory Committee

The Impact of the 1989 Exxon Valdez Oil Spill on Phytoplankton as Seen Through the Dinoflagellate Cyst Record

by

Maximilien Genest
B.Sc., University of Ottawa, 2014

Supervisory Committee

Dr. Vera Pospelova (School of Earth and Ocean Sciences)
Supervisor

Dr. Thomas Pedersen (School of Earth and Ocean Sciences)
Departmental Member

Dr. Richard Hebda (School of Earth and Ocean Sciences)
Departmental Member

Abstract

Supervisory Committee
Dr. Vera Pospelova (School of Earth and Ocean Sciences)
Supervisor
Dr. Thomas Pedersen (School of Earth and Ocean Sciences)
Departmental Member
Dr. Richard Hebda (School of Erath and Ocean Sciences)
Departmental Member

Our knowledge of how oil spills affect coastal environments is severely limited by the shortage of research that addresses the impact of these events on phytoplankton, the single most important group of organisms in the marine ecosystem. This scarcity of knowledge is mainly attributed to the absence of baseline data, preventing the comparison of pre- and post-spill populations. This unique study aims to identify how dinoflagellates and diatoms, the two major groups of phytoplankton in coastal marine environments, have been affected by the 1989 Exxon Valdez oil spill in Prince William Sound (PWS), Alaska. To do this, sedimentary records of dinoflagellate cysts, produced during a dinoflagellate's life cycle and preserved in the sediment, and biogenic silica, a proxy for diatom abundance, were analyzed prior to, during and after the oil spill. The analysis of two well-dated cores in PWS reveals marked increases during the oil spill in the concentrations of total cysts of the species *Operculodinium centrocarpum* sensu Wall and Dale, (1966) and *Dubridinium* spp. Total cyst concentrations doubled in core P-10 from 362 to 749 per g, while in core P-12 the increase was from 1175 to 1771 cysts g^{-1}. During this peak in cyst concentrations, total concentrations were 3 and 2 standard deviations greater than the mean in cores P-10 and P-12, respectively. *Dubridinium* spp. showed a five and sevenfold increase in concentrations in cores P-10 (4 to 20 cysts g^{-1}) and P-12 (16 to 110 cysts g^{-1}), respectively, while *O. centrocarpum* sensu Wall and Dale, (1966) doubled in concentrations in the two cores (P-10: 117 to 276 cysts g-1; P-12: 268 to 495 cysts g^{-1}). Biogenic silica values did

not show significant changes throughout the cores, with values varying between 8% and 9% in core P-10 and 9.0% to 10.9% in core P-12. These changes lie within or very close to the standard deviation of the analyzed standards, suggesting that much of the changes could be analytical noise. The dinoflagellate cyst signals seen in this study are comparable to those seen as a result of nutrient enrichment in estuarine systems, suggesting that the 1989 Exxon Valdez oil spill and its remediation had a stimulatory effect on some taxa of cyst-producing dinoflagellates. This impact appears to be short-lived, with cyst concentrations returning to pre-spill levels within two years of the event. The lack of change in diatom abundance, on the other hand, suggest that diatom abundance remained relatively constant during the entirety of the sample period.

Table of Contents

List of Tables

List of Figures

List of Plates

Acknowledgments

I would like to start off by thanking my supervisor Dr. Vera Pospelova for mentoring me and providing me with a tremendous amount of support, encouragement and guidance. A special thanks to my committee members, Drs. Thomas Pedersen, Richard Hebda, Audrey Dallimore and John Volpe, who provided me in invaluable comments throughout my M.Sc. I would also like to thank our collaborators Drs. Joshua Williams, Steven Kuehl and Tim Dellapenna who provided us with the two well-dated cores from Prince William Sound and to Dr. Kenneth Mertens for his contributions on cyst taxonomy. Finally, I would like to thank my family, especially my parents, who have supported and encouraged me throughout my schooling.

Funding for this project was provided by the Natural Sciences and Engineering Council of Canada (NSERC) through grants to Dr. Vera Pospelova and a CGS-M scholarship to Maximilien Genest. This work was also supported by the American Association of Stratigraphic Palynologists (Student Research Grant), the UVic Graduate Fellowships and President's Research Scholarship, as well as by the Dr. Arne H. Lane Graduate and the Charles S. Humphrey Graduate Student Awards.

Author Contributions

This thesis is a manuscript that will be submitted to the journal of the Science of the Total Environment and is coauthored by M. Genest, V. Pospelova, J.R. Williams, T. Dellapenna, K.N. Mertens, and S.A. Kuehl.

Maximilien Genest – samples acquisition, contributed to the design of the projects, processed 35 samples, microscopy analyses of 35 samples in cores P-10 and P-12, provided funding for BioSi, interpretations of the data and figure construction.

Dr. Vera Pospelova – initiation and design of the project, provided funding for laboratory processing of sediment samples, contributed to sample preparation, counted 20 samples in core P-12, input into the interpretation of the data, figure construction, as well as made edits, comments, suggestions and corrections on the manuscript for publication.

Dr. Kenneth N. Mertens – contributed to taxonomic cyst identification and provided detailed comments, suggestions and corrections on the manuscript.

Dr. Steven A. Kuehl, **Dr. Timothy Dellapenna** and **Dr. Joshua R. Williams** – Provided the cores from Prince William Sound, performed all the dating for the cores and provided detailed comments, suggestions and corrections of the manuscript.

1. Introduction

1.1 General Comments

A large amount of oil that is used globally is extracted from and transported via the oceans, putting marine environments at risk of oil spills (UNCTAD, 2015). It is therefore important for us to understand how such spills affect the sea if we are to better understand both risk and response. Our knowledge of how oil spills affect ecosystems is limited by the lack of scientific research that addresses the impacts of oil on phytoplankton (e.g., Ozhan et al., 2014a). These organisms are the pillars of the marine food chain as they are responsible for marine primary production (Longhurst et al., 1995). The health of the entire marine ecosystem is therefore dependent on the health (diversity and abundance) of these organisms.

This lack of knowledge is due to the absence of baseline data, which prevents the comparison of pre- and post-spill populations (Ozhan et al., 2014a). The very limited research that has been conducted has focused almost entirely on the 2010 Deepwater Horizon oil spill (DHOS) in the Gulf of Mexico (GOM) (e.g., Ozhan et al., 2014a). The conclusions drawn from such rare studies have been contradictory. Some suggest that oil spills promote the growth of phytoplankton biomass (e.g., Hu et al., 2011), whereas others suggest that these spills inhibit phytoplankton growth (e.g., Paul et al., 2013). The wide range of results suggests that we continue to have a very limited understanding of the effects of oil on phytoplankton and that further research is required. Many questions remain unanswered including: What species/groups are stimulated or hindered by spills? How long do communities take to recover? How did the alterations to the phytoplankton communities affect the carbon flux to the benthic environment? It is only once these questions are

answered that environmental stewards will properly understand the impact of such oil spills on marine ecosystems.

Dinoflagellates are the second most abundant phytoplankton group in coastal marine systems and it is therefore important to understand how they are affected by oil in the water column (e.g., Harrison et al., 1983; Radi et al., 2007). There have been very limited studies on the effects that oil spills have on dinoflagellates, with existing research mainly focusing on a few species and none of them looking at how entire populations have been affected by these events (e.g., Tas et al., 2010; Hallare et al., 2011; Ozhan et al., 2014b; Ozhan et al., 2015; Severin et al., 2016). Research suggests that dinoflagellates are inhibited by oil spills, with relative abundances decreasing when exposed to crude oil (e.g., Hallare et al., 2011). Some studies have shown that dinoflagellates are more resilient than other phytoplankton groups, such as diatoms (e.g., Tas et al., 2010; Ozhan et al., 2014b), while other studies indicate that this is not the case (e.g., Hallare et al., 2011).

Approximately half of modern dinoflagellates are heterotrophic, while the other half are autotrophic or mixotrophic (e.g., Jacobson and Anderson, 1996). As part of their life cycle, some dinoflagellates produce very resistant, organic-walled cysts that are typically well preserved in the sedimentary record. Although only about 10% of the total described dinoflagellate species produce these cysts (Dale, 1976; Head, 1996), the cyst record in any coastal site may account for 30 to 40% of species included in local plankton (Dale, 1976). It is widely accepted that the distribution of modern dinoflagellate cysts in marine environments is controlled by salinity, water temperature and nutrient availability (e.g., Dale, 1996; de Vernal et al., 1997; de Vernal et al., 2001; Pospelova et al., 2004; Pospelova et al., 2005; Radi et al., 2007). For this reason, dinoflagellate cysts have been

used to reconstruct sea-surface temperature, salinity and primary productivity (e.g., Dale, 1996; Matsuoka et al., 1999; de Vernal et al., 2001, 2005; Dale et al., 2002; Pospelova et al., 2006, 2015; Bringué et al., 2014; Radi and de Vernal, 2008). They have also been shown to be important tools in studying the effects of industrial pollution and anthropogenic nutrient enrichment, such as sewage outfalls and fertilizer runoff, in coastal regions (e.g., Matsuoka, 1999; Pospelova et al., 2002; Pospelova et al., 2005; Dale, 2009; Krepakevich and Pospelova, 2010; Ellegaard et al., 2017).

The impacts of oil spills on diatoms, the most important group of phytoplankton in coastal marine waters, also require further study (e.g., Harrison et al., 1983; Radi et al., 2007). Much of the research studying the impacts of oil spills on diatoms suggests that diatoms may become more abundant and diverse following exposure to oil (e.g., Hallare et al., 2011; Tas et al., 2010). However, there has been no research of this topic in Arctic/ Sub-Arctic environments, which are known to be much more sensitive to change and should therefore be studied (e.g., Serreze et al., 2000). One method of studying relative diatom abundance is through measuring biogenic silica concentrations. Biogenic silica has been shown to be a strong proxy for diatom abundance in estuarine systems where diatoms are the major type of siliceous phytoplankton. It is a well-accepted proxy that has been used in both sediment trap studies (e.g., Pospelova et al., 2010; Price et al., 2011; Bringué et al., 2013) and surface sediment studies (e.g., Krepakevich and Pospelova, 2010; Heikkilä et al., 2014). In addition, biogenic silica is partially preserved in the sedimentary record and can therefore be used, with caveats, to determine relative diatom abundances throughout the sedimentary record (e.g., Pospelova et al., 2006; Price et al., 2013; Bringué et al., 2014; Pospelova et al., 2015).

1.2 Exxon Valdez Oil Spill

On March 24th, 1989, the Exxon Valdez, an oil tanker bound for Long Beach, California, struck Bligh Reef in Prince William Sound (PWS) spilling nearly 41.6 million liters of Prudhoe Bay crude oil into the ocean waters (Wiens, 2013). Over the next 60 days, the oil spread more than 750 km to the southwest along the Kenai Peninsula, Kodiak archipelago, and the Alaska Peninsula (Wiens, 2013). In total, at least 1900 km of pristine coastline were contaminated to some degree by oil (Shigenaka, 2014).

The effect of this event on marine vertebrates was quite severe. During the timeline of the oil spill, it was estimated that 250,000 seabirds (Piatt and Ford, 1996), 1000 to 2800 sea otters (Garrott and Labs, 1993) and billions of salmon and herring eggs were lost (Shigenaka, 2014). Many of these organisms, including numerous species of seabirds (e.g., Irons et al., 2000) and sea-otters (e.g., Peterson et al., 2003), took several years to recover.

Remediation of the spill was complicated by a variety of different factors including a poor response, remote location, rugged shoreline and severe weather (Wiens, 2013). The remediation of this spill took four years and at its peak included an estimated 10,000 workers, 1,000 vessels and 100 aircraft (Shigenaka, 2014). The most important bioremediation tool that was utilized during this spill was the application of nitrogen and phosphorus, which was done in order to promote microbial degradation of the oil (Pritchard and Costa, 1991; Wiens, 2013). In order to do this, the shorelines of Prince William Sound were treated with an oleophilic liquid fertilizer named Inipol EAP 22 (7.4% N, 7% P) and a slow-release granulated fertilizer named Customblen (28% N, 3.5% P) (Bragg et al., 1994). The amount of fertilizer applied decreased over time, with total nitrogen additions being 23.33, 22.06 and 3.18 tonnes in 1989, 1990 and 1991, respectively (Prince and Bragg,

2008). In total, it is estimated that 50,000 kg of nitrogen and 5,000 kg of phosphorus was applied to the beaches of PWS (Bragg et al., 1994; Prince and Bragg, 2008). Corexit 9527, a type of dispersant composed of 2-butoxyethanol, organic sulfonic acid salt and propylene glycol (NALCO 2008), was also applied to the impacted waters (Shigenaka, 2014). However, its application was quickly halted (within a few weeks), as it showed no significant benefit (Shigenaka, 2014). Despite the unprecedented scale, duration and cost of the cleanup, it was estimated by the National Oceanic and Atmospheric Administration (NOAA) that a little more than 10% of the oil was removed by this cleanup, with the rest being removed by natural weathering and degradation (Shigenaka, 2014).

1.3. Objectives

This study aims to identify how the two major groups of phytoplankton (diatoms and dinoflagellates) in coastal marine environments were impacted by and responded to the 1989 Exxon Valdez oil spill. Pre-1989, during 1989, and post-1989 dinoflagellate populations are assessed using dinoflagellate cysts and diatom abundances, studied through the proxy value of biogenic silica concentrations in the sediments from PWS.

This research provides insight into changes in dinoflagellate species composition and total diatom abundance that resulted from the oil spill. It also establishes a timeframe for the recovery of these two groups of phytoplankton in response to the oil spill.

2. Environmental Setting

2.1 Gulf of Alaska

The Gulf of Alaska (GOA) is a semi-enclosed basin in the North Pacific Ocean (Figure 1). The mountainous coastline of Alaska surrounds the GOA to the west, north, and east, with the open ocean to the south. There are two current systems that dominate the circulation in the GOA: the Subarctic Gyre within the basin and the Alaska Coastal Current (ACC) along its shelf (Figure 1) (e.g., Stabeno et al., 2004). The gyre is formed by the West Wind Drift to the south, which bifurcates when it reaches the west coast of North America into the south-flowing California Current and the north-flowing Alaska Current (e.g., Stabeno et al., 2004). As the Alaska Current reaches the head of the GOA it turns southwestward to become the Alaskan Stream current (Stabeno et al., 2004). The ACC dominates the circulation of the GOA shelf and controls the transport of both dissolved and planktonic materials (e.g., Royer, 1981; Stabeno et al., 1995). This current is driven by winds and freshwater, which can therefore be affected by changes in global circulation patterns (e.g., Stabeno et al., 2004).

The GOA is located at the eastern end of the Pacific storm track, where storms tend to persist as they weaken because of the contact with the mountainous coast of Alaska (Wilson and Overland, 1986). There is a pronounced seasonal weather cycle, with cyclonic winds from fall to spring causing downwelling of surface waters along the coast and upwelling of deep nutrient-rich waters in the central GOA. As discussed below, during the rest of the year, there are periods of high atmospheric pressure which foster intermittent upwelling along the coast (e.g., Stabeno et al., 2004). Overall, the waters of the coastal GOA support a highly productive ecosystem, with large populations of large mammals and

seabirds (Mundy, 2005). This highly productive system suggests that there must be other mechanisms, such as eddies and advection currents in canyons, which replenish nutrients to the shelf (e.g., Stabeno et al., 2004).

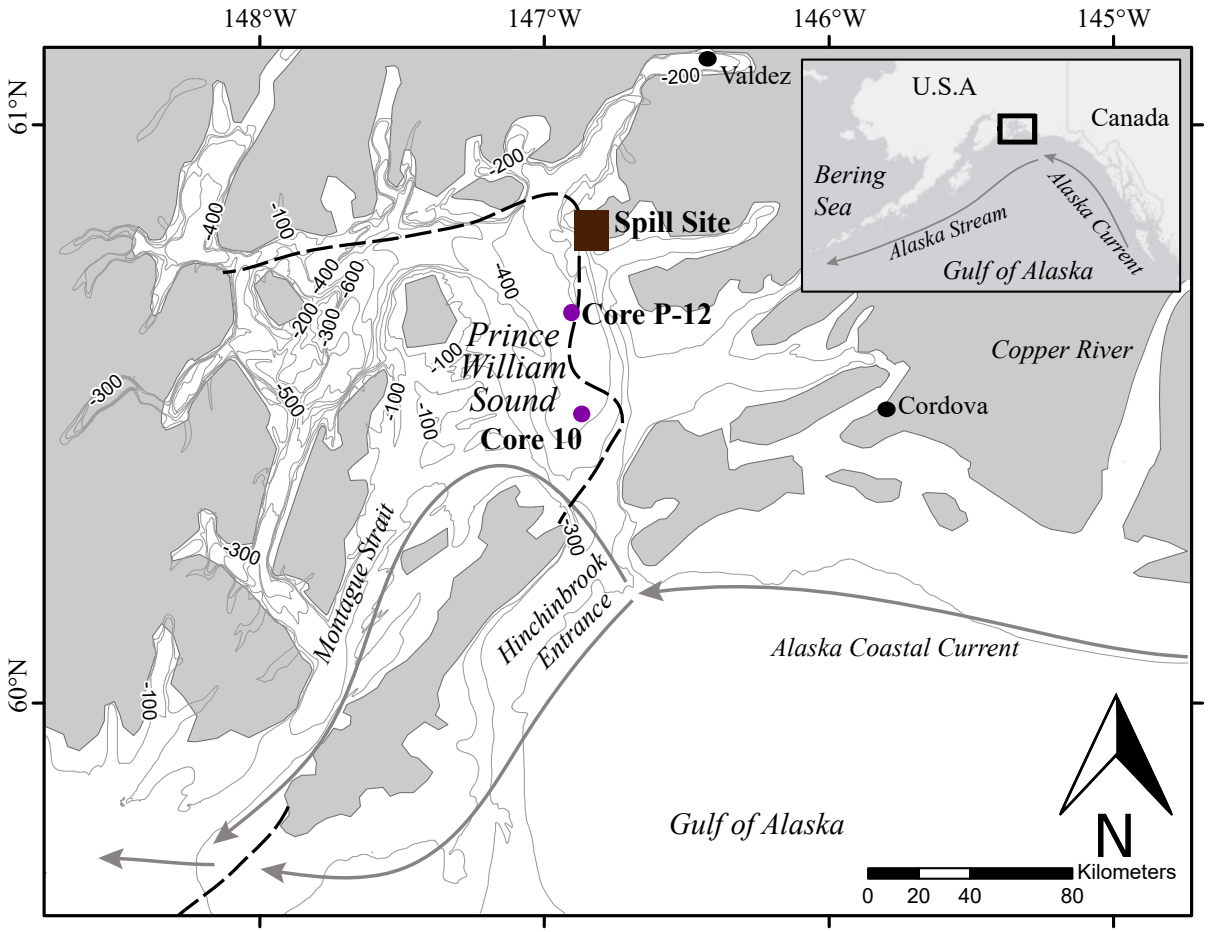

Figure 1: Map showing the general oceanographic circulation and bathymetry of Prince William Sound (Alaska, U.S.A). The location of the sediment cores and the location of the oil spill (brown rectangle) are shown. Also shown is the eastern boundary of the area affected by oil (dashed line); everything to the west of that boundary was coated with oil.

There are periodic changes in oceanic and atmospheric circulation that are important in the long-term variability of the GOA climate. The leading contribution to the regional atmospheric variability is the Pacific-North American teleconnection pattern (PNA) (e.g., Wallace and Gutzler, 1981; Barnston and Livezey, 1987). This mode relates

to the strength and the position of the Aleutian Low and therefore impacts wind, precipitation and temperature patterns in the Gulf (e.g., Stabeno et al., 2004). It has been suggested that the El Niño Southern Oscillation (ENSO) and the Pacific Decadal Oscillation (PDO) (e.g., Hare and Mantua, 2000) events also have an effect on the GOA. ENSO events originate in the eastern equatorial Pacific and have a periodicity from 2 to 5 years. The warm phase, El Niño, is typically associated with positive anomalies in winter air temperature, precipitation, sea level and along-shore wind, with the latter leading to downwelling favorable conditions. The opposite occurs during La Niña, the cold phase of ENSO (e.g., Mantua et al., 1997). However, it has been shown that the effect of ENSO decreases poleward of 31ºN, while the PDO becomes dominant northward of this region (Lluch-Cota et al., 2001). The PDO signal has a decadal-scale periodicity and it has two phases, the warm and the cold, that are believed to influence wind, temperature, precipitation and oceanographic patterns in the northeastern Pacific Ocean (e.g., Stabeno et al., 2004; Mundy, 2005; Harwell et al., 2010). A positive PDO is characterized by warming, intense low-pressure, strong onshore winds and increased precipitation. This, in turn, may cause enhanced coastal downwelling and offshore upwelling in the GOA (e.g., Stabeno et al., 2004; Mundy, 2005; Harwell et al., 2010). The negative PDO phase is characterized by below normal temperatures, winter high-pressure, moderate onshore winds and moderate precipitation (e.g., Stabeno et al., 2004; Mundy, 2005; Harwell et al., 2010). As a result, the GOA can experience reduced coastal downwelling and offshore upwelling during such phases (e.g., Stabeno et al., 2004; Mundy, 2005; Harwell et al., 2010). Although the large-scale linkage between the atmosphere and the ocean is reasonably well understood, how this linkage relates to the coastal and estuarine systems

along the GOA is not (Stabeno et al., 2004). The mountainous coastline of Alaska inhibits the eastward progression of storms and can intensify winds (Stabeno et al., 2004) This can greatly impact along-shore winds, forces cross-shelf Ekman transport and precipitation, leading to changes in the baroclinicity of the upper ocean (Stabeno et al., 2004).

2.2. Prince William Sound

Prince William Sound (PWS) is a 9,000 km^2 semi-enclosed glacial fjord-type estuary located within the GOA, along the south-central coastline of Alaska (Figure 1). The central Sound is roughly 60 km by 90 km with an irregular bathymetry, an average depth >200 m and a maximum depth of ~700 m (Harwell et al., 2010). PWS is characterized by a large number of glacial fjords and tidewater glaciers along its mountainous coastline, which are the main sources of freshwater into the Sound (e.g., Harwell et al., 2010). The freshwater input shows strong seasonality, reaching a maximum during the summer/early fall. In addition, the freshwater input varies spatially with a higher amount of freshwater entering the northern and western parts of PWS (Royer et al., 1990; Okkonen and Bélanger, 2008). Salinity within the Sound is dependent on the influx of freshwater, and as such follows similar trends to the seasonal cycle of freshwater input. In the central part of the Sound, the average salinity ranges from ~32 psu in the winter to ~26 psu in the summer (Musgrave et al., 2013). Similarly, sea surface temperature shows the same seasonal pattern with ranges from ~3°C in the winter to ~13°C in the summer in this sea-ice free estuary (Musgrave et al., 2013).

Circulation within the Sound is complex due to the irregular bathymetry, convoluted coastline, numerous islands, the tidal regime and the spatially and temporally

varying winds and freshwater runoff (e.g., Harwell et al., 2010). In general, PWS has an anticlockwise estuarine flow driven by subtidal currents that are advected into PWS through the Hinchinbrook entrance (Figure 1) before exiting through the Montague Strait and other southwest passages (Niebauer et al., 1994). Occasionally during the summer, the circulation reverses and water enters via the Montague Strait and exits through the Hinchinbrook entrance (Vaughan et al., 2001).

The ACC plays an important role in the exchange between PWS and the GOA shelf waters (Harwell et al., 2010). When the ACC reaches the Hinchinbrook entrance it bifurcates with one arm being directed through the entrance and the other going along the southern part Montague Island (Figure 1) (Harwell et al., 2010). The arm going into the Hinchinbrook entrance is rapidly deflected around the northern part of Montague Island and through the Montague Strait before then rejoining the other arm of the ACC (Figure 1). Furthermore, PWS can communicate directly with deep continental slope waters via the Hinchinbrook Canyon, predominantly in summer (Niebauer et al., 1994; Harwell et al., 2010). These deep waters are relatively rich in nutrients and can therefore be an important source of nutrients to the downwelling favorable waters of PWS (Niebauer et al., 1994; Harwell et al., 2010).

There has been very little research on the sources of sediments in PWS, with a majority of the work relying on ocean-circulation models. One model by Wang et al. (2014) suggests that a third of the suspended sediment delivered by the Copper River enter the Sound, with the remainder being transported southwestward by the ACC. In addition, 60% of the sediment entering the Sound exits via the Montague Strait (Figure 1) (Wang et al., 2014). As such, it is likely that only a small amount of the deposits on the floor of the PWS

originates from the Copper River with the remainder coming from local sources, primarily the Columbia Glacier and local primary production. Finn et al., (2015) noted distinct areas of ponded sediment, which were attributed to inputs from glaciers, indicating that these can be important sources of sediments into PWS.

2.3. Regional Phytoplankton Flora

There is little literature on the diatom and dinoflagellate flora within Prince William Sound. Research from the coastal eastern Gulf of Alaska shows that diatom populations within this region are dominated by species from the genera *Chaetoceros* and *Thalassiosira*, accounting for ~80% of diatoms by cell number (Strom et al., 2016). Although very little information exists on living dinoflagellate populations in GOA, there are a few dinoflagellate cyst studies from the GOA (de Vernal and Pedersen, 1997; Marret et al., 2001; Radi and de Vernal, 2004). The cyst assemblages in the GOA mainly include *Brigantedinium* spp., *Spiniferites ramosus*, *S. elongatus*, *Spiniferites* spp., cysts of *Pentapharsodinium dalei* and *Operculodinium centrocarpum* sensu Wall and Dale, (1966) (see Radi and de Vernal, 2004).

3. Materials and Methods

3.1. Sediment Core Collection, Sampling, and Chronology

Two sediment cores, P-10 and P-12, were collected from the central part of Prince William Sound on board the *M/V Auklet* in June 2012 (Figure 1). These two cores were taken from sites that fell near or within the trajectory of the spilled oil. However, it should be noted that the site of core P-12 is fon the edge of the oil spill and it is possible that this site was not within the plume itself. Both sediment cores were retrieved using a custom-designed gravity corer that utilizes an acrylic barrel (2.0 m length; 8.5 cm inner diameter) with a core catcher. Core P-10 (60° 30' 11N; 146° 58' 3W), a 1.6 m core, was collected from southwestern PWS at a water depth of 419 m. Core P-12 (60° 40' 41N; 146° 54' 11W), a 1.5 m core, was collected in northern PWS at a water depth of 437 m. In general, sediments in both cores are fine-grained, have little structure and showed little lithological change, with the exception of earthquake-generated sediment gravity flow layers. These layers are detected at an original (not corrected) depth between 34 to 38 cm and 65 to 70 cm in core P-12 and between 25 to 27 cm and 45 to 49 cm in core P-10. Although these layers cannot be visually identified in core P-10 (they can in core P-12), they can be recognized geochemically in both cores. XRF and ICPMS analysis revealed long-term variations in Sr/Pb, Cu/Pb, K/Ca and Rb/Sr ratios, which could not be attributed to the seasonal variability (Kuehl et al., 2017). The location of these excursions in the sedimentary record coincides with the timing of known large earthquakes in the region, suggesting that these anomalies were produced by gravity flow deposits triggered by earthquakes (Kuehl et al., 2017). It is therefore concluded that the uppermost set of gravity flow deposits in each core (core P-10 – 25 to 27 cm; core P-12 – 34 to 38 cm) were caused

by a 1983 earthquake (see Kuehl et al., 2017). Only specific sections of each core were used for this study and were chosen to represent the dinoflagellate cyst assemblages before, during and after the oil spill. Sediment was subsampled continuously downcore at every centimeter from 15 to 40 cm for core P-12 and from 11 to 24 cm for core P-10. Approximately from 20 to 30 cc of sediment was subsampled continuously every cm into plastic bags and homogenized. The top portions of each core were not analyzed as our aim was to study 10 years of post-spill measurements. This seemed appropriate as previous research suggested that phytoplankton recovered within a few years of being exposed to oil in the Gulf of Mexico (e.g., Hu et al., 2011; Ozhan et al., 2014a).

The cores were well-dated using ^{210}Pb and ^{137}Cs (see Kuehl et al., 2017), and by gravity flow deposits that are known to correspond to 1964 and 1983 earthquakes (Kuehl et al., 2017). Sediment accumulation rates were determined by using profiles of excess ^{210}Pb determined by either gamma (large samples) or alpha (small samples) spectrophotometry (Kuehl et al., 2017). The excess ^{210}Pb profile in each core showed log-linear decreases with depth, with corresponding sediment accumulations rates of 1.1 and 1.3 cm year^{-1} in cores 10 and 12 respectively (Kuehl et al., 2017). In addition, the sedimentation rate for each core was also determined using the peak fallout ^{137}Cs activities (1964). These sedimentation rates showed good agreement with those determined using the ^{210}Pb profiles, supporting the use of these sedimentation rates in this study (Kuehl et al., 2017).

The sedimentation rates for this study were adjusted in two ways. First, the ^{210}Pb profile was recalculated by removing the gravity flow deposits and using the corrected depth (Figure 2). The sedimentation rate was then re-calculated using the 1983 gravity flow

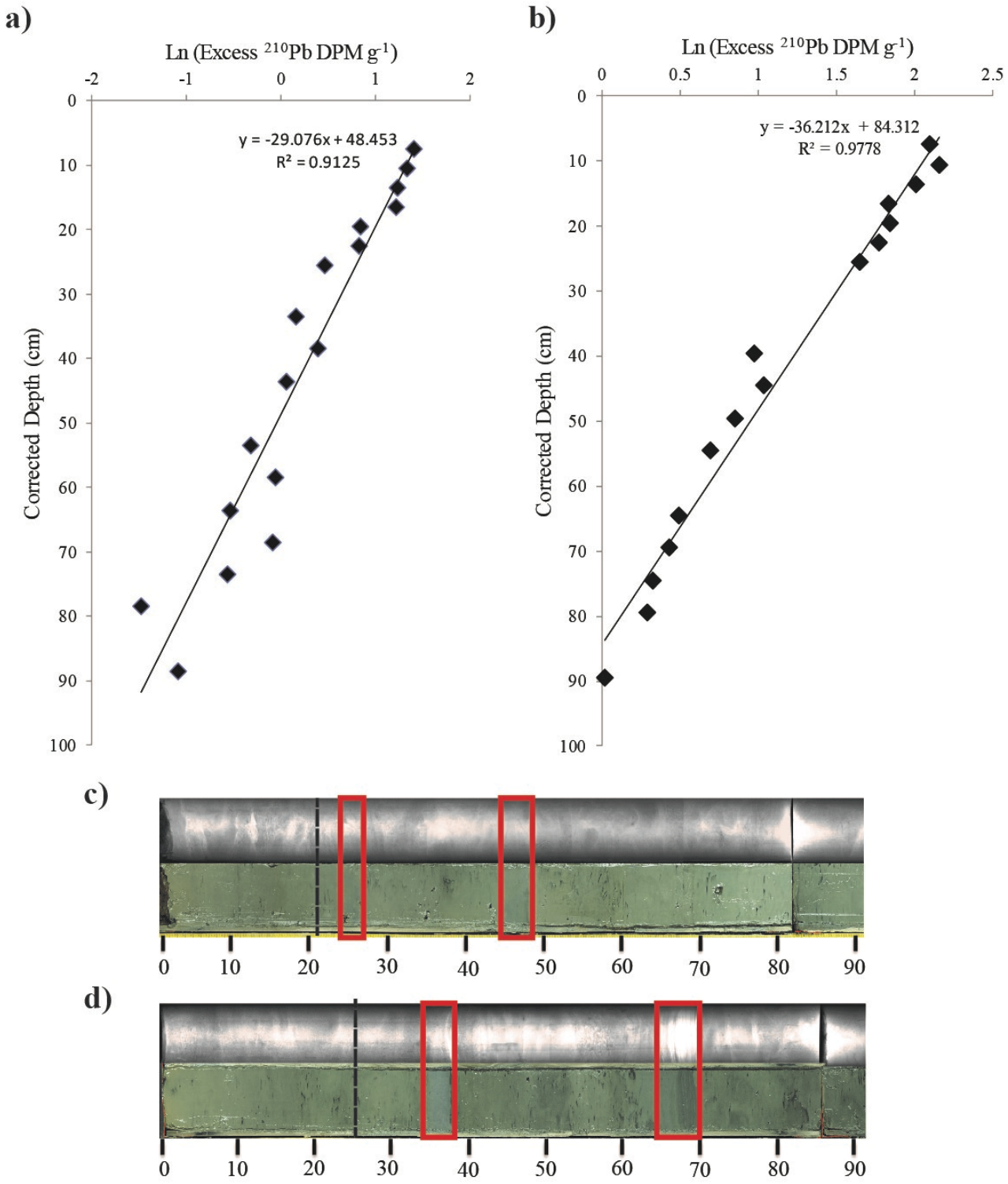

Figure 2: Upper panels: ^{210}Pb profiles used in determining the sedimentation rates for cores P-10 (**a**) and P-12 (**b**) (based on data from Kuehl et al., 2017). Lower panels: Photographs and split core X-radiographs for cores P-10 (**c**) and P-12 (**d**) with the depths corresponding to the timing of the 1964 and 1983 gravity flow deposits highlighted in red. Dashed line represents the approximate location for the oil spill.

deposit as an additional dating horizon, thus yielding sedimentation rates of 0.9 cm $year^{-1}$ and 1.2 cm $year^{-1}$ for the studied sections of cores P-10 and P-12, respectively (Figure 2). The selected sections of both cores provide continuous undisturbed sedimentary records from 1986 to 2000 and from 1982 to 2000 for cores P-10 and P-12, respectively. These values are consistent with those found in another study in PWS, which shows that sedimentation rates varying from ~ 0.8 to 1.6 cm $year^{-1}$ (Jaeger et al., 1998). The sedimentation rates are found to be largest in the central part of the Sound and decrease towards the perimeters (Jaeger et al., 1998). These values are similar to other values in the region. For example, sedimentation rates in the Copper River Delta are roughly 2.0 cm $year^{-1}$ (Jaeger et al., 1998), while between Prince William Sound and the Copper River they vary between 1.0 to 1.8 cm $year^{-1}$ (Jaeger et al., 1998). Eastward of the Copper River, sedimentation rates tend to be lower, between 0.4 and 1.0 cm $year^{-1}$ (Jaeger et al., 1998). Most of the ^{210}Pb profiles that have been measured in PWS exhibit steady-state sediment accumulation, however, nonsteady-state profiles have also been measured in some areas (Jaeger et al., 1998). These nonsteady-state profiles result in part from the episodic deposition near glacier-fed rivers and on the Copper River Delta (Jaeger et al., 1998).

3.2. Biogenic Silica Analysis

Biogenic silica analysis was performed on 11 samples from core P-10 (UVic 2016-78 to 2016-68) and 21 samples from core P-12 (UVic 2016-284 to 2016-259). Each subsample was rinsed three times with distilled water to remove salts, freeze-dried at -80°C, homogenized, powdered, and analyzed at the Pacific Centre for Isotopic and Geochemical Research (PCIGR), University of British Columbia (Vancouver, Canada).

The analysis was done using the alkaline dissolution spectrophotometric method of Mortlock and Froelich (1989). Percent opal was calculated using the following formula: %Opal = 2.4 x $\%Si_{opal}$, an equation that accounts for the average water content of diatomaceous silica (Mortlock and Froelich, 1989). During sample preparation, one sample (UVic 2016-273; ~1987-1988) was lost, and therefore no biogenic silica measurement was obtained for this sample. In addition, a biogenic silica analysis was not performed on samples from the 1983 gravity flow deposit (UVic 2016-282 to 2016-279). Finally, standards from Saanich Inlet and Jervis Inlet in British Columbia were also measured alongside the biogenic silica samples in order to ensure the accuracy of the measurements.

3.3. Dinoflagellate Cyst Preparation and Microscopy

Dinoflagellate cysts were extracted according to the standardized palynological method (e.g., Pospelova et al., 2005, 2010). Samples were rinsed with distilled water to remove salt, oven dried at ~40°C and weighed with an analytical balance (Precisa Type 290-9245/S 303 A). Samples were then treated with 10% room temperature HCl to remove any carbonates. To calculate cyst concentrations based on the dry weight of the sediments, one calibrated tablet of *Lycopodium clavatum* (Stockmarr, 1971; Mertens et al., 2009, 2012) containing 18,584 spores (batch # 177745) was added to each sample, with the exception of one sample (UVic 16-262) where one tablet had only 9,666 spores (batch # 3862). Samples were then sieved through a 120 μm mesh and retained on a 15 μm mesh to eliminate any coarse and fine-grained material. Sediment was treated with 48% room temperature HF (Price et al., 2016) to remove any silicates and 10% room temperature HCl to eliminate any precipitated fluorosilicates, and then sieved once more through a 15 μm

mesh. Between each step, samples were centrifuged at 3500 rpm for 6 minutes. To avoid potential loss of delicate dinoflagellate cysts by oxidation (e.g., Dale, 1976; Zonneveld et al., 1997, 2008), no oxidizing reagents were used in sample preparation (e.g., Marret, 1993; Hopkins and McCarthy, 2002; Mertens et al., 2009).

One or two drops of aliquots of each sample were mounted on microscope slides with glycerin jelly and counted at 400 or 600X magnification on a Nikon Eclipse 80i light transmitted microscope. A minimum of 295 dinoflagellate cysts per sample was counted in core P-10 and 210 dinoflagellate cysts per sample in core P-12. For core P-12, an average of 340 cysts (range of 210 to 417 cysts) was counted in each sample, while in core P-10 an average of 303 (range of 295 to 316 cysts) cysts was counted in each sample. Photomicrographs (bright-field images) of dinoflagellates from Prince William Sound (Alaska) were taken with a Nikon Digital Sight DS-5M microscope camera mounted on a Nikon Eclipse 80i light-transmitting microscope using a 60 or 100X oil immersion objective (Plates I, II and III). All samples and slides are stored at the Paleoenvironmental/Marine Palynology Laboratory, SEOS, University of Victoria (Victoria, Canada).

3.4. Dinoflagellate Cyst Nomenclature

Dinoflagellate cyst identification was performed based on taxonomic descriptions summarized in Zonneveld and Pospelova (2015). When species level identification was not possible, identification was done on a genus level. Some difficult-to-identify cysts were grouped together based on morphological similarities. Thus, there exists a category of unidentifiable spiny brown cysts (see Radi et al., 2013). Cyst folding and orientation can

obscure the archeopyle, making it hard to identify some dinoflagellate cysts to the species level. Because of this, *Brigantedinium* spp. includes *B. cariacoense*, *B. simplex*, and other smooth brown cysts. *Spiniferites* spp. includes all species of *Spiniferites* with the exception of *S. ramosus*. Some rare taxa with similar ecological morphologies or affinities were grouped together. For this reason, counts of cysts of *Polykrikos schwartzii* and *P. kofoidii*, *Echinidinium delicatum* and *E.* cf. *delicatum, as* well *Selenopemphix undulata* and *S. nephroides* were combined. A list of all recorded cysts and their thecal equivalents is provided in Table 1. It should be noted that cysts of cf. *Biecheleria* spp. sensu Price and Pospelova (2011) were observed in the samples but were not counted as most of them are lost during sample preparation due to their small size (from ~8 to 22 μm; Price and Pospelova, 2011; Heikkilä et al., 2016). A total of 39 taxa were identified in both cores, with the average sample being composed of 24 taxa.

3.5. Dinoflagellate Cyst Analysis

Temporal changes in dinoflagellate cysts before, during and after the oil spill were determined by analyzing cyst assemblage composition (relative abundances), total and individual cyst concentrations, expressed as specimens per gram of dry weight (cysts g^{-1}), and species richness (the total number of taxa in a sample). The species richness is preferred over other diversity indices, as it has been found to be a more sensitive indicator of the response of phytoplankton to changes in aquatic ecosystems induced by nutrient enrichment, pollution or environmental stress (e.g., Sommer, 1995; Tsirtis and Karydis, 1998; Pospelova et al., 2002). For convenience, in the rest of the paper, we mention “cysts

Table 1: List of dinoflagellate cysts identified in this study and their theca equivalents based on Zonneveld and Pospelova (2015).

Cyst taxa (Paleontological name)	Dinoflagellate theca (Biological name)
Autotrophic taxa	
-	*Alexandrium* spp.
Ataxiodinium choanum ?	*Gonyaulax spinifera* complex
cf. *Biecheleria* sp.	*Biecheleria* sp. indet
Impagidinium spp.	*Gonyaulax* spp.
Nematosphaeropsis labyrinthus	*Gonyaulax spinifera* complex
Operculodinium centrocarpum sensu Wall and Dale (1966)	*Protoceratium reticulatum*
-	*Pentapharsodinium dalei*
Spiniferites bentorii	*Gonyaulax spinifera* complex, *G. digitalis*
Spiniferites elongatus	*Gonyaulax elongata*
Spiniferites mirabilis	*Gonyaulax spinifera* complex
Spiniferites ramosus	*Gonyaulax spinifera* complex
Spiniferites spp.	*Gonyaulax* spp.
Heterotrophic taxa	
-	*Archaeperidinium* cf. *saanichi*
-	*Archaeperidinium* cf. *minutum*
Brigantedinium cariacoense	*Protoperidinium avellanum*
Brigantedinium simplex	*Protoperidinium conicoides*
Brigantedinium spp.	? *Protoperidinium* spp.
Dubridinium spp.	*Diplopsalid* group
Echinidinium aculeatum	*Diplopsalid* or Protoperidinoid group
Echinidinium delicatum	*Diplopsalid* or Protoperidinoid group
Echinidinium cf. *delicatum*	*Diplopsalid* or Protoperidinoid group
Echinidinium cf. *granulatum*	*Diplopsalid* or Protoperidinoid group
Echinidinium spp.	*Diplopsalid* or Protoperidinoid group
-	*Gymnodinium* spp.
Islandinium cf. *brevispinosum*	*Protoperidinium* spp. indet.
Islandinium minutum	*Protoperidinium* spp. indet.
Islandinium ? cesare	*Protoperidinium* spp. indet.
-	*Polykrikos schwartzii* sensu Matsuoka et al. (2009)
-	*Polykrikos kofoidii* sensu Matsuoka et al. (2009)
-	*Protoperidinium americanum*
-	*Protoperidinium fukuyoi*
	Protoperidinium spp.
Quinquecuspis concreta	*Protoperidinium leonis*
Selenopemphix nephroides	*Protoperidinium* sp. indet.
Selenopemphix quanta	*Protoperidinium conicum*
Selenopemphix undulata	*Protoperidinium* sp. indet.
Votadinium spinosum	*Protoperidinium claudicans*
Spiny brown cysts	?*Protoperidinium* group

Plate I

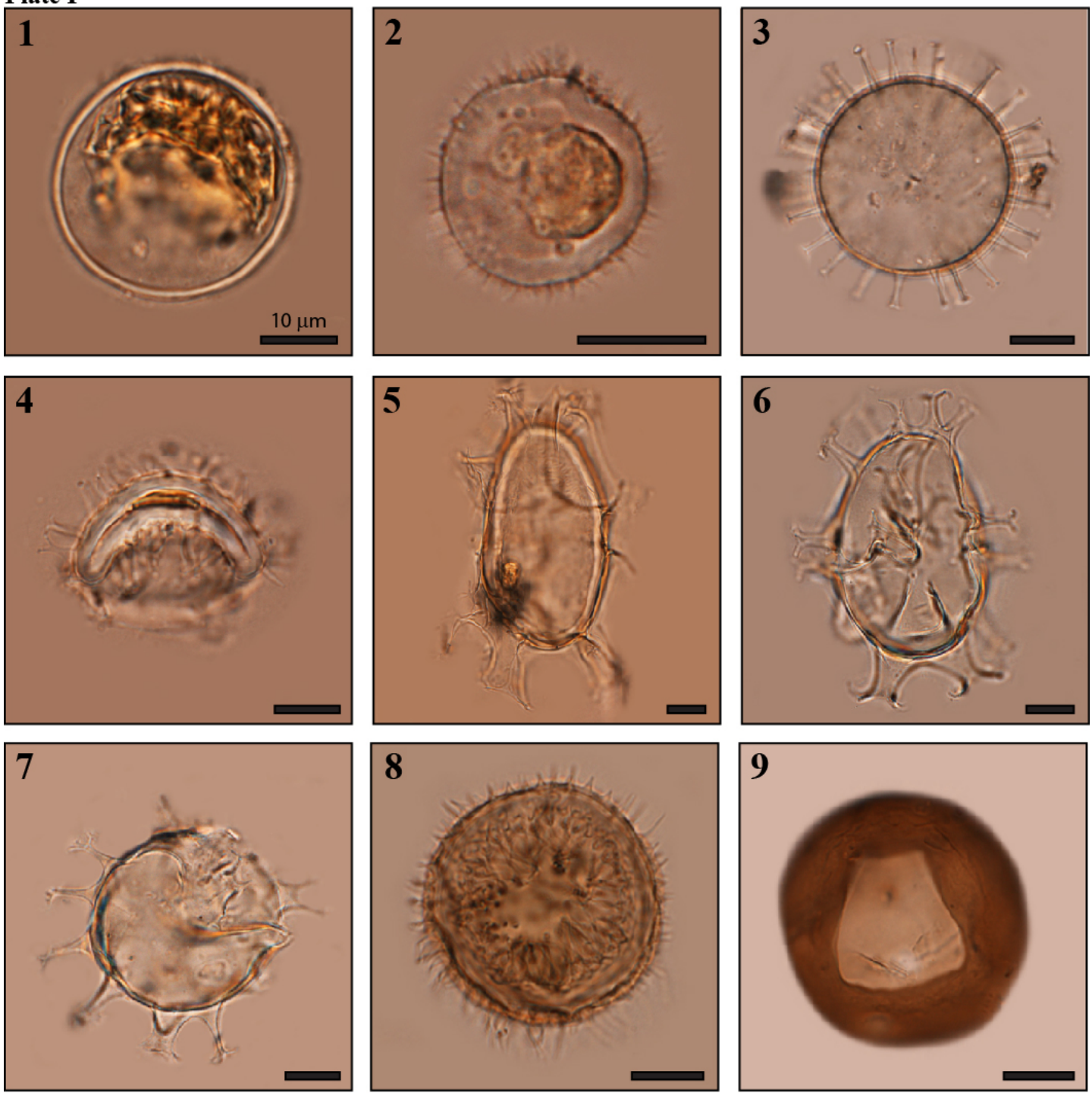

Plate I: Photomicrographs (bright-field images) of dinoflagellates from Prince William Sound (Alaska). 1. Cyst of *Alexandrium* spp. (UVic 16-273 slide 2). 2. cf. *Biecheleria* spp. (UVic 16-281 slide 2). 3. *Operculodinium centrocarpum* sensu Wall and Dale (1966) (UVic 16-271 slide 2). 4. Cyst of *Pentapharsodinium dalei* (UVic 16-263 slide 1). 5. *Spiniferites elongatus* (UVic 16-271 slide 2). 6. *Spiniferites ramosus* (UVic 16-263 slide 1). 7. *Spiniferites* spp. (UVic 16-273 slide 1) 8. Cyst of *Archaeperidinium* cf. *minutum* (UVic 16-271 slide 2). 9. *Brigantedinium simplex* (UVic 16-273 slide 2).

Plate II

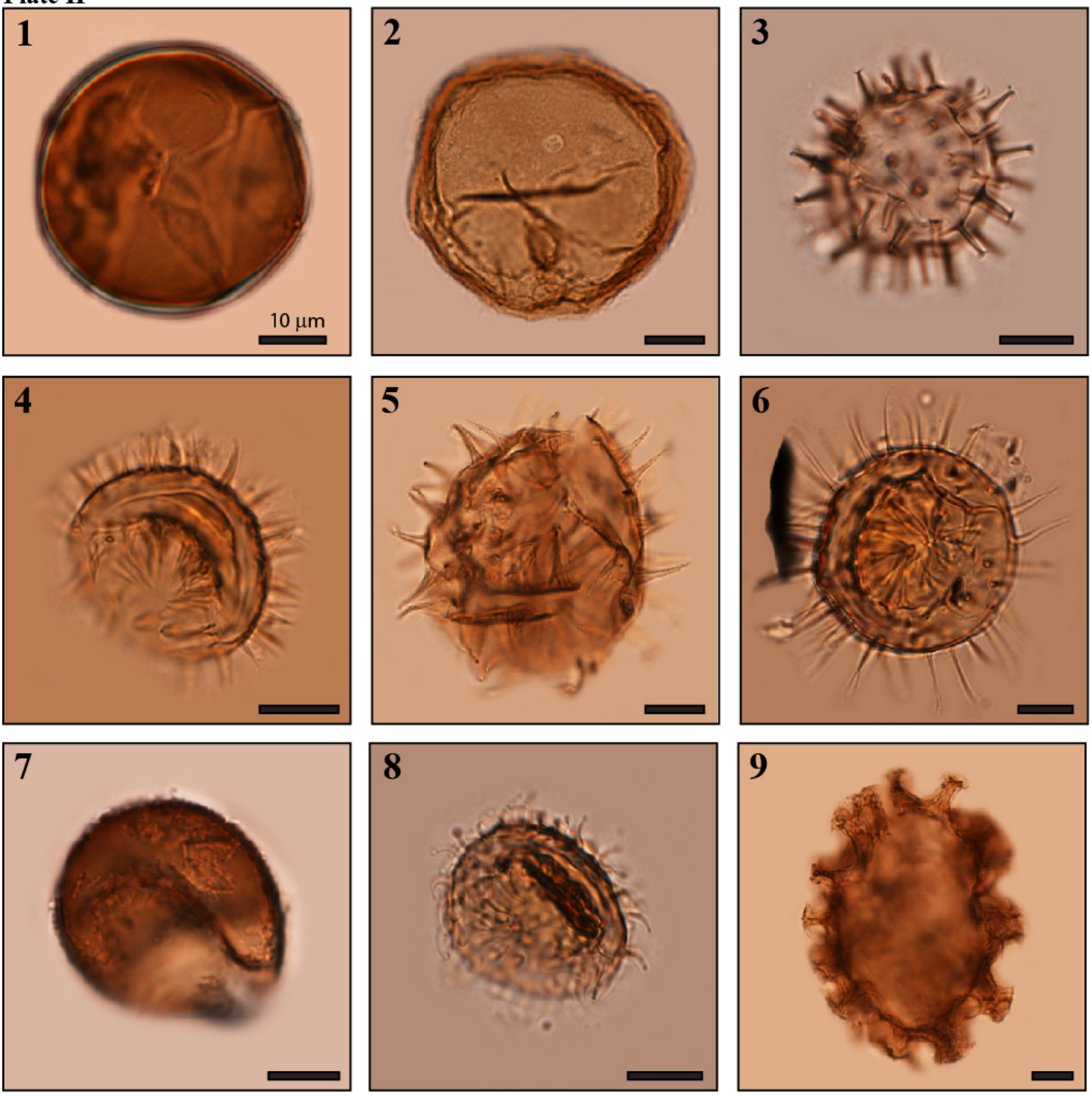

Plate II: Photomicrographs (bright-field images) of dinoflagellates from Prince William Sound (Alaska). 1. *Brigantedinium* spp. (UVic 16-271 slide 2). 2. *Dubridinium* spp. (UVic 16-271 slide 2) 3. *Echinidinium aculeatum* (UVic 16-277 slide 1). 4. *Echinidinium* cf. *delicatum* (UVic 16-250 slide 1). 5. *Echinidinium* cf. *granulatum* (UVic 16-272 slide 1). 6. *Echinidinium* spp. (UVic 16-272 slide 1). 7. *Islandinium* cf. *brevispinosum* (UVic 16-270 slide 2). 8. *Islandinium*? *cesare* (UVic 16-273 slide 1). 9. Cyst of *Polykrikos schwartzii* (UVic 16-271 slide 2).

Plate III

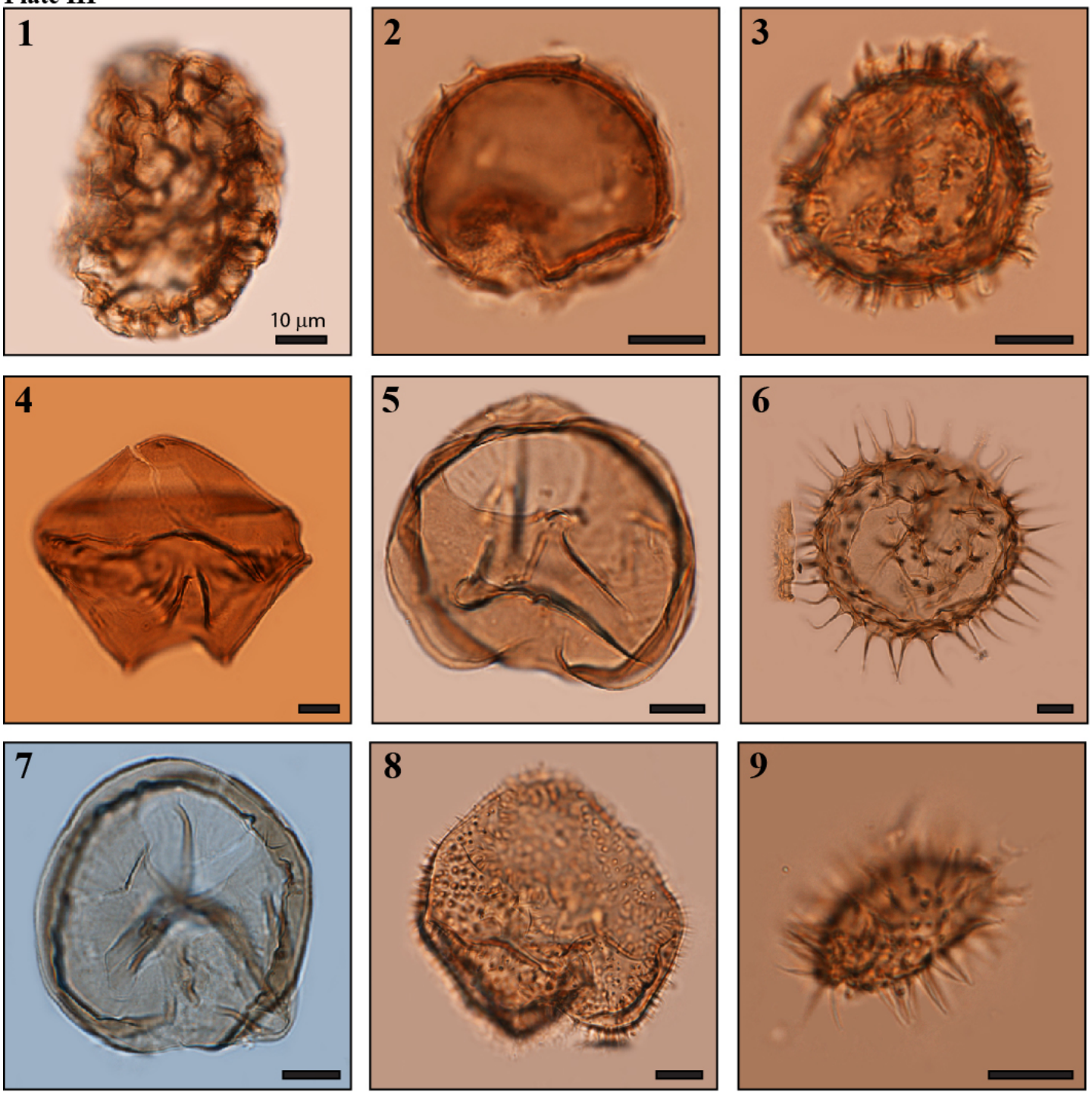

Plate III: Photomicrographs (bright-field images) of dinoflagellates from Prince William Sound (Alaska). 1. Cyst of *Polykrikos kofoidii* (UVic 16-271 slide 2). 2. Cyst of *Protoperidinium americanum* (UVic 16-279 slide 2). 3. Cyst of *Protoperidinium fukuyoi* (UVic 263 slide 2). 4. *Quinquecuspis concreta* (UVic 16-267 slide 2) 5. *Selenopemphix nephroides* (UVic 16-271 slide 2). 6. *Selenopemphix quanta* (UVic 16-280 slide 1) 7. *Selenopemphix undulata* (UVic 17-274 slide 1). 8. *Votadinium spinosum* (UVic 16-271 slide 2). 9. Spiny brown cyst (UVic 16-260 slide 2).

produced by heterotrophic dinoflagellate" as "heterotrophic cysts", and "cysts produced by autotrophic dinoflagellates" as "autotrophic cysts."

Whisker plots of the relative abundance and cyst concentrations in core P-10 and P-12 were produced. These whisker plots display the five-number summary of the data, which includes the minimum, first quartile, median, third quartile, and maximum. These type of plots are commonly used to determine whether the distribution is skewed and whether there are potential unusual observations (Statistics Canada, 2013).

Core P-12 was counted by two individuals (analyst #1 and analyst #2). On average, analyst #1 counted 125 cysts per sample, while analyst #2 counted 231 cysts per sample. These counts were then combined for the analysis of core P-12. To study the similarity in the counts between the two analysts, a comparison of five samples in core P-12 was performed. For each of these five samples (UVic 16-271, 16-269, 16-267, 16-265 and 16-261), a similar number of cysts (~210 cysts) was counted by each analyst. The cyst counts, relative and absolute abundances determined by each individual are compared. The Bray-Curtis similarity was calculated using the following formula:

$$BC_{ij} = \frac{2C_{ij}}{S_i + S_j} \times 100$$

Where C_{ij} is the sum of the lesser values for only those species observed in both counts. S_i and S_j are the total number of specimens counted by each analyst. A value of 100% means that the counts by the two analysts share the same composition.

This similarity measurement was chosen as it has been used in the only other phytoplankton studies looking at inter-observer variability (Kahlert et al., 2010; Lavoie and

Campeau, 2016). As such, it allows for easy comparison with the studies from Kahlert et al (2010) and Lavoie and Campeau (2016).

4. Results

4.1. Count Comparison

As part of this study two analysts (analyst #1 and analyst #2) compared counts from five separate samples (Table 2). The word "difference" in this section refers to the difference in measurements between the two analysts. For example, the difference in the relative abundance of *Brigantedinium* spp. means the difference in the relative abundance of *Brigantedinium* spp. determined by analyst #1 compared to analyst #2.

The difference in the relative abundance of the individual taxa is, for the most part, very small (Table 2). Most taxa show differences of ≤ 3.5%, with an average difference ≤ 2%. The taxa that show the greatest difference include cysts of *Pentapharsodinium dalei* (difference of 0 to 4.4%, average of 2.3%), *Brigantedinium* spp. (difference of 1.4 to 13.7%, average of 6.1%), *Echinidinium aculeatum* (difference of 0.5 to 3.5%, average of 1.9%), cysts of *Protoperidinium americanum* (difference of 0 to 4.0%, average of 1.0%), and spiny brown cysts (difference of 0 to 3.9%, average of 1.7%) (Table 2). The Bray-Curtis similarity between the results by two analysts was also determined for the five samples (Table 2). The similarity ranged from 72 to 88%, with an average of 82% and a standard deviation of 7% relative to the mean similarity (Table 2).

Similar to the differences in relative abundances, the differences in dinoflagellate cyst concentrations are also comparable for the individual taxa, with most taxa having differences of < 60 cysts g^{-1} (Table 2 and 3). There are three exceptions to this: *Operculodinium centrocarpum* sensu Wall and Dale, (1966) (difference of 11 to 71 cysts g^{-1}, average 24 cysts g^{-1}), *Brigantedinium* spp. (difference of 11 to 186 cysts g^{-1}, average of 67 cysts g^{-1}), and spiny brown cysts (difference of 0 to 70 cysts g^{-1}, average 26 cysts g^{-}

Table 2: The number of cysts counted, the relative abundances and the dinoflagellate cyst concentrations determined by each analyst. For each column, the first number represents the data from analyst #1 and the second number represents the data from analyst #2. The dry weight of the samples, the number of *Lycopodium* spores added and counted are shown. The species richness, the total number of cysts counted, and the total dinoflagellate cyst concentrations for each analyst, as well as the Bray-Curtis similarity between the results obtained by the two analysts are presented.

Yr	**UvicID**	Dry weight	*Lycopodium* spores added	*Lycopodium* spores counted		Cysts of *Alexandrium* spp.		*Ataxiodinium choanum*?		*Operculodinium centrocarpum*		Cyst of *Pentapharsodinium dalei*		*Spiniferites elongatus*		*Spiniferites mirabilis*		*Spiniferites ramosus*		*Spiniferites* spp.		Cysts of *Archaeperidinium* cf. *saanich* i		Cysts of *Archaeperidinium* cf. *minutum*		*Brigantedinium cariacoense*		*Brigantedinium simplex*	
Number of dinoflagellate cysts counted																													
2016	**261**	7.673	18584	397	356	6	7	0	0	42	46	6	2	0	0	0	1	5	1	0	2	0	0	0	0	0	0	11	6
2016	**265**	6.226	18584	442	418	12	11	0	0	35	36	0	4	0	0	0	0	3	2	5	3	1	0	0	0	1	1	7	4
2016	**267**	7.191	18584	433	420	10	18	0	1	38	35	1	1	2	1	0	0	5	3	3	0	0	0	0	0	0	1	6	7
2016	**269**	7.262	18584	429	447	3	2	0	0	52	44	9	0	1	2	0	0	3	5	4	0	0	0	0	0	0	0	0	1
2016	**271**	5.275	18584	456	473	6	13	0	0	69	62	9	2	0	0	0	0	9	5	4	1	0	0	0	6	0	1	4	3
	Average			425	410	7	10	0	0	42	45	5	2	1	1	0	0	4	3	3	1	0	0	0	1	0	1	6	4
	Std. Dev			20	39	4	7	0	1	7	6	4	2	1	1	0	1	1	2	2	2	1	0	0	0	1	1	5	3
Relative abundance																													
2016	**261**	7.673	18584	397	356	2.9	3.5	0.0	0.0	20.4	22.8	2.9	1.0	0.0	0.0	0.0	0.5	2.4	0.5	0.0	1.0	0.0	0.0	0.0	0.0	0.0	0.0	5.3	3.0
2016	**265**	6.226	18584	442	418	6.1	5.8	0.0	0.0	17.8	19.0	0.0	2.1	0.0	0.0	0.0	0.0	1.5	1.1	2.5	1.6	0.5	0.0	0.0	0.0	0.5	0.5	3.6	2.1
2016	**267**	7.191	18584	433	420	4.4	7.8	0.0	0.4	16.7	15.2	0.4	0.4	0.9	0.4	0.0	0.0	2.2	1.3	1.3	0.0	0.0	0.0	0.0	0.0	0.0	0.4	2.6	3.0
2016	**269**	7.262	18584	429	447	1.5	1.0	0.0	0.0	25.4	21.9	4.4	0.0	0.5	1.0	0.0	0.0	1.5	2.5	2.0	0.0	0.0	0.0	0.0	0.0	0.0	0.0	0.0	0.5
2016	**271**	5.275	18584	456	473	2.6	5.9	0.0	0.0	29.6	28.2	3.9	0.9	0.0	0.0	0.0	0.0	3.9	2.3	1.7	0.5	0.0	0.0	0.0	2.7	0.0	0.5	1.7	1.4
	Average			425	410	3.5	4.8	0.0	0.1	22.0	21.4	2.3	0.9	0.3	0.3	0.0	0.1	2.3	1.5	1.5	0.6	0.1	0.0	0.0	0.5	0.1	0.3	2.7	2.0
	Std. Dev			20	39	1.8	2.6	0.0	0.2	5.4	4.8	2.0	0.8	0.4	0.4	0.0	0.2	1.0	0.8	0.9	0.7	0.2	0.0	0.0	1.2	0.2	0.3	2.0	1.1
Dinoflagellate cyst concentrations																													
2016	**261**	7.673	18584	397	356	37	48	0	0	256	313	37	14	0	0	0	7	31	7	0	14	0	0	0	0	0	0	67	41
2016	**265**	6.226	18584	442	418	81	79	0	0	236	257	0	29	0	0	0	0	20	14	34	21	7	0	0	0	7	7	47	29
2016	**267**	7.191	18584	433	420	60	111	0	6	227	215	6	6	12	6	0	0	30	18	18	0	0	0	0	0	0	6	36	43
2016	**269**	7.262	18584	429	447	18	11	0	0	310	252	54	0	6	11	0	0	18	29	24	0	0	0	0	0	0	0	0	6
2016	**271**	5.275	18584	456	473	46	97	0	0	533	462	70	15	0	0	0	0	70	37	31	7	0	0	0	45	0	7	31	22
	Average			431	423	48	69	0	1	313	300	33	13	4	4	0	1	34	21	21	8	1	0	0	9	1	4	36	28
	Std. Dev			22	44	24	40	0	3	127	97	30	11	5	5	0	3	21	12	13	9	3	0	0	20	3	4	25	15

Table 2 (continued): The number of cysts counted, the relative abundances and the dinoflagellate cyst concentrations determined by each analyst. For each column, the first number represents the data from analyst #1 and the second number represents the data from analyst #2. The dry weight of the samples, the number of *Lycopodium* spores added and counted are shown. The species richness, the total number of cysts counted, and the total dinoflagellate cyst concentrations for each analyst, as well as the Bray-Curtis similarity between the results obtained by the two analysts are presented.

Yr	UvicID	Dry weight	*Lycopodium* spores added	*Lycopodium* spores counted		*Brigantedinium spp.*		*Dubridinium spp.*		*Echinidinium aculeatum*		*Echinidinium delicatum*		*Echinidinium* cf. *delicatum*		*Echinidinium* cf. *granulatum*		*Echinidinium* spp.		*Islandinium* cf. *brevispinosum*		*Islandinium minutum*		*Islandinium? cesare*		Cysts of *Polykrikos shwartzii*		Cysts of *Polykrikos kofoidii*	
Number of dinoflagellate cysts counted																													
2016	**261**	7.673	18584	397	356	71	62	6	6	1	7	8	4	1	0	3	0	5	6	0	0	1	5	5	3	0	1	2	5
2016	**265**	6.226	18584	442	418	83	89	6	5	2	0	5	3	0	0	1	0	1	6	0	0	0	1	4	1	0	0	2	2
2016	**267**	7.191	18584	433	420	103	108	9	10	1	1	10	2	0	0	1	1	5	1	0	0	0	1	2	1	0	1	1	1
2016	**269**	7.262	18584	429	447	101	112	5	6	4	0	1	2	0	0	2	0	2	0	0	0	0	0	0	0	0	0	0	2
2016	**271**	5.275	18584	456	473	56	83	15	14	5	1	9	3	1	0	7	0	9	2	0	1	0	3	3	1	1	0	1	0
	Average			425	410	90	91	7	8	3	2	7	3	0	0	3	0	3	3	0	0	0	2	3	1	0	0	1	2
	Std. Dev			20	39	15	23	2	2	1	3	4	1	1	0	1	1	2	3	0	0	1	2	2	1	0	1	1	2
Relative abundance																													
2016	**261**	7.673	18584	397	356	34.5	30.7	2.9	3.0	0.5	3.5	3.9	2.0	0.5	0.0	1.5	0.0	2.4	3.0	0.0	0.0	0.5	2.5	2.4	1.5	0.0	0.5	1.0	2.5
2016	**265**	6.226	18584	442	418	42.1	47.1	3.0	2.6	1.0	0.0	2.5	1.6	0.0	0.0	0.5	0.0	0.5	3.2	0.0	0.0	0.0	0.5	2.0	0.5	0.0	0.0	1.0	1.1
2016	**267**	7.191	18584	433	420	45.4	46.8	4.0	4.3	0.4	0.4	4.4	0.9	0.0	0.0	0.4	0.4	2.2	0.4	0.0	0.0	0.0	0.4	0.9	0.4	0.0	0.4	0.4	0.4
2016	**269**	7.262	18584	429	447	49.3	55.7	2.4	3.0	2.0	0.0	0.5	1.0	0.0	0.0	1.0	0.0	1.0	0.0	0.0	0.0	0.0	0.0	0.0	0.0	0.0	0.0	0.0	1.0
2016	**271**	5.275	18584	456	473	24.0	37.7	6.4	6.4	2.1	0.5	3.9	1.4	0.4	0.0	3.0	0.0	3.9	0.9	0.0	0.5	0.0	1.4	1.3	0.5	0.4	0.0	0.4	0.0
	Average			425	410	39.1	43.6	3.8	3.9	1.2	0.9	3.0	1.4	0.2	0.0	1.3	0.1	2.0	1.5	0.0	0.1	0.1	1.0	1.3	0.6	0.1	0.2	0.6	1.0
	Std. Dev			20	39	10.0	9.6	1.6	1.5	0.8	1.5	1.6	0.5	0.3	0.0	1.0	0.2	1.3	1.5	0.0	0.2	0.2	1.0	1.0	0.5	0.2	0.3	0.4	0.9
Dinoflagellate cyst concentrations																													
2016	**261**	7.673	18584	397	356	433	422	37	41	6	48	49	27	6	0	18	0	31	41	0	0	6	34	31	20	0	7	12	34
2016	**265**	6.226	18584	442	418	561	636	41	36	14	0	34	21	0	0	7	0	7	43	0	0	0	7	27	7	0	0	14	14
2016	**267**	7.191	18584	433	420	615	665	54	62	6	6	60	12	0	0	6	6	30	6	0	0	0	6	12	6	0	6	6	6
2016	**269**	7.262	18584	429	447	602	641	30	34	24	0	6	11	0	0	12	0	12	0	0	0	0	0	0	0	0	0	0	11
2016	**271**	5.275	18584	456	473	433	618	116	104	39	7	70	22	8	0	54	0	70	15	0	7	0	22	23	7	8	0	8	0
	Average			431	423	529	596	55	55	18	12	44	19	3	0	19	1	30	21	0	1	1	14	19	8	2	3	8	13
	Std. Dev			22	44	90	99	35	29	14	20	25	7	4	0	20	3	25	20	0	3	3	14	12	7	3	4	5	13

Table 2 (continued): The number of cysts counted, the relative abundances and the dinoflagellate cyst concentrations determined by each analyst. For each column, the first number represents the data from analyst #1 and the second number represents the data from analyst #2. The dry weight of the samples, the number of *Lycopodium* spores added and counted are shown. The species richness, the total number of cysts counted, and the total dinoflagellate cyst concentrations for each analyst, as well as the Bray-Curtis similarity between the results obtained by the two analysts are presented.

Yr	UvicID	Dry weight	*Lycopodium* spores added	*Lycopodium* spores counted		*Cyst* of *Protoperidinium americanum*		Cysts of *Protoperidinium fukuyoi*		Cysts of *Protoperidinium* spp.		*Quinquecuspis concreta*		*Selenopemphix undulata*		*Selenopemphix quanta*		*Votadinium spinosum*		Spiny brown cysts		Spiny brown cysts (small)		Unknown cysts		Total		Species richness		Bray-Curtis similarity (%)
Number of dinoflagellate cysts counted																														
2016	**261**	7.673	18584	397	356	5	13	2	1	11	12	3	4	5	3	2	2	0	0	4	0	1	0	0	3	206	202	23	22	N/A
2016	**265**	6.226	18584	442	418	4	3	1	1	13	7	4	2	4	4	1	1	0	1	1	1	0	1	1	0	197	189	22	23	N/A
2016	**267**	7.191	18584	433	420	3	3	2	0	11	15	4	8	3	5	3	3	0	0	3	0	0	2	1	1	227	231	22	24	N/A
2016	**269**	7.262	18584	429	447	1	1	0	0	6	9	5	7	2	5	0	2	0	1	3	0	1	0	0	0	205	201	18	15	N/A
2016	**271**	5.275	18584	456	473	3	2	4	0	4	9	1	0	0	3	0	3	1	1	9	0	2	0	1	1	233	220	23	21	N/A
	Average			425	410	3	4	1	0	9	10	3	4	3	4	2	2	0	1	3	0	1	1	1	1	214	209	22	21	N/A
	Std. Dev			20	39	2	5	1	1	3	4	1	3	1	1	1	1	0	1	1	1	1	1	1	1	13	18	2	4	N/A
Relative abundance																														
2016	**261**	7.673	18584	397	356	2.4	6.4	1.0	0.5	5.3	5.9	1.5	2.0	2.4	1.5	1.0	1.0	0.0	0.0	1.9	0.0	0.5	0.0	0.0	1.5	N/A	N/A	N/A	N/A	78
2016	**265**	6.226	18584	442	418	2.0	1.6	0.5	0.5	6.6	3.7	2.0	1.1	2.0	2.1	0.5	0.5	0.0	0.5	0.5	0.5	0.0	0.5	0.5	0.0	N/A	N/A	N/A	N/A	88
2016	**267**	7.191	18584	433	420	1.3	1.3	0.9	0.0	4.8	6.5	1.8	3.5	1.3	2.2	1.3	1.3	0.0	0.0	1.3	0.0	0.0	0.9	0.4	0.4	N/A	N/A	N/A	N/A	87
2016	**269**	7.262	18584	429	447	0.5	0.5	0.0	0.0	2.9	4.5	2.4	3.5	1.0	2.5	0.0	1.0	0.0	0.5	1.5	0.0	0.5	0.0	0.0	0.0	N/A	N/A	N/A	N/A	84
2016	**271**	5.275	18584	456	473	1.3	0.9	1.7	0.0	1.7	4.1	0.4	0.0	0.0	1.4	0.0	1.4	0.4	0.5	3.9	0.0	0.9	0.0	0.4	0.5	N/A	N/A	N/A	N/A	72
	Average			425	410	1.5	2.1	0.8	0.2	4.3	4.9	1.6	2.0	1.4	1.9	0.6	1.0	0.1	0.3	1.8	0.1	0.4	0.3	0.3	0.5	N/A	N/A	N/A	N/A	82
	Std. Dev			20	39	0.7	2.4	0.6	0.3	2.0	1.2	0.8	1.5	0.9	0.5	0.6	0.3	0.2	0.3	1.3	0.2	0.4	0.4	0.3	0.6	N/A	N/A	N/A	N/A	7
Dinoflagellate cyst concentrations																														
2016	**261**	7.673	18584	397	356	31	88	12	7	67	82	18	27	31	20	12	14	0	0	24	0	6	0	0	20	1257	1374	N/A	N/A	N/A
2016	**265**	6.226	18584	442	418	27	21	7	7	88	50	27	14	27	29	7	7	0	7	7	7	0	7	7	0	1330	1350	N/A	N/A	N/A
2016	**267**	7.191	18584	433	420	18	18	12	0	66	92	24	49	18	31	18	18	0	0	18	0	0	12	6	6	1355	1421	N/A	N/A	N/A
2016	**269**	7.262	18584	429	447	6	6	0	0	36	52	30	40	12	29	0	11	0	6	18	0	6	0	0	0	1223	1151	N/A	N/A	N/A
2016	**271**	5.275	18584	456	473	23	15	31	0	31	67	8	0	0	22	0	22	8	7	70	0	15	0	8	7	1800	1639	N/A	N/A	N/A
	Average			431	423	21	30	12	3	57	68	21	26	17	26	7	15	2	4	27	1	6	4	4	7	1393	1387	N/A	N/A	N/A
	Std. Dev			22	44	10	33	11	4	24	19	9	20	12	4	8	6	3	4	24	3	6	6	4	8	234	175	N/A	N/A	N/A

Table 3: The difference in dinoflagellate cyst concentrations between the results obtained by the two analysts. The percent difference in total concentration and the difference in the number of *Lycopodium* spores counted are shown.

Yr	UvicID	*Echinidinium* cf. *delicatum*	*Echinidinium* cf. *granulatum*	*Echinidinium* spp.	*Islandinium* cf. *brevispinosum*	*Islandinium minutum*	*Islandinium? cesare*	Cysts of *Polykrikos shwartzii*	Cysts of *Polykrikos kofoidii*	*Cyst* of *Protoperidinium americanum*	Cysts of *Protoperidinium fukuyoi*	Cysts of *Protoperidinium* spp.	*Quinquecuspis concreta*	*Selenopemphix undulata*	*Selenopemphix quanta*	*Votadinium spinosum*	Spiny brown cysts	Spiny brown cysts (small)	Unknown cysts	Difference in total concentration	% difference of total concentration
Absolute difference in cyst concentration																					
2016	**261**	6	18	10	0	28	10	7	22	58	5	15	9	10	1	0	24	6	20	118	8.9
2016	**265**	0	7	36	0	7	20	0	1	6	0	38	13	2	0	7	0	7	7	19	1.4
2016	**267**	0	0	24	0	6	6	6	0	1	12	27	25	13	1	0	18	12	0	67	4.8
2016	**269**	0	12	12	0	0	0	0	11	0	0	16	10	17	11	6	18	6	0	72	6.1
2016	**271**	8	54	55	7	22	16	8	8	8	31	36	8	22	22	0	70	15	0	162	9.4
	Mean	3	18	27	1	13	10	4	8	15	10	26	13	13	7	3	26	9	6	87	6
	Std. dev.	4	21	18	3	12	8	4	9	25	13	11	7	8	10	4	26	4	9	54	3

Yr	UvicID	*Echinidinium* cf. *delicatum*	*Echinidinium* cf. *granulatum*	*Echinidinium* spp.	*Islandinium* cf. *brevispinosum*	*Islandinium minutum*	*Islandinium? cesare*	Cysts of *Polykrikos shwartzii*	Cysts of *Polykrikos kofoidii*	*Cyst* of *Protoperidinium americanum*	Cysts of *Protoperidinium fukuyoi*	Cysts of *Protoperidinium* spp.	*Quinquecuspis concreta*	*Selenopemphix undulata*	*Selenopemphix quanta*	*Votadinium spinosum*	Spiny brown cysts	Spiny brown cysts (small)	Unknown cysts	Difference in total concentration	% difference of total concentration
Absolute difference in cyst concentration																					
2016	**261**	6	18	10	0	28	10	7	22	58	5	15	9	10	1	0	24	6	20	118	8.9
2016	**265**	0	7	36	0	7	20	0	1	6	0	38	13	2	0	7	0	7	7	19	1.4
2016	**267**	0	0	24	0	6	6	6	0	1	12	27	25	13	1	0	18	12	0	67	4.8
2016	**269**	0	12	12	0	0	0	0	11	0	0	16	10	17	11	6	18	6	0	72	6.1
2016	**271**	8	54	55	7	22	16	8	8	8	31	36	8	22	22	0	70	15	0	162	9.4
	Mean	3	18	27	1	13	10	4	8	15	10	26	13	13	7	3	26	9	6	87	6
	Std. dev.	4	21	18	3	12	8	4	9	25	13	11	7	8	10	4	26	4	9	54	3

^{1}) (Table 2 and 3). The standard deviation of the absolute difference in concentration of the individual taxa is < 30 cysts g^{-1}, except for *Brigantedinium* spp., which is 67 cysts g^{-1} (Table 3).

The total dinoflagellate cyst concentrations are very similar between the two analysts (Table 2 and 3). The absolute difference in total cyst concentrations ranges from 19 to 162 cysts g^{-1}, representing a percent difference ranging from 1.4 to 9.4% (Table 3). The average difference in total cyst concentrations is 87 cysts g^{-1}, with a standard deviation of 54 cysts g^{-1}, representing an average percent difference of 6.1% with a standard deviation of 3.3% (Table 3).

4.2. Dinoflagellate Cyst Record

Dinoflagellate cysts are abundant and well-preserved in both cores, with a total of 39 taxa being identified (Table 1). Bright-field photomicrographs of the most common cyst taxa are presented in Plates I-III. Total cyst concentrations in core P-10 range from 327 to 749 cysts g^{-1} (Figure 3 and 4), with an average of 476 cysts g^{-1}, whereas those of core P-12 range between 638 and 1771 cysts g^{-1}, with an average of 1221 cysts g^{-1} (Figure 5 and 6). In general, dinoflagellate cyst assemblages are dominated by cysts produced by heterotrophic dinoflagellates (~65%), with an average heterotrophic to autotrophic (H/A) ratio of 2.0 (Figure 7 and 8). The most abundant heterotrophic taxon is *Brigantedinium* spp., with an average relative abundance of 41.6% (Figure 7) and average cyst concentrations of

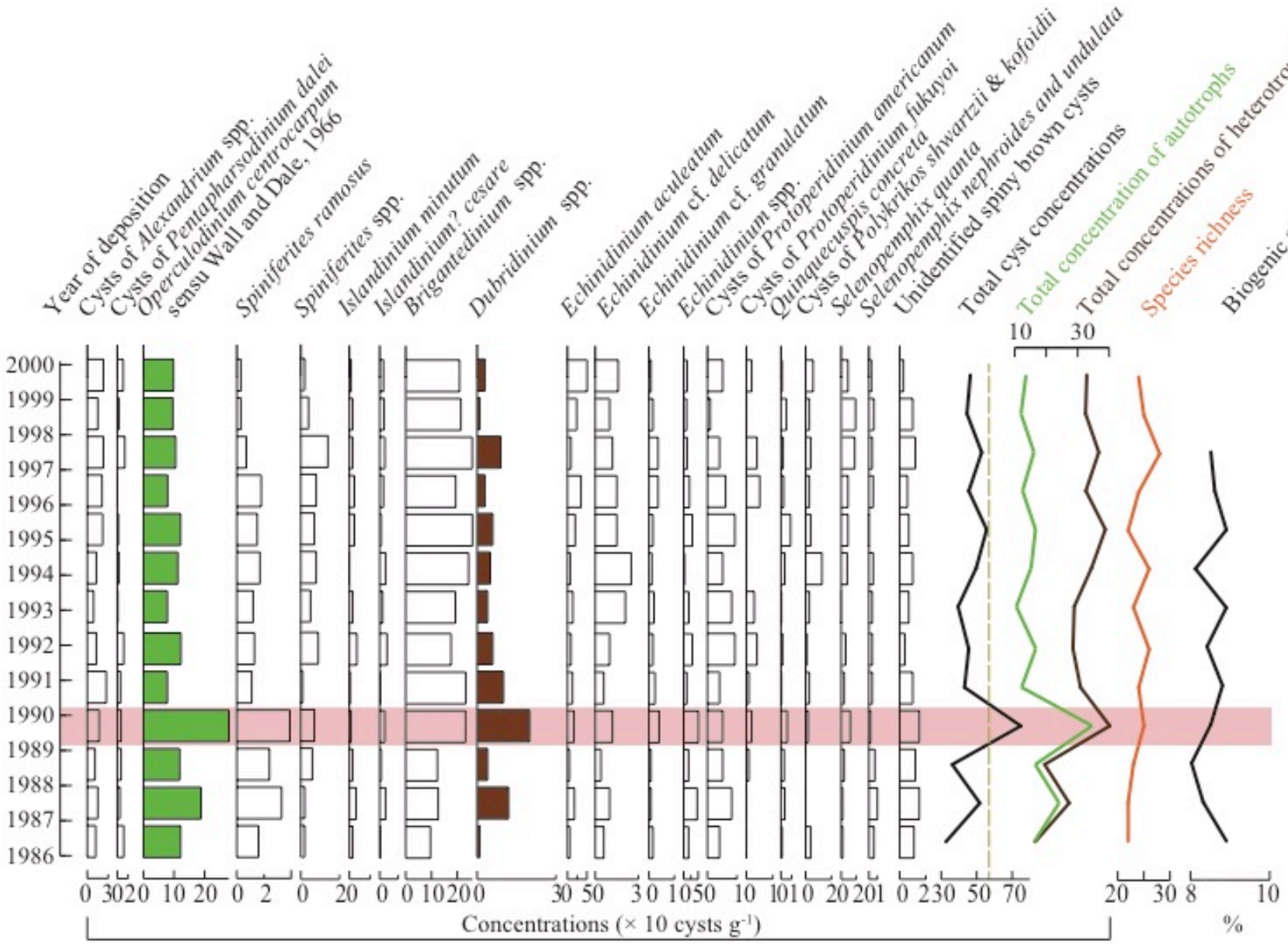

Figure 3: Dinoflagellate cyst concentrations for the individual taxa found in core P-10, including total cyst concentrations and total concentrations of cysts produced by autotrophic and heterotrophic dinoflagellates. The proportion (%) of biogenic silica and species richness (number of taxa) are also shown. The red area marks the timing of the 1989 Exxon Valdez oil spill

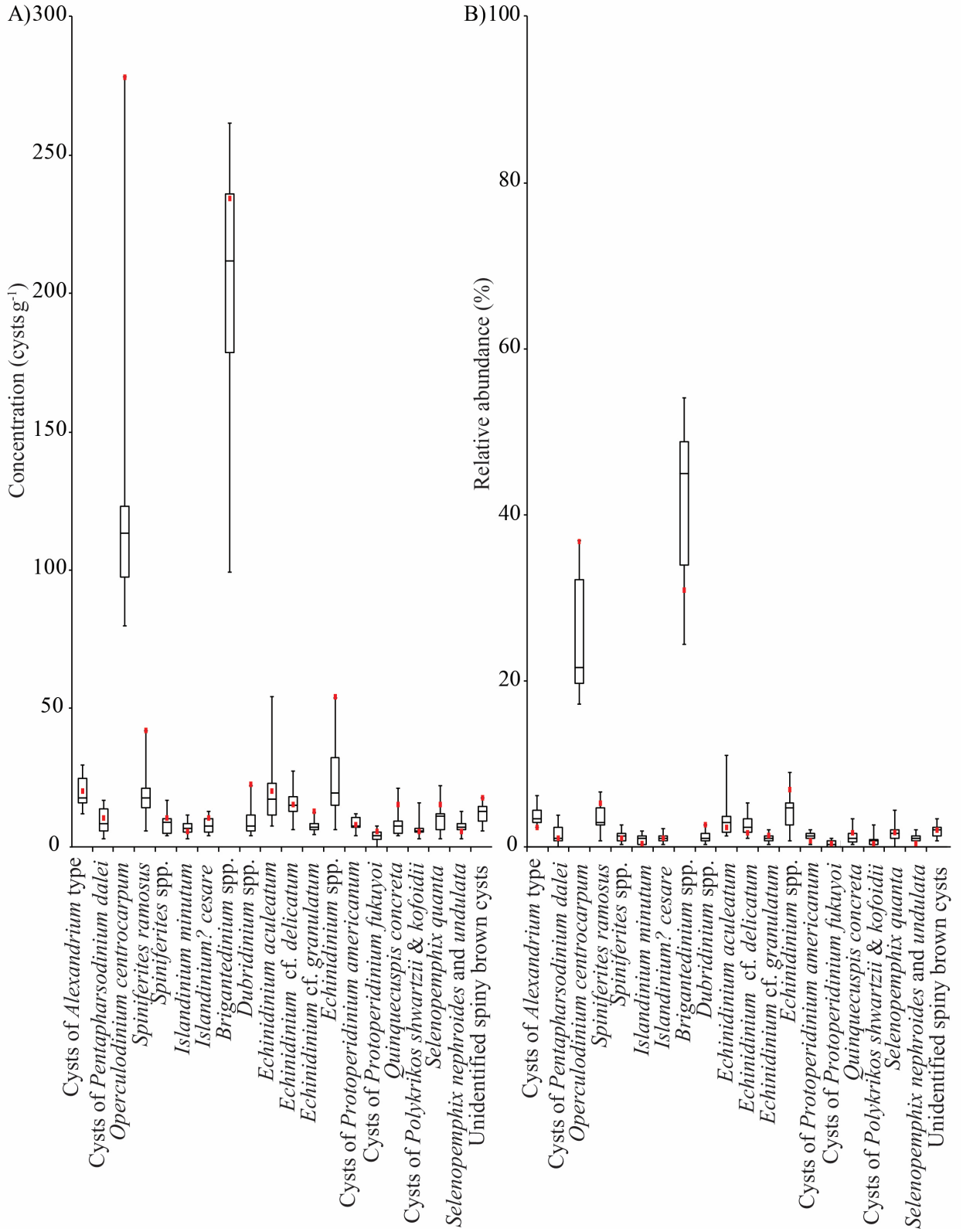

Figure 4: Whisker-plot of **(A)** cyst concentrations and **(B)** relative abundances showing the median, first quartile, third quartile, maximum and minimum for the taxa found in core P-10. The red dots represent the concentrations and relative abundances for sample deposited during the oil spill (UVic 16-75).

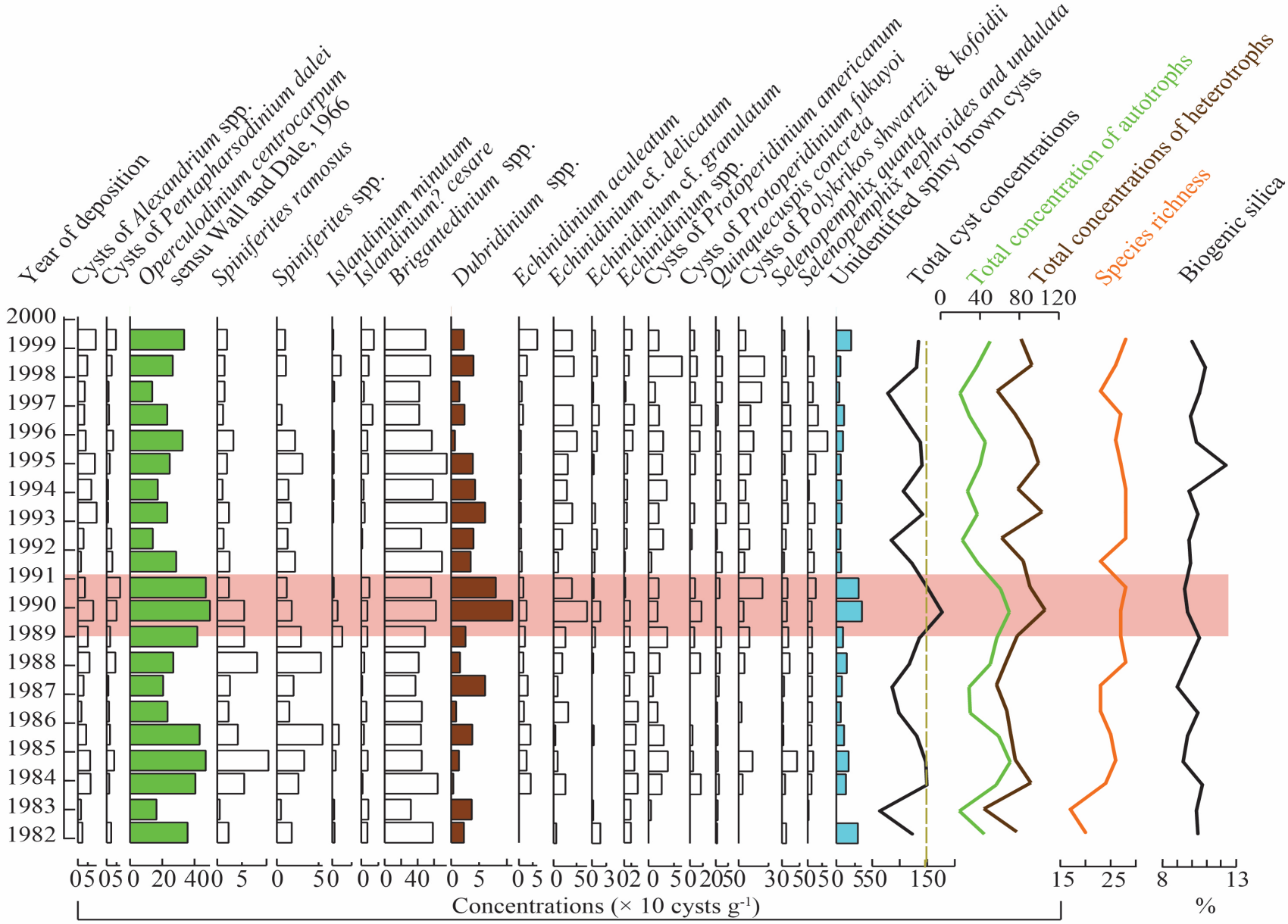

Figure 5: Dinoflagellate cyst concentrations for the individual taxa found in core P-12, including total cyst concentrations and total concentrations of cysts produced by autotrophic and heterotrophic dinoflagellates. The proportion (%) of biogenic silica and species richness (number of taxa) are also shown. The red area marks the timing of the 1989 Exxon Valdez oil spill.

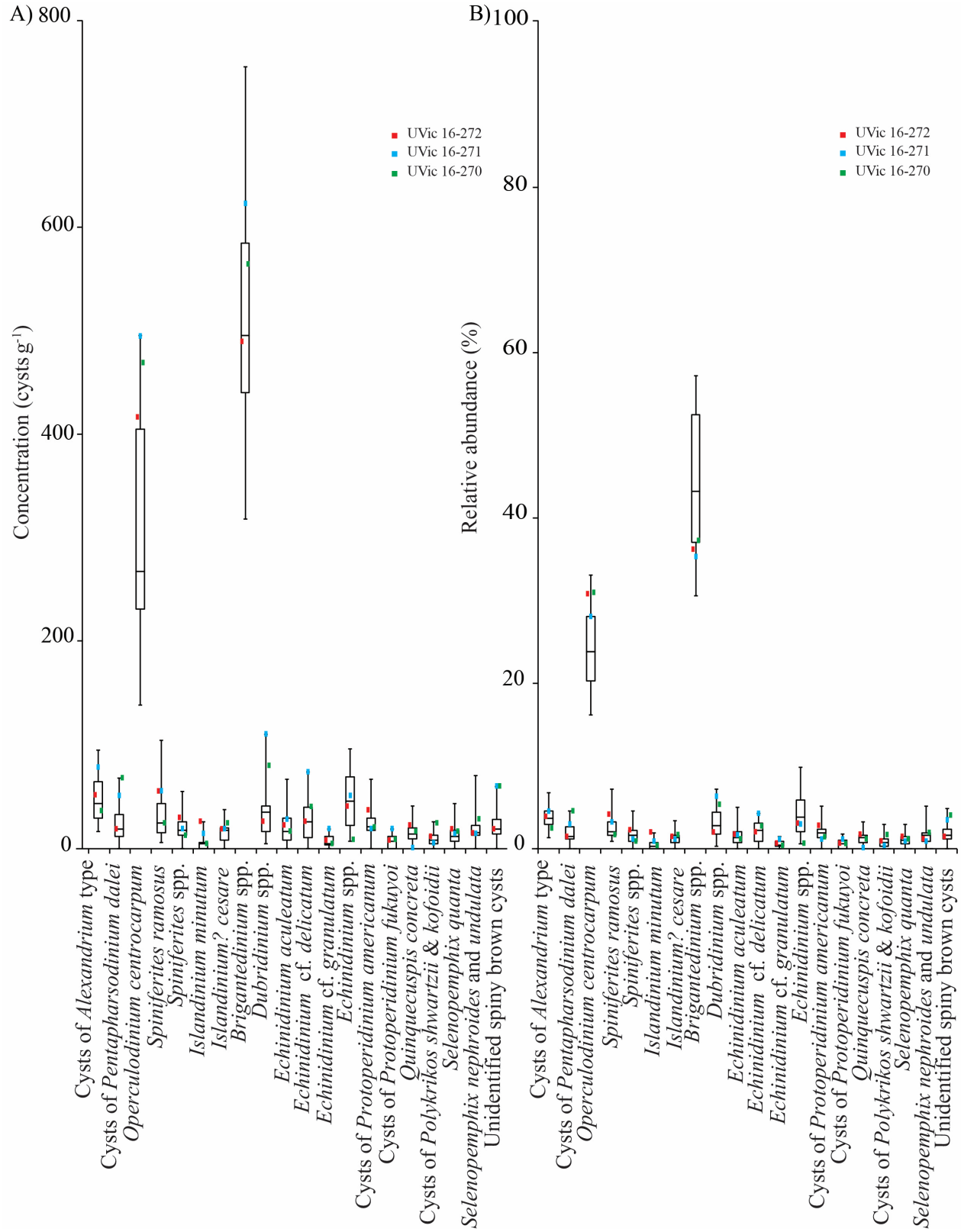

Figure 6: Whisker-plot of **(A)** cyst concentrations and **(B)** relative abundances showing the median, first quartile, third quartile, maximum and minimum for the taxa found in core P-12. Coloured dots represent the concentrations and relative abundances for the samples deposited during the oil spill (Green: UVic 16-270; Blue: UVic 16-271; Red: UVic 16-272).

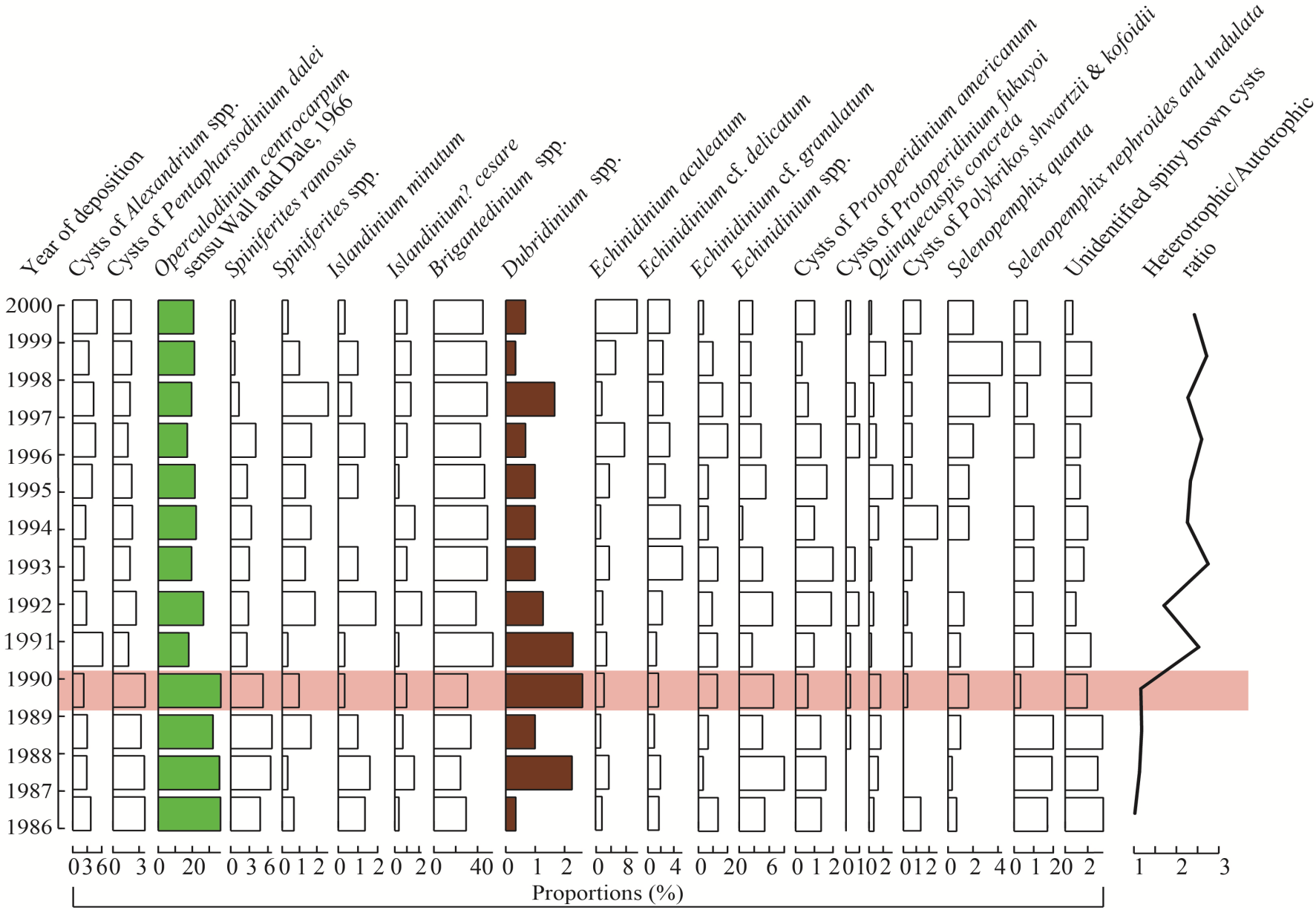

Figure 7: Relative abundances for the individual dinoflagellate taxa found in core P-10, and the **heterotrophic to autotrophic ratio. The red area marks the timing of the 1989 Exxon Valdez oil spill.**

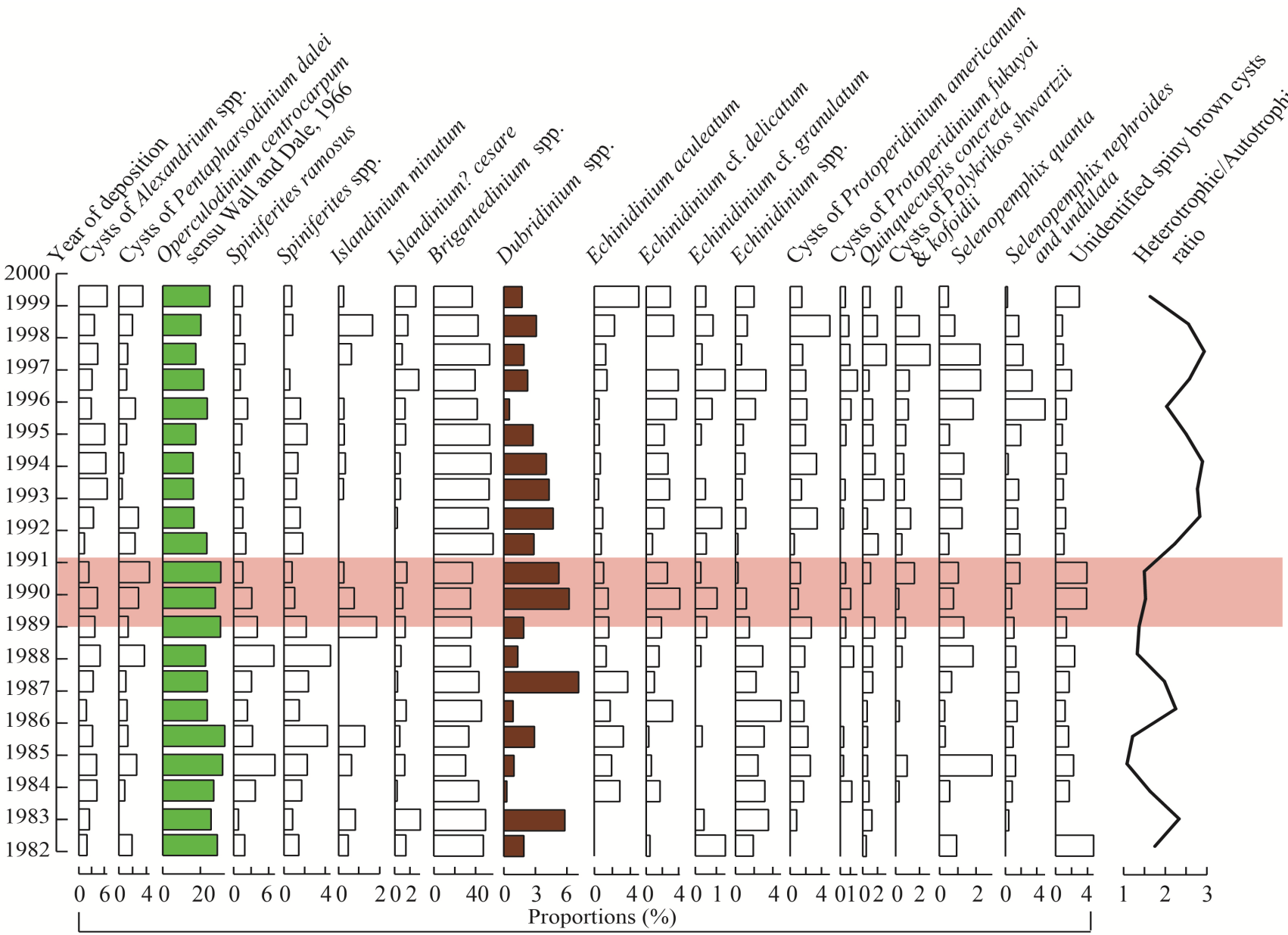

Figure 8: Relative abundances for the individual dinoflagellate taxa found in core P-12, and the heterotrophic to autotrophic ratio. The red area marks the timing of the 1989 Exxon Valdez oil spill.

259 cysts g^{-1} (range from 96 to 259 cysts g^{-1}) (Figure 3) in core P-10. In core P-12 the average relative abundance and average cyst concentration of *Brigantedinium* spp. is 44.0% (Figure 8) and 527 cysts g^{-1} (range from 318 to 755 cysts g^{-1}) (Figure 5), respectively. The remainder of the heterotrophic taxa have relative abundances ≤ 5% (Figure 4, 6, 7 and 8) and concentrations on an order of magnitude less than the concentration of *Brigantedinium* spp. in both cores (Figure 3 and 5). On average, the most abundant are *Echinidinium* spp., *Dubridinium* spp., *E.* cf. *delicatum*, *E. aculeatum*, and other spiny brown cysts (Figures 7 and 8). Autotrophic cysts contribute on average 34.4% of the relative abundance in both cores (Figures 7 and 8). *Operculodinium centrocarpum* sensu Wall and Dale, (1966) is the most common autotrophic species identified in the cores, with an average relative abundance of 25.3% and 24.0% in cores P-10 and P-12, respectively (Figures 7 and 8). Average concentrations of *O. centrocarpum* sensu Wall and Dale, (1966) are 121 cysts g^{-1} in core P-10 (ranges from 77 to 276 cysts g^{-1}) (Figure 3 and 4) and 299 cysts g^{-1} in core P-12 (ranges from 138 to 495 cysts g^{-1}) (Figure 5 and 6). The remaining autotrophic taxa have relative abundances ≤ 5.0% (Figure 4, 5, 7 and 8) and average cyst concentrations approximately one order of magnitude or less than those of *Operculodinium centrocarpum* sensu Wall and Dale, (1966) (Figure 3, 4, 5, 6).

4.3. Dinoflagellate Cysts in Core P-10

Pre-spill (pre-1989) cyst concentrations in core P-10 change from 327 to 518 cysts g^{-1} (Figure 3) with an equal number of cysts produced by heterotrophic and autotrophic dinoflagellates (Figure 7). Concentrations of total heterotrophic cysts range from 165 to 273 cysts g^{-1}, while total autotrophic cyst concentrations range from 162 to 241 cysts g^{-1}

(Figure 3). *Brigantedinium* spp. is the most common heterotrophic taxon with relative abundances between 24.4% and 33.9% (Figure 7), and concentrations between 96 and 126 cysts g^{-1} (Figure 3). *Echinidinium* spp. is also common prior to the spill, with relative abundances between 4.7% and 9.0% (Figure 7), and concentrations varying from 17 to 47 cysts g^{-1} (Figure 3). The remainder of the heterotrophic taxa have relative abundances ≤ 4.0% (Figure 7) and concentrations ≤ 20 cysts g^{-1} (Figure 3). These include *Dubridinium* spp., which has relative abundances ranging from 0.3 to 2.3% (Figure 7) and concentrations changing from 1 to 12 cysts g^{-1} (Figure 3). The most common autotrophic species in this core during this time are *Operculodinium centrocarpum* sensu Wall and Dale, (1966) and *Spiniferites ramosus*. *O. centrocarpum* sensu Wall and Dale, (1966) has a relative abundance ranging from 32.2% to 36.6% (Figure 7), with concentrations changing from 117 to 186 cysts g^{-1} (Figure 3). *S. ramosus* has relative abundances between 4.7% and 6.6% (Figure 7), and concentrations between 16 and 33 cysts g^{-1} (Figure 3). Relative abundances of all other autotrophic taxa are <4.0% (Figure 7), with concentrations ≤ 20 cysts g^{-1} (Figure 3).

From 1989 to 1990, a notable increase in dinoflagellate cyst concentrations is observed and coincides with the Exxon Valdez oil spill and peak remediation. During this time, total cyst concentrations doubled (from 362 cysts g^{-1} in 1988, to 749 cysts g^{-1} in 1990), and this is the highest observed cyst concentration in the section of the core (Figure 3). This increase is three standard deviations greater than the average total cyst concentration of the samples in core P-10. Both heterotrophic and autotrophic dinoflagellates cyst concentrations increased in these samples (UVic 2016-76 – 2016-75), rising from 195 to 402 cysts g^{-1} and 165 to 346 cysts g^{-1} (Figure 3), respectively. The

increase in heterotrophic cysts is mainly driven by an increase in *Brigantedinium* spp., increasing from 123 to 232 cysts g^{-1} (Figure 3). *Echinidinium* spp. triples in concentration, from 17 to 51 cysts g^{-1} (Figure 3). This represents the highest concentration of *Echinidinium* spp. during the sample period (Figure 4) and is two standard deviations greater than the mean (Appendix table 3). Although *Dubridinium* spp. does not contribute considerably to the overall increase in total cyst concentrations, this taxon exhibits a fourfold increase from 4 to 20 cysts g^{-1} (Figure 3). This is the highest *Dubridinium* spp. concentration seen in core P-10 (Figure 4) and is three standard deviations greater than the mean *Dubridinium* spp. concentration (Appendix Table 3). *Operculodinium centrocarpum* sensu Wall and Dale, (1966) is the main driver of the increase in autotrophic cyst concentrations, with concentrations roughly doubling from 117 to 276 cysts g^{-1} between 1988 and 1990 (Figure 3), representing the highest peak in the concentration of *O. centrocarpum* sensu Wall and Dale, (1966) (Figure 4). In addition, this peak is roughly three standard deviations greater than the mean (Appendix Table 3). The remaining heterotrophic and autotrophic taxa show a change of fewer than 15 cysts g^{-1} during the timing of the oil spill (Figure 3).

Although an increase in dinoflagellate cyst concentrations is seen between 1989 and 1990, this increase is not reflected in major changes in relative abundances of any of the taxa during the same time period. The H/A ratio remains unchanged between 1988 and 1990 at 1.2 (Figure 5). *Operculodinium centrocarpum* sensu Wall and Dale, (1966) which shows a large increase in cyst concentrations during this time, only displayed a slight increase in relative abundance, from 32.2% in 1988 to 36.8% in 1990 (Figure 7). Although this is the highest relative abundance in core P-10 (Figure 4), it is less than two standard

deviations greater than the mean (Appendix Table 1). *Brigantedinium* spp. showed a decrease from 33.9% to 30.9% (Figure 7). Although this relative abundance lies below the lower quartile range (Figure 4), it is only approximately one standard deviation less than the mean (Appendix Table 1). *Echinidinium* spp. shows a slight increase in relative abundance, from 4.7% to 6.8% (Figure 7). This value lies above the upper quartile (Figure 4) and it is only one standard deviation greater than the mean (Appendix Table 1). *Dubridinium* spp. exhibits an increase from 1.0% to 2.6%, between 1988 and 1990 (Figure 7). This is the highest relative abundance of *Dubridinium* spp. in core P-10 (Figure 4) and it is roughly two standard deviations greater than the mean (Appendix Table 1). The remainder of the taxa show changes ≤1% (Figure 7).

Following the increase in total cyst concentrations, it then declines from 749 cysts g^{-1} around 1990 to 431 cysts g^{-1} by the beginning of 1991 (Figure 3). During this time, cysts of autotrophic dinoflagellates have a considerable decline in concentrations, whereas heterotrophic dinoflagellate cysts have a little decline, thus increasing the H/A ratio to 2.5 (Figure 5). Autotrophic cyst concentrations decrease to a third, with concentrations changing from 346 to 122 cyst g^{-1} (Figure 3). The main contributor to this change is *Operculodinium centrocarpum* sensu Wall and Dale, (1966) which exhibits an 18.9% decrease in relative abundance (from 36.8% to 17.9%) (Figure 7) and an approximate fourfold decrease in concentration from 276 to 77 cysts g^{-1} (Figure 3). *Spiniferites ramosus* concentrations change from 39 to 11 cysts g^{-1} (Figure 3), a noticeable threefold decrease, while its relative abundance decreases from 5.2% to 2.6% (Figure 7). All other cysts of autotrophic dinoflagellates show a change of fewer than 15 cysts g^{-1} (Figure 3). Total concentrations of heterotrophic cysts, on the other hand, show very little change, with

concentration only decreasing from 402 to 309 cysts g^{-1} (Figure 3). Although the concentration of *Brigantedinium* spp. remains unchanged (Figure 3), it does experience an important increase in relative abundance, from 30.9% to 54.1 by 1991 (Figure 7). *Echinidinium* spp. concentrations displayed roughly a fivefold decrease from 51 to 11 cysts g^{-1} (Figure 3), with the relative abundance decreasing from 6.8% to 2.6% (Figure 7). The relative abundance of *Dubridinium* spp. decreases slightly from 2.6 to 2.3% (Figure 7), while its concentration decreases from 20 to 10 cysts g^{-1} (Figure 3). All other heterotrophic cysts exhibit changes in relative abundances ≤ 1% (Figure 7) and changes in cysts concentrations ≤ 15 cysts g^{-1} (Figure 3).

Following 1991, total dinoflagellate cyst concentrations range from 431 to 556 cysts g^{-1} (Figure 3). The cyst assemblages consist primarily of cysts produced by heterotrophic dinoflagellates, with the H/A varying from 1.7 to 2.8 (Figure 7) and total heterotrophic cyst concentrations varying between 285 and 388 cysts g^{-1} (Figure 3). The most abundant heterotrophic taxon continues to be *Brigantedinium* spp., with relative abundances between 38.2% and 49.2% (Figure 7) and concentrations between 176 to 259 cysts g^{-1} (Figure 3). *Echinidinium* spp. contributes between 11 and 30 cysts g^{-1}, except for one sample that has the lowest concentration of 3 cysts g^{-1} (~1994) (Figure 3). *Dubridinium* spp. displays changes in concentrations between 1 and 10 cysts g^{-1} (Figure 3) and relative abundances between 0.3% and 1.3% (Figure 7). The remainder of heterotrophic taxa have relative abundances ≤ 5% (Figure 7) and concentrations ≤ 20 cysts g^{-1} (Figure 3), with the exception of *Echinidinium aculeatum* and *E.* cf. *delicatum* that have cyst concentrations from 7 to 51 cysts g^{-1} and 6 to 25 cysts g^{-1}, respectively (Figure 3). The relative abundance of *E. aculeatum* and *E.* cf. *delicatum* during this time varies between 1.7% to 11.1% and

1.3% to 5.3%, respectively (Figure 7). Cysts produced by autotrophic dinoflagellates now only form approximately a third of the dinoflagellate cyst assemblage (Figure 7), with concentrations changing between 105 and 167 cysts g^{-1} (Figure 3). *Operculodinium centrocarpum* sensu Wall and Dale, (1966) concentrations fluctuate between 77 and 121 cysts g^{-1} (Figure 3) and it is the most abundant autotrophic species with relative abundances between 17.1% and 26.6% (Figure 7). All other autotrophic taxa, with the exception of cysts of *Alexandrium* spp., remain unchanged with relative abundances and concentrations $\leq$ 4.0% (Figure 7) and $\leq$ 20 cysts g^{-1} (Figure 3), respectively. Cysts of *Alexandrium* spp. occasionally have concentrations marginally above this value (maximum of 27 cysts g^{-1}) (Figure 3).

The average species richness (total number of taxa) seen in the samples of core P-10 is 24 taxa, with a minimum of 22 taxa and maximum of 28 taxa (Figure 3). Although species richness has seen to change by a maximum of four species from one sample to another (Figure 3), this is not seen during the timing of the oil spill. Between 1988 and 1990, dinoflagellate species richness only increases by two from 23 to 25 taxa (Figure 3).

4.4. Dinoflagellate Cysts in Core P-12

Two prominent peaks in total dinoflagellate cysts concentrations were observed in core P-12. The first peak occurs between 1983 and 1984, where there is a doubling of total cyst concentrations, from 638 to 1492 cysts g^{-1} (Figure 5). This increase in total cyst concentrations matches the timing of a large 1983 earthquake and the gravity-flow deposit it produced (Figure 2; Kuehl et al., 2017). It could be expected that a debris flow would lead to increase in sediments, causing a decrease in dinoflagellate cyst concentrations.

However, the sediment flow deposits were removed and not included in the dinoflagellate cyst analysis. As such, none of the samples analyzed were affected by an increase in sedimentation. This peak is mainly driven by a tripling in autotrophic cyst concentrations, from 191 to 563 cysts g^{-1} between 1983 and 1984 (UVic 2016-283 and 2016-278; Figure 5). This further increased to 706 cysts g^{-1} by 1985 marking an approximate overall fourfold increase in the total autotrophic cyst concentrations (Figure 5). *Operculodinium centrocarpum* sensu Wall and Dale, (1966) is the main contributor to this increase, with concentrations increasing threefold from 164 cysts g^{-1} in 1983 to 469 cysts g^{-1} in 1985 (Figure 5). *Spiniferites ramosus* also shows a noticeable change in these samples, with concentrations increasing from 5 to up to 104 cysts g^{-1} in 1985 (Figure 5). Cyst concentrations of other *Spiniferites* spp. increase from 5 cysts g^{-1} in 1983 to 55 cysts g^{-1} by 1986 (Figure 5). Heterotrophic cysts exhibit a twofold rise in concentrations, from 445 cysts g^{-1} in 1983 to 921 cysts g^{-1} in 1984 (Figure 5). *Brigantedinium* spp. are the main contributors to this increase, with concentration doubling from 318 cysts g^{-1} to 644 cysts g^{-1} (Figure 5). The other heterotrophic taxa show changes in cyst concentrations $\leq$ 50 cysts g^{-1} (Figure 5).

This first peak is not very noticeable when looking at the relative abundance of the different taxa between 1983 and 1984 (Figure 8). Although there is a decrease in the H/A, from 2.3 in 1983 to 1.1 in 1984 (Figure 8), it is mainly driven by a decrease in the relative abundance of *Brigantedinium* spp., from 49.8% to 30.5% (Figure 8). The relative abundance of *Dubridinium* spp. also decreases from 5.8% to 0.3% (Figure 8), while the relative abundance of *Spiniferites* spp. increases from 0.3% to 7.1% (Figure 8). *Operculodinium centrocarpum* sensu Wall and Dale, (1966) also shows a slight increase

in relative abundance, from 25.7% to 33.0% (Figure 8). The remainder of taxa display changes in relative abundance ≤ 3% (Figure 8).

Between 1986 and 1988, the total cyst concentrations decline and range only from 986 to 1175 cysts g^{-1} (Figure 5). Cysts of heterotrophic dinoflagellates continue to be slightly more abundant than those produced by autotrophic dinoflagellates, with an H/A between 1.3 and 2.3 (Figure 8). Heterotrophic cyst concentrations, which range from 573 and 677 cysts g^{-1} (Figure 5), are dominated by *Brigantedinium* spp. During this time period the relative abundance of *Brigantedinium* spp. ranges from 35.3% to 45.9% (Figure 8), with concentrations changing between 374 to 452 cysts g^{-1} (Figure 5). *Echinidinium* spp. are also common during this time, with a relative abundance and concentration ranging from 4.4% to 9.8% (Figure 8) and 39 to 96 cysts g^{-1} (Figure 5), respectively. *Dubridinium* spp. has a relative abundance that fluctuates between 0.9% and 7.1% (Figure 8), while concentrations fluctuate between 9 and 61 cysts g^{-1} (Figure 5). The remainder of the heterotrophic taxa have relative abundances ≤ 5% (Figure 8) and contribute ≤50 cysts g^{-1} from 1986 to 1988 (Figure 5). Autotrophic cysts have concentrations slightly lower than those produced by heterotrophic dinoflagellates, with concentrations changing from 289 to 505 cysts g^{-1} (Figure 5). *Operculodinium centrocarpum* sensu Wall and Dale, (1966) continues to be the most common autotrophic species, with a relative abundance from 22.8% to 23.7% (Figure 8) and concentrations between 205 and 268 cysts g^{-1} (Figure 5). *Spiniferites ramosus* has a relative abundance from 2.4% to 6.9% (Figure 8) and concentrations changing from 23 to 81 cysts g^{-1} (Figure 5), while other *Spiniferites* spp. has a relative abundance of 1.5% to 4.5% (Figure 8) and concentrations varying from 15 and 53 cysts g^{-1} (Figure 5). Cysts of *Alexandrium* spp. and cysts of *Pentapharsodinium*

dalei are in low relative abundance, from 1.8% to 5% and 1% to 3.7%, respectively (Figure 8). The concentrations are also low, from 18 to 59 cysts g^{-1} for cysts of *Alexandrium* spp. and 9 to 44 cysts g^{-1} for cysts of *Pentapharsodinium dalei* (Figure 5).

An increase in the total cyst concentrations occurs at ~1989 (UVic 2016-273 and 2016-271), which coincides with the timing of the Exxon Valdez oil spill. Total cyst concentrations increase by two standard deviations, from 1175 (~1988) to 1771 cysts g^{-1} (~1990), reaching the maximum value for the record (Figure 5). Both cysts of heterotrophic and autotrophic dinoflagellates show noticeable increases in concentrations. Heterotrophic cyst concentrations increase by approximately two, from 670 to 1064 cysts g^{-1}, while autotrophic cysts increase from 505 to 697 cysts g^{-1} (Figure 5). Although most of the taxa do not show noticeable changes in cyst concentrations, there are a few that do. *Operculodinium centrocarpum* sensu Wall and Dale, (1966) exhibits an increase in concentration from 268 to 495 cysts g^{-1}, and it remains abundant (~470 cysts g^{-1}) until 1991 (Figure 5). This represents the highest peak in the concentrations of *O. centrocarpum* sensu Wall and Dale, (1966) (Figure 6), and it is almost two standard deviations greater than the mean (Appendix Table 4). *Brigantedinium* spp., the most abundant species during this time, has concentrations that change only between 490 and 624 cysts g^{-1} (Figure 5). The concentration of *Brigantedinium* spp. lie within the lower (UVic 16-272) and upper (UVic 16-270) quartile, as well as just above the upper quartile (UVic 16-271; Figure 6). There are three heterotrophic taxa that exhibit noticeable increases in concentrations with the remainder showing very little change. *Dubridinium* spp. becomes sevenfold more abundant from 16 cysts g^{-1} in 1988 to 110 cysts g^{-1} in 1990, and its values remain elevated until 1991 (~80 cysts g^{-1}) (Figure 5). This marks the highest concentration of *Dubridinium* spp. during

the sample period of core P-12 (Figure 6) and it is approximately three standard deviations greater than the mean (Appendix Table 4). *Echinidinium* cf. *delicatum* exhibits a fourfold increase in cyst concentration during the oil spill interval, from 19 to 73 cysts g^{-1}. This is the highest concentration of *E.* cf. *delicatum* in core P-12 (Figure 6), which is two standard deviations greater than its mean concentration (Appendix Table 4). The spiny brown cysts taxon increases from 28 to 69 cysts g^{-1} between 1988 and 1990 (Figure 5), the highest concentration of spiny brown cysts in core P-12 (Figure 6), the concentration of which is two standard deviations greater than its mean (Appendix Table 4). The concentration of spiny brown cysts remains high (~60 cysts g^{-1}) until 1991 (Figure 5).

The relative abundances of the different taxa do not appear to change considerably during the timing of the oil spill. Between 1989 and 1991, the H/A remains stable between 1.4 and 1.5. The most abundant autotrophic species during this time is *Operculodinium centrocarpum* sensu Wall and Dale, (1966), which increases from 22.8% to 30.7% in 1989, remaining elevated (~30%) until the start of 1991 (Figure 8), representing relative abundances above the upper quartile range (Figure 6). *Brigantedinium* spp., the most abundant taxa, does not change, with relative abundances remaining between 35.2% and 37.2% during the timing of the event (Figure 8). These relative abundances are in or below the lower quartile (Figure 6). *Dubridinium* spp. shows an increase in relative abundance, from 1.3% in 1988 to 6.2% around 1990 (Figure 8). This represents the highest relative abundance of *Dubridinium* spp. in core P-12 (Figure 6), and it is approximately two standard deviations greater than its average relative abundance (Appendix Table 3). The remaining taxa show changes in relative abundance ≤ 3.0% between 1988 and 1991 (Figure 8)

Following 1991, the total cyst concentrations range from 784 to 1414 cysts g^{-1}, averaging at ~1154 cysts g^{-1} (Figure 5). Cysts produced by heterotrophic dinoflagellates contribute ~70% to the cyst assemblages between 1991 and 2000, whereas those produced by autotrophic dinoflagellates constitute ~30% (Figure 8). Heterotrophic cysts, with concentrations ranging from 581 to 1034 cysts g^{-1}, consist mainly of *Brigantedinium* spp. (366 to 755 cysts g^{-1}; Figure 5), which has relative abundances between 37.0% and 47.0% (Figure 8). *Echinidinium* cf. *delicatum* and other spiny brown cysts have concentrations between 0 to 51 cysts g^{-1} and 8 to 40 cysts g^{-1}, respectively (Figure 5). The relative abundance of *E.* cf. *delicatum* is between 0.5% and 1.4%, while that of the other spiny brown cysts is between 0.8% and 3% (Figure 8). *Dubridinium* spp. concentrations are between 7 and 61 cysts g^{-1}, averaging at 32 cysts g^{-1} (Figure 5), with a relative abundance ranging from 0.5% and 4.7% (Figure 8). Cysts produced by autotrophic dinoflagellates change in concentrations from 198 to 503 cysts g^{-1}, and are dominated by *Operculodinium centrocarpum* sensu Wall and Dale, (1966) (141 to 336 cysts g^{-1}; Figure 5), the relative abundance of which is between 16.2% and 25.1% (Figure 8). The relative abundance of cysts of *Alexandrium* spp. ranges from 1.3% to 6.7% (Figure 8), while concentrations range from 16 to 95 cysts g^{-1} (Figure 5) The remainder of the autotrophic taxa have relative abundances $\leq$ 3% (Figure 8) and concentrations $\leq$ 50 cysts g^{-1} between 1991 and 2000 (Figure 5).

Species richness varies throughout core P-12, with the number of taxa ranging from 17 to 28, with an average of 25 taxa (Figure 5). The lowest species richness is found following the 1983 gravity-flow deposit (UVic 2016-283 and 2016-277) when it varies

from 17 to 24 taxa (Figure 5). During the timing of the oil spill the number of taxa only declines from 28 to 27 taxa between 1988 and 1991 (Figure 5).

4.5. Biogenic Silica – Cores P-10 and P-12

Biogenic silica in core P-10 remains constant throughout the core with the values changing from 8.0 to 9.0% (Figure 3). Between 1988 and 1990 (UVic 2016-76 and 2016-75), biogenic silica abundance only increases from 8.0 to 8.5% (Figure 3).

Biogenic silica in core P-12 changes from 9.0% to 10.9%, with the exception of one sample from 1994 (UVic 2016-265) with a value of 12.3% (Figure 5). Following the 1983 gravity flow deposit, biogenic silica increases slightly between 1983 and 1984, from 10.3% to 10.8% and then decreased to 9.4% in 1985 (Figure 5). The sample (UVic 2016-273), just prior to one corresponding to the timing of the oil spill, was lost and therefore no biogenic silica measurement was available for ~1988. The sample just before this (UVic 2016-274) has 9.0% biogenic silica and during the timing of the oil spill, it increases by 0.5% to 1.0% (10.5 and 9.5%) (Figure 5).

The standard deviation for the Saanich Inlet standard is 1.5% and for the Jervis Inlet standard it is 1.3%. Any change seen during the timing of the oil spill in both PWS cores is less than 1 standard deviation of the standards. As such, the changes in biogenic silica seen in the cores and not significant and are most likely analytical noise as this method is not able to differentiate at the fraction of a percent level.

5. Discussion

The two cores from PWS provide dinoflagellate cyst records and total diatom abundance (in the form of biogenic silica) for two sites in the central part of Prince William Sound, Alaska. The records presented cover the period from 1986 to 2000 (core P-10) and 1982 to 2000 (core P-12), providing ample coverage for studying the impact of the 1989 Exxon Valdez oil spill on phytoplankton. One of the greatest challenges when attempting to assess the impact of oil spills on phytoplankton is the lack of baseline data. This constrains the comparison of pre-spill and post-spill phytoplankton concentrations (Ozhan et al., 2014a). By using sedimentary proxies, this study provides a comparison between pre-spill and post-spill dinoflagellate and diatom abundances.

5.1. Dinoflagellate Cyst Preservation

Dinoflagellate cysts have occasionally been shown to have selective preservation issues, especially because of oxidation. These different sensitivities to degradation can introduce a systemic error in the data, adversely affecting the environmental reconstructions (e.g., Dale, 1976; Zonneveld et al., 1997, 2007, 2008). In the PWS study, there is no reason to believe that poor preservation of the selected taxa was an issue. All taxa are well preserved and show very little breakage. *Brigantedinium* spp., cysts of *Protoperidinium* spp., and *Echinidinium* spp., which have been shown to be sensitive to oxidative degeneration (e.g., Dale, 1976; Zonneveld et al., 1997, 2007, 2008), do not exhibit breakage. The high sedimentation rates (P-10 = 0.9 cm year^{-1}; P-12 = 1.2 cm year^{-1}) observed in the cores limited the time that the cysts were in contact with oxygenated bottom waters.

5.2. Count Comparison Between Two Analysts

The comparison between the five samples counted by two analysts provides insight into inter-observer variability. Although the variability in this study includes both inter-observer and inter-slide variability, the latter is assumed to be negligible. Therefore, this discussion focuses on the inter-observer variability.

There are few published studies that investigate inter-observer variability in phytoplankton assemblages, although they focus on diatoms and not on dinoflagellates (Kahlert et al., 2010; Lavoie and Campeau, 2016). The inter-observer variability seen in our study are comparable, if not substantially better than what has been documented in the studies by Kahlert et al. (2012) and Lavoie and Campeau (2016). Using Bray-Curtis similarities, values found in our study range from 72 to 87%. In Kahlert et al. (2012) the Bray-Curtis similarities were in many cases < 60%, while in Lavoie and Campeau (2016), most were between 70 and 85%, although some were between 60 and 70%.

It is important to understand the potential sources of inter-observer variability in this study. Most of the variability in other studies has been explained by differences in identification of taxa (Kahlert et al., 2012; Lavoie and Campeau, 2016). In these studies, the difference in the number of taxa identified differed by as much as 55 taxa (Kahlert et al., 2012; Lavoie and Campeau, 2016). In our study, the maximum number of taxa differs by no more than three.

The main source of variability between the results obtained by analyst #1 and analyst #2 can be attributed to differences in cyst identification skills. For example, one analyst (analyst #2) identifies spiny brown cysts or *Spiniferites* to the species level, whereas the other analyst (analyst #1) tends to group them. For example, the counts for spiny brown

cyst and *Spiniferites* spp. are much higher by analyst #1 (Table 2). Another source of variability can be the counts of rare taxa when only a few specimens were observed. For example, *Islandinium minutum* was only identified in one sample by analyst #1 but was identified in four of the five samples by analyst #2. Overall, this highlights the importance of counting 300 cysts per sample, which has been shown to produce more accurate counts (e.g., Mertens et al., 2009). This is one of the most standard recommendations in palynology (e.g., Mertens et al., 2009).

5.3. Eutrophication Signal

Dinoflagellate cysts have been used to study eutrophication, the signal of which resembles the variations seen in this study (e.g., Matsuoka, 1999; Pospelova et al., 2004, 2005; Dale, 2009; Ellegaard et al., 2017). Since the signal of eutrophication, as seen through the dinoflagellate cyst record, can vary from one location to another, it is important to compare our results to the most similar environments for which nutrient versus dinoflagellate concentrations have been made.

Large fluctuations in total dinoflagellate cyst concentrations have been associated with a high nutrient loading (eutrophication) and toxic pollution in estuaries (e.g., Pospelova et al., 2002, 2005). However, when nutrients are plentiful and toxic pollutants are minimal, dinoflagellate cyst concentrations are steadily high. For example, near sewage outfalls in Victoria (BC, Canada) total cyst concentrations are five times higher than those in the surrounding waters (Krepakevich and Pospelova, 2010). Similar high cyst concentrations have also been observed in coastal upwelling regions (e.g., Dale 1996; Pospelova et al., 2008, Zonneveld et al., 2013). During the temporal span of the oil spill,

an increase in the total cyst concentrations was observed in both cores, with concentrations reaching their maximum value for the entire studied record, values that were roughly three (core P-10) and two (core P-12) standard deviations greater than the mean. However, the amplitude of this increase, two-fold in core P-10 and by 50% (from 1175 to 1771 cysts g^{-1}) in core P-12, is much smaller than is typically associated with the eutrophication signal, an indication that there may have been only a small effect on cyst-producing dinoflagellates.

Sedimentary records of dinoflagellate cysts from several coastal areas and estuaries affected by anthropogenic nutrient enrichment exhibit higher proportions of cysts produced by heterotrophic dinoflagellates and are often marked by increases in the abundances of cysts of *Polykrikos kofoidii* and *P. schwartzii*, as well as *Dubridinium* species (e.g., Matsuoka, 1999; Pospelova et al., 2002, 2005; Pospelova and Kim, 2010; Ellegaard et al., 2017). Although the two PWS cores do not show increases in *P. kofoidii* and *P. schwartzii* in sediments deposited in the 1989-90 period, they do exhibit noticeable increases in *Dubridinium* spp. (Figure 4 and 6), with concentrations of *Dubridinium* spp. during this time being three standard deviations greater than the average (Appendix Table 3 and 4). *Dubridinium* spp. are produced by marine dinoflagellates belonging to the Diplopsalid group. These species have a more varied diet, which consists mainly of diatoms and other types of phytoplankton such as flagellates (Jacobson and Anderson, 1986; Jeong, 1999). Increases in heterotrophic dinoflagellates are generally related to increases in their prey (e.g., Hansen, 1991; Landry et al., 2000), and they can therefore help understand how their prey are responding during this time. This interpretation can be further narrowed by looking at the *Brigantedinium* spp. Although there is some increase in the concentration of

Brigantedinium spp. during the timing of the oil spill in the cores, this increase lies within the natural variability of the system (Figures 3, 4, 5 and 6). These species feed primarily on diatoms (e.g., Wall et al., 1977; Zonneveld et al., 2001; Dale et al., 2002, Pospelova et al., 2006, 2008), and therefore this suggests that there was no abnormal change in diatom abundance during the timing of the Exxon Valdez oil spill. In support of this statement, the biogenic silica values (Figures 3 and 5) show little variation in the studied sections of both cores, suggesting that diatom abundance remains relatively unchanged during that time, including the oil spill. Although there are other types of siliceous material that can contribute to biogenic silica (e.g., sponges, silicoflagellates), diatoms are typically the most abundant group of siliceous phytoplankton in estuarine and coastal waters, making biogenic silica a common proxy for diatom abundance (e.g., Nelson et al., 1995; Ragueneau et al., 2000). This was also confirmed through the analysis of smear-slides of our samples that diatoms were, in fact, the dominant group of siliceous microfossils.

Bacteria are known to play an important role in the degradation of oil in the natural environment (e.g., Kostka et al., 2011; Santisi et al., 2015). A wide variety of marine bacteria degrade crude oil by oxidizing its different components (e.g., alkenes, alkanes, aromatics) and converting them into energy, cell mass as well as biological waste products (e.g., Santisi et al., 2015). This degradation of oil in the natural environment involves a succession of different species, as each species can metabolize only a limited range of hydrocarbon substrates (e.g., Santisi et al., 2015). The degradation of oil by bacteria is typically limited by the availability of nitrogen and phosphorus in marine systems (e.g., Yakimov et al., 1998; Kasai et al., 2002a, b). As such, it is a common bioremediation practice to stimulate the growth of oil-degrading bacteria by adding nutrients to the system.

During the oil spill, bioremediation involving the addition of ~50,000 kg of nitrogen and 5,000 kg of phosphorus was done during the summers of 1989 to 1992 in order to stimulate bacterial growth (Bragg et al., 1994). The nitrogen and phosphorous was added to the Sound in the form of an oleophilic liquid fertilizer named Inipol EAP 22 (7.4% N, 7% P) and a slow-release granulated fertilizer named Customblen (28% N, 3.5% P) (Bragg et al., 1994). This addition of nutrients could lead to an increase in heterotrophic dinoflagellate cyst concentrations and could therefore be responsible for the increase seen during the timing of the oil spill. However, this does not appear to be the case as diatom abundance remained unchanged during this time. In coastal regions, where dissolved silica is not limiting, diatoms are typically the first phytoplankton group to prosper from a nutrient enrichment (e.g., Matsuoka, 1999). Therefore, the absence of any noticeable increases in diatom abundance makes it unlikely that the addition of nutrients had a direct positive effect on dinoflagellate cyst concentrations.

Our results imply that the increase in *Dubridinium* spp. concentrations cannot be explained by increases in diatom abundances (BioSi%) during the timing of the oil spill. However, increases in *Dubridinium* spp. could be explained by increases in flagellate abundance, another very common prey of *Dubridinium* spp. (Jacobson and Anderson, 1986; Jeong, 1999). Flagellates are a diverse group of unicellular organisms which possess a flagellum. Although there is no direct measurement of flagellate abundances in our study, this could explain why the abundance of *Dubridinium* spp. increased. This increase in flagellate concentrations is also supported by other research, mainly in macrocosms, that have found that flagellate abundance increased following exposure to oil and increased nutrients (e.g., Gertler et al., 2010; Jung et al., 2012). The explanation for this is that many

flagellates graze on bacteria, which have been shown to thrive in oil-rich aquatic environments (e.g., Hazen et al., 2010; Edwards et al., 2011; Ziervogel et al., 2012). As such, it is possible that the addition of nutrients, which was done to promote the growth of oil-degrading bacteria (Bragg et al., 1994), led to an increase in *Dubridinium* spp. concentrations by increasing the concentrations of their prey. The increase in *Dubridinium* spp. follows similar trends to the addition of nutrients during the bioremediation. Although the bioremediation continued into 1991, by which point concentration had already decreased to pre-spill levels, the amount of nutrients added in 1991 (3.18 tonnes of N) was drastically less than in 1989 (23.33 tonnes of N) and 1990 (22.06 tonnes of N) (Prince and Bragg, 2008). This could explain why *Dubridinium* spp. concentrations had decreased by 1991.

Operculodinium centrocarpum sensu Wall and Dale, (1966) is also a species that showed a noticeable increase during the time of the oil spill (Figures 3, 4, 5 and 6). The concentration of this species during the timing of the oil spill was three and two standard deviations greater than their respective mean in core P-10 and P-12, respectively (Appendix Table 3 and 4). *O. centrocarpum* sensu Wall and Dale, (1966) is a cosmopolitan and opportunistic species able to tolerate a wide range of temperatures and salinities, and as such it is found from the tropics to the poles (e.g., Zonneveld et al, 2013). Opportunistic species are adapted to rapidly exploit newly opened habitats or resources, typically found in environments with high physiological stress (e.g., Levinton, 1970). The increase in *O. centrocarpum* sensu Wall and Dale, (1966) during the timing of the oil spill suggests that the spill and its bioremediation added stress to the environment, opening new niches for this species to exploit.

There has been little research on how oil spills affect phytoplankton (Ozhan et al., 2014b). However, studies following the 2010 Deepwater Horizon oil spill (DHOS) in the Gulf of Mexico (GOM) observed similar trends to those see seen in this study (e.g., Hu et al., 2011; Ozhan et al., 2014b). Although no in-depth work was done on how dinoflagellates were affected, fluorescence line height data from the GOM show increased concentrations of chlorophyll following the spill (Hu et al., 2011). The mechanism by which oil promotes phytoplankton growth is poorly understood, but it is known that a close relationship between bacteria and phytoplankton exists (e.g., McGenity et al., 2012; Amin et al., 2015). It is thought that when exposed to hydrocarbons, phytoplankton can provide bacteria with oxygen, dissolved and volatile organic matter, as well as extracellular polymeric substances. The bacteria than in turn can provide phytoplankton with CO_2, exopolysaccharides, vitamins, nutrients, enzymes and iron (e.g., McGenity et al., 2012).

5.4. Variations in the Heterotrophic to Autotrophic Ratio (H/A)

In general, the ratio of heterotrophic to autotrophic (H/A) dinoflagellate cysts has been seen to be high in high primary productivity regions and to increase as a result of increased coastal upwelling (e.g., Dale, 1996; Pospelova et al., 2008; Bringué et al., 2013). The H/A is commonly used as a proxy for nutrient availability and coastal proximity (e.g. Dale 1996, Ellegaard et al., 2017; de Vernal et al., 2001).

Before assessing the changes in H/A in cores P-10 and P-12, it is important to understand the differences between relative abundance and concentrations of dinoflagellate cysts. The main limitation of relative abundances is that it reflects proportions of dinoflagellate cysts and how common or rare a taxon is relative to other taxa in the

assemblages. Because of this, cysts concentrations are preferred as these values do provide absolute abundances of dinoflagellate cysts. However, dinoflagellate cyst concentrations can be affected by differences in sedimentation rates and physical properties of sediments. Thus, cyst sedimentary concentrations should be used in settings where sediment types (lithology) do not show much variation and sedimentations rates arecomparable and well known. As previously discussed, the sedimentation rates for cores P-10 and P-12 are well known and do not show much variability over time. Therefore, dinoflagellate cyst concentrations are the preferred measurement for this study.

The changes in H/A ratio seen in cores P-10 and P-12 are almost all driven by changes in the cyst concentrations of *Operculodinium centrocarpum* sensu Wall and Dale, (1966), while cyst concentrations of heterotrophic taxa exhibit little change. An example of this can be seen shortly after the oil spill when cores P-10 and P-12 exhibit the largest increase in H/A during the sample period. The H/A in core P-10 increases from 1.2 to 2.5 between ~1990 and ~1991, whereas in core P-12 it increases from 1.5 to 2.8 between ~1990 and ~1993. During this time, heterotrophic cyst concentrations decrease from 402 to 309 cysts g^{-1} and from 912 to 627 cysts g^{-1} in cores P-10 and P-12, respectively. Meanwhile, autotrophic cyst concentrations show a much greater change, with cyst concentrations decreasing from 346 to 122 cysts g^{-1} in core P-10 and from 609 to 221 cysts g^{-1} in core P-12. *Operculodinium centrocarpum* sensu Wall and Dale, (1966) is the main driver of this decrease, with concentrations decreasing by ~200 cysts g^{-1} in core P-10 and ~330 cysts g^{-1} in core P-12. This species accounts for ~89% (core P-10) and 85% (core P-12) of the decrease in the concentrations of autotrophic dinoflagellate cysts, suggesting that *Operculodinium centrocarpum* is the main driver of the observed change in H/A.

5.5. Recovery Time

One of the main objectives of this research was to determine a timeframe for the recovery of phytoplankton following the 1989 Exxon Valdez oil spill. The results show that by 1991, total cyst concentrations for *Dubridinium* spp. and *O. centrocarpum* sensu Wall and Dale, (1966) had returned to the pre-spill values in both cores. This suggests that the impact of the oil spill was short-lived and that dinoflagellate communities appeared to recover within the first two years after the oil spill. Although no other work has been done in PWS, this two year recovery period is similar to those found by studies monitoring phytoplankton recovery after the 2010 Deepwater Horizon oil spill (e.g., Hu et al., 2011; Ozhan et al., 2014a). These studies have shown that phytoplankton biomass, measured by MODIS fluorescence line height, increased following the DHOS and then returned to pre-spill conditions within a year of the spill (e.g., Hu et al., 2011; Ozhan et al., 2014a). The apparently longer recovery time of the Exxon Valdez oil spill might be explained by its location. When compared to the GOM (e.g., Sturges et al., 2013), ocean circulation is much more limited in PWS (e.g., Niebauer et al., 1994) and therefore the oil may not have been dispersed as quickly as in the GOM.

It is important to note that this research was unable to differentiate between the effects of the oil itself versus the effects of the bioremediation of the spill. Althoug, it was suggested that nutrient input from the bioremediation did not directly affect cyst concentrations and diatom abundances, it promoted bacterial growth, which in turn may have promoted flagellate growth and consequently *Dubridinium* spp. However, other tactics were also undertaken to try and remediate the spill. Most notably was the use of Corexit 9527, a type of dispersant, which was applied to PWS (Shigenaka, 2014). Although

the exact chemical composition of this dispersant is proprietary, it does contain 30-60% 2-Butoxyethanol, 10-30% organic sulfonic acid salt and 1-5% propylene glycol (NALCO, 2008). These dispersants have been shown to be even more toxic to phytoplankton than the crude oil itself (e.g., Hook and Osborn, 2012; Gar et al., 2014). For example, it was found that crude oil mixed with dispersants inhibited cell division and motility in *Isochrysis galbana* (haptophytes species) and *Chaetoceros* spp. (diatom genus), while the same species were unaffected when only exposed to crude oil (e.g., Gar et al., 2014). However, the impact of the dispersant on phytoplankton was most likely short-lived as its application was stopped after just three weeks (March 24th to April 13th) (Shigenaka, 2014).

5.6. Turbidite Signal

Core P-12 provides the opportunity to assess the impact of the 1983 earthquake which caused the gravity deposit seen in the cores. Similar to the oil spill response, the changes seen following the 1983 earthquake may be indicative of nutrient enrichment. The natural variability of the system can be defined as the maximum and minimum total cyst concentrations throughout the core without including the values during the timing of the turbidite deposit and the oil spill. As such, the natural variability of the system, in terms of dinoflagellate cyst concentrations, is between 327 and 556 cysts g^{-1} in core P-10 and between 784 and 1414 cysts g^{-1} in core P-12. The total cyst concentrations associated with the earthquake event is outside the range of natural variation but only slightly so, suggesting that the nutrient input was not higher than during times without disturbance. The absence of any noticeable increase in *Polykrikos kofoidii* and *P. schwartzii*, or *Dubridinium* spp., further suggests that nutrient input did not change during this time

period as these taxa have been shown to be good indicators of eutrophication (e.g., Matsuoka, 1999; Pospelova et al., 2002, 2005; Dale, 2009; Ellegaard et al., 2017). Much of the increase in the total cyst concentrations following the earthquake is primarily driven by an increase in *Operculodinium centrocarpum* sensu Wall and Dale, (1966) and to a lesser degree by *Spiniferites ramosus* and *Spiniferites* spp. The increase in *O. centrocarpum* sensu Wall and Dale, (1966), from 164 (~1983) to 469 cysts g^{-1} (~1985) suggests that there is instability in the system following the earthquake. *Spiniferites ramosus* and *Spiniferites* spp. increased from 5 to 104 cysts g^{-1} (between 1983 and 1985) and 5 to 55 cysts g^{-1} (between 1983 and 1986) in cores P-10 and P-12, respectively (Figures 3 and 5). Spiniferites may be an indicator of instability in an estuarine system (e.g., eutrophication) (Pospelova et al., 2002; 2005), however the increases seen in PWS are only marginally higher than the ranges of these cyst concentrations through the studied sections of the core (*S. ramosus*: 11 to 81 cysts g^{-1}; *Spiniferites* spp.: 0 to 53 cysts g^{-1}). It is important to note that these observations are only drawn from one core (P-12) and were therefore not reported in other parts of PWS. Dinoflagellate cyst counts and biogenic silica analysis only date back to 1986 in core P-10 and there is therefore no data during the timing of the 1983 earthquake for this core.

5.7. PWS Cyst Assemblage Comparison with Other Locations in the Northern and Eastern Pacific Ocean

The dinoflagellate cyst assemblages in PWS are characterized by very low numbers of open water taxa, a dominance of *Brigantedinium* spp. and other cysts of the Protoperidiniaceae, as well as by high proportions of *Operculodinium centrocarpum* sensu

Wall and Dale, (1966). In general, PWS assemblages are similar to what has previously been observed in coastal and estuarine systems of the northeastern Pacific (e.g., Radi and de Vernal, 2004; Pospelova et al., 2008), including the Strait of Georgia (SOG) (Radi et al., 2007; Pospelova et al., 2010) and southern Vancouver Island (VI) (Krepakevich and Pospelova, 2010), British Columbia, Canada. For the most part, the assemblage of PWS and the northeastern Pacific (e.g Radi and de Vernal, 2004; Pospelova et al., 2008) are comparable to those from coastal zones of the eastern and western North Atlantic (e.g., Harland et al., 2004; Pospelova et al., 2005), although important differences do exist. Most notably is the presence of *Echinidinium* species, which are less common in the North Atlantic (e.g., Bonnet et al., 2013; Zonneveld et al., 2013). In addition, *Selenopemphix undulata*, a species observed in PWS, appears to be endemic to the Pacific Ocean (Verleye et al., 2011). Finally, warm water species, *Bitectatodinium spongium*, *Tuberculodinium vancampoae,* and *Lingulodinium machaerophorum* were not identified in PWS (e.g., Pospelova et al., 2008; Zonneveld et al., 2013).

The dinoflagellate cyst assemblages in PWS are similar to the assemblages reported from surface sediment samples along the western coast of the Gulf of Alaska with respect to the relative abundance of the most abundant taxa. Both of the assemblages in PWS and along the western coast of the GOA are dominated by *Brigantedinium* spp. with relative abundances ranging from 24 to 57% and 25 to 70%, respectively. *Operculodinium centrocarpum* sensu Wall and Dale, (1966) also shows comparable abundances between the two areas, with relative abundances from 16 to 37% in PWS and from 15 to 25% along the western coast of the GOA. Other taxa in PWS include cysts of *Pentapharsodinium dalei* (0-5%), *Spiniferites ramosus* (1-7%), *Spiniferites elongatus* (0-1.5%), *Spiniferites*

spp. (0-4%) and *Nematosphaeropsis labyrinthus* (0-17%) (Radi and de Vernal, 2004). *N. labyrinthus* in core P-10 and P-12 are occasionally present, however, never reaching a relative abundance > 1%. This is not surprising as this species is most commonly found in open ocean environments that are characterized by low primary productivity and nutrient concentrations (e.g., Dale, 1996; Rochon et al., 1999; Pospelova et al., 2008). Many of the taxa identified in cores P-10 and P-12 have never been reported within the GOA (Radi and de Vernal, 2004), including cysts of *Archaeperidinium* cf. *saanichi*, cysts of *Archaeperidinium* cf. *minutum*, *Dubridinium* spp., *E. delicatum*, *E.* cf *delicatum*, *Islandinium* cf. *brevispinosum*, cysts of *Protoperidinium americanum* and cysts of *Protoperidinium fukuyoi*. Some of these taxa have only recently been described and this may explain why they were not identified in samples from the GOA as these were counted as "spiny brown cysts" in Radi and de Vernal (2004). In Radi and de Vernal, (2004), undescribed taxa at the time included cysts of *Archaeperidinium* cf. *saanichi* (Mertens et al., 2012a), cysts of *Archaeperidinium* cf. *minutum* (Yamaguchi et al., 2011) and cysts of *Protoperidinium fukuyoi* (Mertens et al., 2013). The lack of studies from estuaries of the GOA might also explain why many of these taxa had not been identified in this region until now.

The assemblages of PWS are comparable, in terms of species richness and assemblage composition, to those reported in the SOG and surrounding areas (Radi et al., 2007; Pospelova et al., 2010; Price and Pospelova, 2011). Similar to PWS, the SOG and southern VI have a high species diversity, with a total of 30 to 36 taxa identified (Radi et al., 2007; Pospelova et al., 2010; Krepakevich and Pospelova, 2010). Similar to PWS, the

dinoflagellate cyst assemblages from the SOG and southern VI are dominated by *Brigantedinium* spp. and other cysts of Protoperidiniaceae, as well as by *Operculodinium centrocarpum* sensu Wall and Dale, (1966) (Radi et al., 2007; Pospelova et al., 2010). One important difference between the assemblage of PWS and that of the SOG is the relative abundance of *Quinquecuspis concreta*, which is much higher in the SOG (0 - 30%; Radi et al., 2007; Pospelova et al., 2010). This could be related to the abundance of diatoms, fluxes of which have been shown to correlate with that of *Q. concreta* in the SOG (Pospelova et al., 2010).

When comparing the cyst assembles from PWS to glacial fjords along the western coast of North America, the species composition is similar, however, the relative abundances of the taxa do vary (Kumar and Patterson, 2001; Radi et al., 2007; Bringue et al., 2016). This can be explained by the differences in estuarine settings.

Finally, dinoflagellate cyst concentrations observed in the SOG are most comparable to those of PWS, which had an average concentration of 1200 and 750 cysts g^{-1} in cores P-10 and P-12, respectively. Near the Fraser River delta concentrations are on average ~1800 cysts g^{-1} (Radi et al., 2007), which is comparable to those seen in PWS. However, further from the Fraser River total dinoflagellate cyst concentration increases reaching a maximum of 13,000 cysts g^{-1} (Radi et., 2007) and even higher in Saanich Inlet (Price and Pospelova, 2011). Dinoflagellate cyst concentrations along southern VI are similar to those seen in PWS, with concentrations ranging from 500 to 5,000 cysts g^{-1}. The concentrations seen in PWS, the SOG and southern VI are comparable to those seen in other European (e.g., Dale el at., 1999; Harland et al., 2004a,b) and North American estuaries (e.g., Pospelova et al., 2004, 2005; Price et al., 2016). However, these values are

low in comparison to values for Effingham and Seymour–Belize inlets, which are higher than 25,000 cysts g^{-1} (Radi et al., 2007; Bringue et al., 2016).

5.8. Large Scale Climate Variability

Changes in dinoflagellate cyst abundances have been shown to reflect climate variability, including ENSO and PDO in the temperate northeastern Pacific (e.g., Pospelova et al., 2010; Bringué et al., 2014). It is therefore important to understand if the PWS was subjected to these climatic phenomena and whether such features influenced the dinoflagellate cyst record. With respect to climatic variation, the large-scale linkage between the ocean and the atmosphere in the North Pacific is well established, but how this relates to the coastal zone along the GOA is not yet known (Stabeno et al., 2004). The reason for this is mainly attributed to the mountainous coastline of Alaska, which influences along-shore winds (e.g., Royer et al, 1990; Stabeno et al., 2004). This effect in turn forces cross-shelf Ekman transport and precipitation, thus affecting the upper ocean's baroclinicity (e.g., Royer et al., 1990; Stabeno et al., 2004). As such, the relationship of these climatic phenomena to dinoflagellate populations and communities is unknown in PWS. However, considering that PWS is located at 60ºN it is unlikely that ENSO has large effects on the Sound (e.g., Lluch-Cota et al., 2001).

The studied sections of the cores span from 1986 to 2000 in core P-10 and 1982 to 2000 in core P-12. This timeframe covers a number of El Niño (1983, 1987, 1988, 1992, 1995, 1998; NOAA) and La Niña (1989, 1999, 2000; NOAA) events in the tropics and mid-latitudes. There is a strong La Niña event between 1988 and 1989, which coincides with the timing of the peak in cyst concentrations. However, other such events do not seem

to manifest themselves in the samples. For example, sediments deposited during the 1997-1998 El Niño, which prior to the 2016 event was regarded as the strongest on record (e.g., Lynn et al., 1998), or the moderately strong 1998-2000 La Niña event (e.g., Shabbar and Yu, 2009), showed very little changes in dinoflagellate cyst concentrations and biogenic silica content. During the 1997-1998 El Niño, total cyst concentrations fluctuate between 455 and 528 cysts g^{-1} (core P-10; Figure 3) and between 784 and 1341 cysts g^{-1} (core P-12; Figure 5), with no cyst taxa showing noticeable changes in concentrations. Biogenic silica also remains relatively unchanged, with values between 8.5 and 8.6% in core P-10 (Figure 3) and 9.9 to 10.5% in core P-12 (Figure 5). Similarly, during the 1998-2000 La Niña event, total cyst concentrations do not exhibit a noticeable change, with concentrations between 528 and 445 cysts g^{-1} (core P-10) (Figure 3) and 874 to 1341 cysts g^{-1} (core P-12) (Figure 5). In addition, individual dinoflagellate cyst taxa do not show any visible changes in concentrations or assemblage composition. Although there are no biogenic silica measurements from P-10 during this time (Figure 3), the values in core P-12 are between 10.0 and 10.8% (Figure 5). Thus, there is no evidence in the sedimentary record that shows that ENSO influenced the dinoflagellate cyst assemblage concentrations or diatom abundances (biogenic silica) in the interval of the study.

The PDO is believed to be related to wind, temperature, precipitation and oceanographic patterns in the Gulf of Alaska (e.g., Stabeno et al., 2004; Mundy, 2005; Harwell et al., 2010). However, how PDO affects the coastal and estuarine systems along the GOA is not very well understood (e.g., Stabeno et al., 2004) and it is therefore possible that the PDO is having an influence on PWS. Although changes in dinoflagellate cyst concentrations and fluxes in the Santa Barbara Basin (Bringué et al., 2014), Effingham

Inlet (Bringué et al., 2016), and the Beaufort Sea (Durantou et al., 2012) were linked to the PDO, it cannot be used to explain the peaks in concentrations observed in the PWS cores during the timing of the oil spill. The abrupt changes seen in both cores ~1989 occur over a very small time interval (1-2 years). The time frame for the distinct phases of the PDO is much larger, with the average duration of a regime lasting 23 years, and therefore cannot account for the changes seen during the timing of the oil spill. Furthermore, a positive PDO (warm) phase lasted between 1977 to at least the mid-1990's (e.g., Mantua and Hare, 1990), further supporting that the change in concentrations seen during the timing of the oil spill cannot be explained by a shift in the PDO.

6. Conclusion

Understanding the effects that oil spills have on phytoplankton is crucial for our understanding of how these events affect coastal environments. This study is the first to use dinoflagellate remains and biogenic silica to examine how marine primary productivity was affected by the 1989 Exxon Valdez oil spill in Prince William Sound Alaska. These two indicators allowed for the determination of pre-spill, during and post-spill conditions. Dinoflagellate cysts assemblages and biogenic silica were measured every centimeter, for the interval of 1986 to 2000 with an annual to bi-annual resolution. The most noticeable shift in dinoflagellate abundances occurs during the timing of the oil spill, with notable increases in total cyst concentrations, as well as in the abundance of *Operculodinium centrocarpum* Wall and Dale, (1966) and *Dubridinium* spp. This signal is similar to that seen as a result of nutrient enrichment or eutrophication in coastal regions. There was however a major La Niña event between 1988 and 1989 which could explain these changes. Other ENSO events apparently did not manifest themselves in the dinoflagellate cyst and biogenic silica records. As such, it seems that the oil spill and its bioremediation are responsible for the observed changes. Assuming this interpretation, the effect of the spill appears to have been short-lived, with dinoflagellate cyst abundances returning to pre-spill values within two years of the event.

However, there does not appear to be a major shift in the relative abundance of the different taxa during the timing on the oil spill. During this time a majority of the cyst taxa display very little changes in relative abundance. *Dubridinium* spp. did exhibited a 1.6% (core P-10) and 4.3% (Core P-12) increase in relative abundance.

Diatom abundances, as inferred by biogenic silica content, on the other hand, appear to have been unaffected by the spill. This inference is supported by the lack of change in *Brigantedinium* spp. abundances during the timing of the oil spill. It is also suggested that flagellate concentrations may have increased following the Exxon Valdez oil spill, as this would explain the increase in *Dubridinium* spp. concentrations.

This study provides valuable information on how phytoplankton might respond to an oil spill and shows that dinoflagellate cysts and biogenic silica can be useful tools in studying these events. It is important to apply this methodology to other oil-affected locations, such as the DHOS in the GOM. Although this research does show that some dinoflagellate cyst taxa were impacted by the spill, it does not account for all dinoflagellate species in the water column. Furthermore, there remains an absence of knowledge on how individual species in other groups of phytoplankton, such as diatoms and flagellates, have responded to the Exxon Valdez oil spill. Regardless, there is a need for continuous monitoring of areas that are at high risk of oil spills so that when such events do happen the impacts of spills on phytoplankton can be properly assessed.

Bibliography

Amin, S.A., Hmelo, L.R., van Tol, H.M., Durham, B.P., Carlson, L.T., Heal, K.R., Morales, R.L., Berthiaume, C.T., Parker, M.S., Djunaedi, B., Ingalls, A.E., Parsek, M.R., Moran, M.A., Armbrust, E. V., 2015. Interaction and signalling between a cosmopolitan phytoplankton and associated bacteria. Nature 522, 98–101. doi:10.1038/nature14488

Barnston, A.G., Livezey, R.E., 1987. Classification, Seasonality and Persistence of Low-Frequency Atmospheric Circulation Patterns. Mon. Weather Rev. 1083-1126 doi:10.1175/1520-0493(1987)115≤ 1083:CSAPOL>2.0.CO;2

Bonnet, S., De Vernal, A., Henry, M., 2013. Dinoflagellate cyst assemblage distributions as tracers of Pacific v. Atlantic water masses in the Northern Hemisphere, in: Lewis, JM and Marret, F and Bradley, LR (Ed.), BIOLOGICAL AND GEOLOGICAL PERSPECTIVES OF DINOFLAGELLATES, Micropaleaeontological Society Special Publications. Geological Soc Publishing House, Unit 7, Brassmill Enterprice CTR, Brassmill Lane, Bath BA1 3JN, Avon, England, pp. 55–63.

Bragg, J.R., Prince, R.C., Harner, J.E., Atlas, R.M., 1994. Effectiveness of bioremediation for the Exxon Valdez oil spill. Nature 367, 532–8. doi:10.1038/367532a0

Bringué, M., Pospelova, V., Pak, D., 2013. Seasonal production of organic-walled dinoflagellate cysts in an upwelling system: A sediment trap study from the Santa Barbara Basin, California. Mar. Micropaleontol. 100, 34–51. doi:10.1016/j.marmicro.2013.03.007

Bringué, M., Pospelova, V., Field, D.B., 2014. High resolution sedimentary record of dinoflagellate cysts reflects decadal variability and 20th century warming in the Santa Barbara Basin. Quat. Sci. Rev. 105, 86–101. doi:10.1016/j.quascirev.2014.09.022

Bringué, M., Pospelova, V., Calvert, S.E., Enkin, R.J., Lacourse, T., Ivanochko, T., 2016. High resolution dinoflagellate cyst record of environmental change in Effingham Inlet (British Columbia, Canada) over the last millennium. Palaeogeogr. Palaeoclimatol. Palaeoecol. 441, 787–810. doi:10.1016/j.palaeo.2015.10.026

Dale, B., 1976. Cyst formation, sedimentation, and preservation: Factors affecting dinoflagellate assemblages in recent sediments from trondheimsfjord, Norway. Rev. Palaeobot. Palynol. 22, 39–60. doi:10.1016/0034-6667(76)90010-5

Dale, B., 1996. Dinoglagellate Cyst Ecology: Modeling and Geological Application, in: Jansonius, J., McGregor, D.C. (Eds.), Palynology: Principles and Applications. AASP, Dallas, Texas, pp. 1249–1275.

Dale, B., 2009. Eutrophication signals in the sedimentary record of dinoflagellate cysts in coastal waters. J. Sea Res. 61, 103–113. doi:10.1016/j.seares.2008.06.007

Dale, B., Dale, A.L., Jansen, J.H.F., 2002. Dinoflagellate cysts as environmental indicators in surface sediments from the Congo deep-sea fan and adjacent regions. Palaeogeogr. Palaeoclimatol. Palaeoecol. 185, 309–338. doi:10.1016/S0031-0182(02)00380-2

de Vernal, A., Pedersen, T. F., 1997. Micropaleontology and palynology of core PAR87A-10: A 23,000 year record of paleoenvironmental changes in the Gulf of Alaska, northeast North Pacific Anne 12, 821–830.

de Vernal, A., Rochon, A., Turon, J.-L., Matthiessen, J., 1997. Organic-walled dinoflagellate cysts: Palynological tracers of sea-surface conditions in middle to high latitude marine environments. Geobios 30, 905–920. doi:10.1016/S0016-6995(97)80215-X

de Vernal, A., Henry, M., Matthiessen, J., Mudie, P.J., Rochon, A., Boessenkool, K.P., Eynaud, F., Grosfjeld, K., Guiot, J., Hamel, D., Harland, R., Head, M.J., Kunz-Pirrung, M., Levac, E., Loucheur, V., Peyron, O., Pospelova, V., Radi, T., Turon, J.-L., Voronina, E., 2001. Dinoflagellate cyst assemblages as tracers of sea-surface conditions in the northern North Atlantic, Arctic and sub-Arctic seas: the new "n = 677" data base and its application for quantitative palaeoceanographic reconstruction. J. Quat. Sci. 16, 681–698. doi:10.1002/jqs.659

de Vernal, A., Eynaud, F., Henry, M., Hillaire-Marcel, C., Londeix, L., Mangin, S., Matthiessen, J., Marret, F., Radi, T., Rochon, a., Solignac, S., Turon, J.L., 2005. Reconstruction of sea-surface conditions at middle to high latitudes of the Northern Hemisphere during the Last Glacial Maximum (LGM) based on dinoflagellate cyst assemblages. Quat. Sci. Rev. 24, 897–924. doi:10.1016/j.quascirev.2004.06.014

Durantou, L., Rochon, A., Ledu, D., Massé, G., Schmidt, S., Babin, M., 2012. Quantitative reconstruction of sea-surface conditions over the last 150 yr in the Beaufort Sea based on dinoflagellate cyst assemblages: The role of large-scale atmospheric circulation patterns. Biogeosciences 9, 5391–5406. doi:10.5194/bg-9-5391-2012

Edwards, B.R., Reddy, C.M., Camilli, R., Carmichael, C.A., Longnecker, K., Van Mooy, B.A.S., 2011. Rapid microbial respiration of oil from the Deepwater Horizon spill in offshore surface waters of the Gulf of Mexico. Environ. Res. Lett. 6, 35301. doi:10.1088/1748-9326/6/3/035301

Ellegaard, M., Dale, B., Mertens, K.N., Pospelova, V., Ribeiro, S., 2017. Dinoflagellate Cysts as Proxies for Holocene Environmental Change in Estuaries: Diversity, Abundance and Morphology, in: Applications of Paleoenvironmental Techniques. (eds.), Springer, pp. 295–310. doi:10.1007/978-94-024-0990-1_12

Finn, S.P., Liberty, L.M., Haeussler, P.J., Pratt, T.L., 2015. Landslides and Megathrust Splay Faults Captured by the Late Holocene Sediment Record of Eastern Prince William Sound, Alaska. Bull. Seismol. Soc. Am. 105, 2343–2353. doi:10.1785/0120140273

Garr, A.L., Laramore, S., Krebs, W., 2014. Toxic effects of oil and dispersant on marine microalgae. Bull. Environ. Contam. Toxicol. 93, 654–659. doi:10.1007/s00128-014-1395-2

Garrott, R.A., Labs, R., 1993. Mortality of Sea Otters in Prince William Sound Following the Exxon Valdez Oil Spill. Mar. Mammal Sci. 9, 343–359. doi: 10.1111/j.1748-7692.1993.tb00468.x

Gertler, C., Näther, D.J., Gerdts, G., Malpass, M.C., Golyshin, P.N., 2010. A mesocosm study of the changes in marine flagellate and ciliate communities in a crude oil bioremediation trial. Microb. Ecol. 60, 180–191. doi:10.1007/s00248-010-9660-3

Hallare, A.V., Lasafin, K.J.A., Magalanes, J.R., 2011. Shift in phytoplankton community structure in a tropical marine reserve before and after a major oil spill event. Int. J. Environ. Res. 5, 651–660.

Hansen, P.J., 1991. Quantitative importance and trophic role of heterotrophic dinoflagellates in a coastal pelagial food web. Mar. Ecol. Prog. Ser. 73, 253–261. doi:10.3354/meps073253

Hare, S.R., Mantua, N.J., 2000. Empirical evidence for North Pacific regime shifts in 1977 and 1989. Prog. Oceanogr. 47, 103–145. doi:10.1016/S0079-6611(00)00033-1

Harland, R., Nordberg, K., Filipsson, H.L., 2004a. The seasonal occurrence of dinoflagellate cysts in surface sediments from Koljo Fjord, west coast of Sweden - A note. Rev. Palaeobot. Palynol. 128, 107–117. https://doi.org/10.1016/S0034-6667(03)00115-5

Harland, R., Nordberg, K., Filipsson, H.L., 2004b. A high-resolution dinoflagellate cyst record from latest Holocene sediments in Kolj?? Fjord, Sweden. Rev. Palaeobot. Palynol. 128, 119–141. https://doi.org/10.1016/S0034-6667(03)00116-7

Harrison, P.J., Fulton, J.D., Taylor, F.J.R., Parsons, T.R., 1983. Review of the Biological Oceanography of the Strait of Georgia: Pelagic Environment. Can. J. Fish. Aquat. Sci. 40, 1064–1094. doi:10.1139/f83-129

Harwell, M. A, Gentile, J.H., Cummins, K.W., Highsmith, R.C., Hilborn, R., McRoy, C.P., Parrish, J., Weingartner, T., 2010. A Conceptual Model of Natural and

Anthropogenic Drivers and Their Influence on the Prince William Sound, Alaska, Ecosystem. Hum. Ecol. Risk Assess. 16, 672–726. doi:10.1080/10807039.2010.501011

Hazen, T.C., Dubinsky, E.A., Desantis, T.Z., Andersen, G.L., Piceno, M., Singh, N., Jansson, J.K., Probst, A., Borglin, S.E., Julian, L., Stringfellow, W.T., Bill, M., Conrad, M.E., Tom, L.M., Krystle, L., Alusi, T.R., Lamendella, R., Joyner, D.C., Spier, C., Auer, M., Zemla, M.L., Chakraborty, R., Sonnenthal, E.L., 2010. Deep-Sea Oil Plume Enriches Indigenous Oil-Degrading Bacteria. Science. 330, 204–208.

Head, M.J., 1996. Chapter 30. Modern dinoflagellate cysts and their biological affinities. Palynol. Princ. Appl. Am. Assoc. Stratigr. Palynol. Found. Dallas, TX 3, 1197–1248.

Heikkilä, M., Pospelova, V., Hochheim, K.P., Kuzyk, Z.Z.A., Stern, G.A., Barber, D.G., Macdonald, R.W., 2014. Surface sediment dinoflagellate cysts from the Hudson Bay system and their relation to freshwater and nutrient cycling. Mar. Micropaleontol. 106, 79–109. doi:10.1016/j.marmicro.2013.12.002

Heikkilä, M., Pospelova, V., Forest, A., Stern, G.A., Fortier, L., Macdonald, R.W., 2016. Dinoflagellate cyst production over an annual cycle in seasonally ice-covered Hudson Bay. Mar. Micropaleontol. 125, 1–24. doi.org/10.1016/j.marmicro.2016.02.005

Hook, S.E., Osborn, H.L., 2012. Comparison of toxicity and transcriptomic profiles in a diatom exposed to oil, dispersants, dispersed oil. Aquat. Toxicol. 124–125, 139–151. doi:10.1016/j.aquatox.2012.08.005

Hopkins, J.A., Mccarthy, F.M.G., 2002. Post-depositional palynomorph degradation in quaternary shelf sediments: A laboratory experiment studying the effects of progressive oxidation. Palynology 26, 167–184. doi:10.1080/01916122.2002.9989571

Hu, C., Weisberg, R.H., Liu, Y., Zheng, L., Daly, K.L., English, D.C., Zhao, J., Vargo, G.A., 2011. Did the northeastern Gulf of Mexico become greener after the Deepwater Horizon oil spill? Geophys. Res. Lett. 38, 1–5. doi:10.1029/2011GL047184

Irons, D.B., Kendall, S.J., Erickson, W.P., McDonald, L.L., Lance, B.K., 2000. Nine years after the Exxon Valdez oil spill: Effects on marine bird populations in Prince William Sound, Alaska 102, 723–737. doi: 10.1650/00105422(2000)102[0723:NYATEV]2.0.CO;2

Jacobson, D.M., Anderson, D.M., 1986. Thecate heterotrophic dinoflagellates: feeding behavior and mechanisms. J. Phycol. 22, 249–258. doi:10.1111/j.1529-8817.1986.tb00021.x

Jacobson, D.M., Anderson, D.M., 1996. Widespread Phagocytosis of Ciliates and Other Protists By Marine Mixotrophic and Heterotrophic Thecate Dinoflagellates1. J. Phycol. 32, 279–285. doi:10.1111/j.0022-3646.1996.00279.x

Jaeger, J.M., Nittrouer, C.A., Scott, N.D., Milliman, J.D., 1998. Sediment accumulation along a glacially impacted mountainous coastline: north-east Gulf of Alaska. Basin Res. 10, 155–173. doi:10.1046/j.1365-2117.1998.00059.x

Jeong, H.J., 1999. The Ecological Roles of Heterotrophic Dinoflagellates in Marine Planktonic Community. J. Eukaryot. Microbiol. 46, 390–396. doi:10.1111/j.1550-7408.1999.tb04618.x

Jung, S.W., Kwon, O.Y., Joo, C.K., Kang, J.H., Kim, M., Shim, W.J., Kim, Y.O., 2012. Stronger impact of dispersant plus crude oil on natural plankton assemblages in short-term marine mesocosms. J. Hazard. Mater. 217–218, 338–349. doi:10.1016/j.jhazmat.2012.03.034

Kahlert, M., Kelly, M., Salome, R.A., 2012. Identification versus counting protocols as sources of uncertainty in diatom-based ecological status assessments. https://doi.org/10.1007/s10750-012-1115-z

Kasai, Y., Kishira, H., Harayama, S., 2002a. Bacteria Belonging to the Genus Cycloclasticus Play a Primary Role in the Degradation of Aromatic Hydrocarbons Released in a Marine Environment Bacteria Belonging to the Genus Cycloclasticus Play a Primary Role in the Degradation of Aromatic Hydrocarbons. Appl. Environ. Microbiol. 68, 5625–5633. doi:10.1128/AEM.68.11.5625

Kasai, Y., Kishira, H., Sasaki, T., Syutsubo, K., Watanabe, K., Harayama, S., 2002b. Predominant growth of Alcanivorax strains in oil-contaminated and nutrient-supplemented sea water. Environ. Microbiol. 4, 141–147. doi:10.1046/j.1462-2920.2002.00275.x

Kostka, J.E., Prakash, O., Overholt, W.A., Green, S.J., Freyer, G., Canion, A., Delgardio, J., Norton, N., Hazen, T.C., Huettel, M., 2011. Hydrocarbon-degrading bacteria and the bacterial community response in Gulf of Mexico beach sands impacted by the deepwater horizon oil spill. Appl. Environ. Microbiol. 77, 7962–7974. doi:10.1128/AEM.05402-11

Kumar, A., Patterson, R.T., 2002. Dinoflagellate cyst assemblages from Effingham Inlet, Vancouver Island, British Columbia, Canada. Paleogeography, Paleoclimatology, Paleoecol. 180, 187–206. doi: 10.1016/S0031-0182(01)00428-X

Krepakevich, A., Pospelova, V., 2010. Tracing the influence of sewage discharge on coastal bays of Southern Vancouver Island (BC, Canada) using sedimentary records of phytoplankton. Cont. Shelf Res. 30, 1924–1940. doi:10.1016/j.csr.2010.09.002

Kuehl, S.A., Miller, E.J., Marshall, N.R., Dellapenna, T.M., 2017. Recent paleoseismicity record in Prince William Sound, Alaska, USA. Geo-Marine Lett. doi:10.1007/s00367-017-0505-7

Landry, M., Constantinou, J., Latasa, M., Brown, S., Bidigare, R., Ondrusek, M., 2000. Biological response to iron fertilization in the eastern equatorial Pacific (IronEx II). III. Dynamics of phytoplankton growth and microzooplankton grazing. Mar. Ecol. Prog. Ser. 201, 57–72. doi:10.3354/meps201057

Lavoie, I., Campeau, S., 2016. Assemblage diversity , cell density and within-slide variability : Implications for quality assurance / quality control and uncertainty assessment in diatom-based monitoring. Ecol. Indic. 69, 415–421. https://doi.org/10.1016/j.ecolind.2016.05.001

Levinton, J.S., 1970. The Paleoecological Significance of Opportunistic Species. Lethaia 3, 69–78. doi:10.1111/j.1502-3931.1970.tb01264.x

Lluch-Cota, D.B., Wooster, W.S., Hare, S.R., 2001. Sea surface temperature variability in coastal areas of the Northeastern Pacific related to the El Nino-Southern oscillation and the Pacific decadal oscillation. Geophys. Res. Lett. 28, 2029–2032. doi:10.1029/2000GL012429

Longhurst, A., Sathyendranath, S., Platt, T., Caverhill, C., 1995. An estimate of global primary production in the ocean from satellite radiometer data. J. Plankton Res. 17, 1245–1271. doi: 10.1093/plankt/17.6.1245

Lynn, R.J., Baumgartner, T., Garcia, J., Collins, C.A., Hayward, T.L., Hyrenbach, K.D., Mantyla, A.W., Murphree, T., Shankle, A., Schwing, F.B., Sakuma, K.M., Tegner, M.J., 1998. The state of the California current, 1997-1998: Transition to El Nino conditions. Calif. Coop. Ocean. Fish. Investig. REPORTS 39, 25–49.

Mantua, N.J., Hare, S.R., Zhang, Y., Wallace, J.M., Francis, R.C., 1997. A Pacific Interdecadal Climate Oscillation with Impacts on Salmon Production. Bull. Am. Meteorol. Soc. 78, 1069–1079. doi: 10.1175/1520-0477(1997)078<1069:APICOW>2.0.CO;2

Marret, F., 1993. Les effets de l'acetolyse sur les assemblages des kystes de dinoflagelles. Palynosciences 2, 267–272.

Marret, F., 1994. Distribution of dinoflagellate cysts in recent marine sediments from the east Equatorial Atlantic (Gulf of Guinea) 84, 1–22. doi: 10.1016/0034-6667(94)90038-8

Marret, F., Vernal, A. De, Pedersen, T.F., Mcdonald, D., 2001. Middle Pleistocene to Holocene palynostratigraphy of Ocean Drilling Program Site 887 in the Gulf of Alaska , northeastern North Pacific 38, 373–386. doi:10.1139/cjes-38-3-373

Matsuoka, K., 1999. Eutrophication process recorded in dinoflagellate cyst assemblages - A case of Yokohama Port, Tokyo Bay, Japan. Sci. Total Environ. 231, 17–35. doi:10.1016/S0048-9697(99)00087-X

McGenity, T.J., Folwell, B.D., McKew, B. a, Sanni, G.O., 2012. Marine crude-oil biodegradation: a central role for interspecies interactions. Aquat. Biosyst. 8, 10. doi:10.1186/2046-9063-8-10

Mertens, K.N., Verhoeven, K., Verleye, T., Louwye, S., Amorim, A., Ribeiro, S., Deaf, A.S., Harding, I.C., De Schepper, S., Gonz??lez, C., Kodrans-Nsiah, M., De Vernal, A., Henry, M., Radi, T., Dybkjaer, K., Poulsen, N.E., Feist-Burkhardt, S., Chitolie, J., Heilmann-Clausen, C., Londeix, L., Turon, J.L., Marret, F., Matthiessen, J., McCarthy, F.M.G., Prasad, V., Pospelova, V., Kyffin Hughes, J.E., Riding, J.B., Rochon, A., Sangiorgi, F., Welters, N., Sinclair, N., Thun, C., Soliman, A., Van Nieuwenhove, N., Vink, A., Young, M., 2009. Determining the absolute abundance of dinoflagellate cysts in recent marine sediments: The *Lycopodium* marker-grain method put to the test. Rev. Palaeobot. Palynol. 157, 238–252. doi:10.1016/j.revpalbo.2009.05.004

Mertens, K.N., Yamaguchi, A., Kawami, H., Ribeiro, S., Leander, B.S., Price, A.M., Pospelova, V., Ellegaard, M., Matsuoka, K., 2012a. *Archaeperidinium saanichi* sp. nov.: A new species based on morphological variation of cyst and theca within the *Archaeperidinium minutum* Jorgensen 1912 species complex. Mar. Micropaleontol. 96–97, 48–62. https://doi.org/10.1016/j.marmicro.2012.08.002

Mertens, K.N., Bringué, M., Van Nieuwenhove, N., Takano, Y., Pospelova, V., Rochon, A., De Vernal, A., Radi, T., Dale, B., Patterson, R.T., Weckström, K., Andrén, E., Louwye, S., Matsuoka, K., 2012b. Process length variation of the cyst of the dinoflagellate Protoceratium reticulatum in the North Pacific and Baltic-Skagerrak region: Calibration as an annual density proxy and first evidence of pseudo-cryptic speciation. J. Quat. Sci. 27, 734–744. https://doi.org/10.1002/jqs.2564

Mertens, K.N., Yamaguchi, A., Takano, Y., Pospelova, V., Head, M.J., Radi, T., Pieńkowski, A.J., De Vernal, A., Kawami, H., Matsuoka, K., 2013. A new heterotrophic dinoflagellate from the north-eastern pacific, Protoperidinium fukuyoi: Cyst-theca relationship, phylogeny, distribution and ecology. J. Eukaryot. Microbiol. 60, 545–563. https://doi.org/10.1111/jeu.12058

Mortlock, R.A., Froelich, P.N., 1989. A simple method for the rapid determination of biogenic opal in pelagic marine sediments. Deep. Sea. Res. A. 36, 1415–1426. doi: 10.1016/0198-0149(89)90092-7

Mundy, P.R., 2005. The Gulf of Alaska Biology and Oceanography. Alaska Seat Grant College Program, University of Alaska, Fairbanks, Fairbanks. 1-214.

Musgrave, D.L., Halverson, M.J., Scott Pegau, W., 2013. Seasonal surface circulation, temperature, and salinity in Prince William Sound, Alaska. Cont. Shelf Res. 53, 20–29. doi:10.1016/j.csr.2012.12.001

Nalco Company, 2008. Corexit Ec9527a Safety Data Sheet.

Nelson, D.M., Tréguer, P., Brzezinski, M. a., Leynaert, A., Quéguiner, B., 1995. Production and dissolution of biogenic silica in the ocean: Revised global estimates, comparison with regional data and relationship to biogenic sedimentation. Global Biogeochem. Cycles 9, 359. doi:10.1029/95GB01070

Niebauer, H.J., Royer, C., Weingartner, T.J., Royer, T.C., Weingartner, T.J., Royer, C., Weingartner, T.J., 1994. Circulation of Prince William Sound. J. Geophys. Res. 99, 14113–14126. doi:10.1029/94JC00712

NOAA, n.d. El Niño Southern Oscillation (ENSO). URL https://www.esrl.noaa.gov/psd/enso/past_events.html (accessed 10.1.17).

Okkonen, S.R., Bélanger, C., 2008. Annual period temperature and salinity signals of surface waters in Prince William Sound, Alaska. Geophys. Res. Lett. 35. doi:10.1029/2008GL034456

Ozhan, K., Parsons, M.L., Bargu, S., 2014a. How were phytoplankton affected by the deepwater horizon oil spill? Bioscience 64, 829–836. doi:10.1093/biosci/biu117

Özhan, K., Miles, S.M., Gao, H., Bargu, S., 2014b. Relative phytoplankton growth responses to physically and chemically dispersed South Louisiana sweet crude oil. Environ. Monit. Assess. 186, 3941–3956. doi:10.1007/s10661-014-3670-4

Ozhan, K., Zahraeifard, S., Smith, A.P., Bargu, S., 2015. Induction of reactive oxygen species in marine phytoplankton under crude oil exposure. Environ. Sci. Pollut. Res. 22, 18874–18884. doi:10.1007/s11356-015-5037-y

Paul, J.H., Hollander, D., Coble, P., Daly, K.L., Murasko, S., English, D., Basso, J., Delaney, J., McDaniel, L., Kovach, C.W., 2013. Toxicity and mutagenicity of gulf of mexico waters during and after the Deepwater Horizon oil spill. Environ. Sci. Technol. 47, 9651–9659. doi:10.1021/es401761h

Peterson, C., Rice, S., Short, J., Esler, D., 2003. Long-term ecosystem response to the Exxon Valdez oil spill. Science 302, 2082–2086. doi:10.1126/science.1084282

Piatt, J.F., Ford, R.G., 1996. How Many Seabirds Were Killed by the Exxon Valdez Oil Spill? Am. Fish. Soc. Symp. 18, 712–719.

Pospelova, V., Kim, S.-J., 2010. Dinoflagellate cysts in recent estuarine sediments from aquaculture sites of southern South Korea. Mar. Micropaleontol. 76, 37–51. doi:10.1016/j.marmicro.2010.04.003

Pospelova, V., Chmura, G.L., Boothman, W.S., Latimer, J.S., 2002. Dinoflagellate cyst records and human disturbance in two neighboring estuaries , New Bedford Harbor and Apponagansett. Sci. Total Environ. 298, 81–102. doi: 10.1016/S0048-9697(02) 00195-X

Pospelova, V., Chmura, G.L., Walker, H. a., 2004. Environmental factors influencing the spatial distribution of dinoflagellate cyst assemblages in shallow lagoons of southern New England (USA). Rev. Palaeobot. Palynol. 128, 7–34. doi:10.1016/S0034-6667(03)00110-6

Pospelova, V., Chmura, G.L., Boothman, W.S., Latimer, J.S., 2005. Spatial distribution of modern dinoflagellate cysts in polluted estuarine sediments from Buzzards Bay (Massachusetts, USA) embayments. Mar. Ecol. Prog. Ser. 292, 23–40. doi:10.3354/meps292023

Pospelova, V., Pedersen, T.F., de Vernal, A., 2006. Dinoflagellate cysts as indicators of climatic and oceanographic changes during the past 40 kyr in the Santa Barbara Basin , southern California. Paleoceanography 21(2), 1-16. doi:10.1029/2005PA001251

Pospelova, V., de Vernal, A., Pedersen, T.F., 2008. Distribution of dinoflagellate cysts in surface sediments from the northeastern Pacific Ocean (43 – 25 ° N) in relation to sea-surface temperature , salinity , productivity and coastal upwelling. Mar. Micropaleontol. 68, 21–48. doi:10.1016/j.marmicro.2008.01.008

Pospelova, V., Esenkulova, S., Johannessen, S.C., O'Brien, M.C., Macdonald, R.W., 2010. Organic-walled dinoflagellate cyst production, composition and flux from 1996 to 1998 in the central Strait of Georgia (BC, Canada): A sediment trap study. Mar. Micropaleontol. 75, 17–37. doi:10.1016/j.marmicro.2010.02.003

Pospelova, V., Price, A.M., Pedersen, T.F., 2015. Palynological evidence for late Quaternary climate and marine primary productivity changes along the California margin 1–18. doi:10.1002/2014PA002728.

Price, A.M., Pospelova, V., 2011. High-resolution sediment trap study of organic-walled dinoflagellate cyst production and biogenic silica flux in Saanich Inlet (BC, Canada). Mar. Micropaleontol. 80, 18–43. doi:10.1016/j.marmicro.2011.03.003

Price, A.M., Mertens, K.N., Pospelova, V., Pedersen, T.F., Ganeshram, R.S., 2013. Late Quaternary climatic and oceanographic changes in the Northeast Pacific as recorded by dinoflagellate cysts from Guaymas Basin, Gulf of California (Mexico).

Paleoceanography 28, 200–212. doi:10.1002/palo.20019

Price, A.M., Gurdebeke, P.R., Mertens, K.N., Pospelova, V., 2016. Determining the absolute abundance of dinoflagellate cysts in recent marine sediments III: Identifying the source of *Lycopodium* loss during palynological processing and further testing of the *Lycopodium* marker-grain method. Rev. Palaeobot. Palynol. 226, 78–90. doi:10.1016/j.revpalbo.2015.12.009

Prince, R.C., Bragg, J.R., 2008. Shoreline Bioremediation Following the Exxon Valdez Oil Spill in Alaska. Bioremediat. J. 1, 97–104. doi:10.1080/10889869709351324

Pritchard, P.H., Costa, C.F., 1991. EPA's Alaska oil spill bioremediation project: Final part of a five-part series. Environ. Sci. Technol. 25, 372–379. doi:10.1021/es00015a002

Radi, T., de Vernal, A., 2004. Dinocyst distribution in surface sediments from the northeastern Pacific margin (40-60°N) in relation to hydrographic conditions, productivity and upwelling. Rev. Palaeobot. Palynol. 128, 169–193. doi:10.1016/S0034-6667(03)00118-0

Radi, T., de Vernal, A., 2008. Last glacial maximum (LGM) primary productivity in the northern North Atlantic OceanThis article is one of a series of papers published in this Special Issue on the theme Polar Climate Stability Network . Can. J. Earth Sci. 45, 1299–1316. doi:10.1139/E08-059

Radi, T., Bonnet, S., Cormier, M.A., de Vernal, A., Durantou, L., Faubert, É., Head, M.J., Henry, M., Pospelova, V., Rochon, A., Van Nieuwenhove, N., 2013. Operational taxonomy and (paleo-)autecology of round, brown, spiny dinoflagellate cysts from the Quaternary of high northern latitudes. Mar. Micropaleontol. 98, 41–57. doi:10.1016/j.marmicro.2012.11.001

Radi, T., Pospelova, V., de Vernal, A., Barrie, J.V., 2007. Dinoflagellate cysts as indicators of water quality and productivity in British Columbia estuarine environments 62, 269–297. doi:10.1016/j.marmicro.2006.09.002

Ragueneau, O., Tréguer, P., Leynaert, a., Anderson, R.F., Brzezinski, M. a., DeMaster, D.J., Dugdale, R.C., Dymond, J., Fischer, G., François, R., Heinze, C., Maier-Reimer, E., Martin-Jézéquel, V., Nelson, D.M., Quéguiner, B., 2000. A review of the Si cycle in the modern ocean: Recent progress and missing gaps in the application of biogenic opal as a paleoproductivity proxy. Glob. Planet. Change 26, 317–365. doi:10.1016/S0921-8181(00)00052-7

Rochon, A., de Vernal, A., Turon, J.L., Matthiessen, J., Head, M.J., 1999. Distribution of recent dinoflagellate cysts in surface sediments from the North Atlantic Ocean and adjacent seas in relation to sea-surface parameters. Contribution Series No. 35. American Association of Stratigraphic Palynologists Foundation, Dallas, TX.

Royer, T.C., 1981. Baroclinic Transport in the Gulf of Alaska. Part II. A Freshwater driven coastal current. J. Mar. Res. 39, 251–266.

Royer, T.C., Vermersch, J.A., Weingartner, T.J., Niebauer, H.J., Muench, R.D., 1990. Ocean circulation influencing the Exxon Valdez oil spill. Oceanography. 3, 3–10.

Santisi, S., Cappello, S., Catalfamo, M., Mancini, G., Hassanshahian, M., Genovese, L., Giuliano, L., Yakimov, M.M., 2015. Biodegradation of crude oil by individual bacterial strains and a mixed bacterial consortium. Brazilian J. Microbiol. 46, 377–387. doi:10.1590/S1517-838246120131276

Serreze, M.C., Walsh, J.E., Chapin, F.S.I., Osterkamp, T., Dyurgerov, M., Romanovsky, V., Oechel, W.C., Morison, J., Zhang, T., Barry, R.G., 2000. Observational evidence of recent change in the northern high- latitude environment. Clim. Change 46, 159–207. doi:10.1023/A:1005504031923

Severin, T., Bacosa, H.P., Sato, A., Erdner, D.L., 2016. Dynamics of Heterocapsa sp. and the associated attached and free-living bacteria under the influence of dispersed and undispersed crude oil. Lett. Appl. Microbiol. 63, 419–425. doi:10.1111/lam.12661

Shabbar, A., Yu, B., 2009. The 1998-2000 la Ni??a in the context of historically strong la Nina events. J. Geophys. Res. Atmos. 114, 1–14. doi:10.1029/2008JD011185

Shigenaka, G., 2014. Twenty-Five Years After the Exxon Valdez Oil Spill: NOAA's Scientific Support, Monitoring, and Research. Seattle: NOAA Office of Response and Restoration. 78 pp.

Sommer, U., 2009. An Experimental Test of the Intermediate Disturbance Hypothesis Using Cultures of Marine Phytoplankton. Limnol. Oceanogr. 40, 1271–1277. doi: 10.4319/lo.1995.40.7.1271

Stabeno, P.J., Reed, R.K., Schumacher, J.D., 1995. The Alaska Coastal Current: Continuity of transport and forcing. J. Geophys. Res. 100, 2477. doi:10.1029/94JC02842

Stabeno, P.J., Bond, N.A., Hermann, A.J., Kachel, N.B., Mordy, C.W., Overland, J.E., 2004. Meteorology and oceanography of the Northern Gulf of Alaska, Continental Shelf Research. doi:10.1016/j.csr.2004.02.007

Statistics Canada, 2013. Constructing box and whisker plots. URL https://www.statcan.gc.ca/edu/power-pouvoir/ch12/5214889-eng.htm

Stockmarr, J., 1971. Tablets with spores in absolute pollen analysis. Pollen et Spores 13, 615–621.

Strom, S.L., Fredrickson, K.A., Bright, K.J., 2016. Spring phytoplankton in the eastern coastal Gulf of Alaska: Photosynthesis and production during high and low bloom years. Deep. Res. Part II Top. Stud. Oceanogr. 132, 107–121. doi:10.1016/j.dsr2.2015.05.003

Sturges, W., Lugo-Fernandez, A., Shargel, M.D., 2013. Introduction to Circulation in the Gulf of Mexico. Circ. Gulf Mex. Obs. Model. 161, 1–10. doi:10.1029/161GM02

Taş, S., Okuş, E., Ünlü, S., Altiok, H., 2010. A study on phytoplankton following "Volgoneft-248" oil spill on the north-eastern coast of the Sea of Marmara. J. Mar. Biol. Assoc. United Kingdom 91, 715–725. doi:10.1017/S0025315410000330

Tsirtsis, G., Karydis, M., 1998. Evaluation of phytoplankton community indices for detecting eutrophic trends in the marine environment. Environ. Monit. Assess. 50, 255–269. doi:10.1023/A:1005883015373

UNCTAD, 2015. Review of maritime transport 2015, United Nations.

Vaughan, S.L., Mooers, C.N.K., Gay, S.M., 2001. Physical variability in Prince William Sound during the SEA study (1994-98). Fish. Oceanogr. 10, 58–80. doi:10.1046/j.1054-6006.2001.00034.x

Verleye, T.J., Pospelova, V., Mertens, K.N., Louwye, S., 2011. The geographical distribution and (palaeo)ecology of *Selenopemphix undulata* sp. nov., a new late Quaternary dinoflagellate cyst from the Pacific Ocean. Mar. Micropaleontol. 78, 65–83. https://doi.org/10.1016/j.marmicro.2010.10.001

Wall, D., Dale, B., 1966. "Living fossils" in western Atlantic plankton. Nature 211, 1025–1026. doi:10.1038/211676a0

Wall, D., Dale, B., Lohmann, G.P., Smith, W.K., 1977. The environmental and climatic distribution of dinoflagellate cysts in modern marine sediments from regions in the North and South Atlantic Oceans and adjacent seas. Mar. Micropaleontol. 2, 121–200. doi:10.1016/0377-8398(77)90008-1

Wallace, J.M., Gutzler, D.S., 1981. Teleconnections in the Geopotential Height Field during the Northern Hemisphere Winter. Mon. Weather Rev. doi:10.1175/1520-0493(1981)109≤ 0784:TITGHF>2.0.CO;2

Wang, Y., Xue, H., Chai, F., Chao, Y., Farrara, J., 2014. A model study of the Copper River plume and its effects on the northern Gulf of Alaska Topical Collection on the 5th International Workshop on Modelling the Ocean (IWMO) in Bergen, Norway 17-20 June 2013. Ocean Dyn. 64, 241–258. doi:10.1007/s10236-013-0684-3

Wiens, J.A., 2013. Oil in the Environment: Legacies and Lessons of the Exxon Valdez Oil Spill, 1st ed. New York. doi:10.1017/CBO9781139225335

Wilson, J.G., Overland, J.E., 1986. Meteorology of the northern Gulf of Alaska, in: Hood, D.W., Zimmerman, S.T. (Eds.), The Gulf of Alaska: Physical Environment and Biological Resources. DOC/NOAA, pp. 31–54.

Yakimov, M.M., Golyshin, P.N., Lang, S., Moore, E.R.B., Abraham, W., Lunsdorf, H., Timmis, K.N., 1972. a New , Hydrocarbon-Degrading and Surfactant-Producing Marine Bacterium. Int. J. Syst. Bacteriol. 48, 339–348. doi:10.1099/00207713-48-2-339

Yamaguchi, A., Hoppenrath, M., Pospelova, V., Horiguchi, T., Leander, B.S., 2011. Molecular phylogeny of the marine sand-dwelling dinoflagellate herdmania litoralis and an emended description of the closely related planktonic genus archaeperidinium jörgensen. Eur. J. Phycol. 46, 98–112. https://doi.org/10.1080/09670262.2011.564517

Ziervogel, K., McKay, L., Rhodes, B., Osburn, C.L., Dickson-Brown, J., Arnosti, C., Teske, A., 2012. Microbial activities and dissolved organic matter dynamics in oil-contaminated surface seawater from the deepwater horizon oil spill site. PLoS One 7. doi:10.1371/journal.pone.0034816

Zonneveld, K. a. F., Pospelova, V., 2015. A determination key for modern dinoflagellate cysts. Palynology 39, 1–23. doi:10.1080/01916122.2014.990115

Zonneveld, K.A.F., Versteegh, G.J.M., De Lange, G.J., 1997. Preservation of organic-walled dinoflagellate cysts in different oxygen regimes: A 10,000 year natural experiment. Mar. Micropaleontol. 29, 393–405. doi:10.1016/S0377-8398(96)00032-1

Zonneveld, K.A.F., P. Hoek, R., Brinkhuis, H., Helmut Willems, 2001. Geographical distributions of organic-walled dinoflagellate cysts in surficial sediments of the Benguela upwelling region and their relationship to upper ocean conditions. Prog. Oceanogr. 48, 25–72. doi:10.1016/S0079-6611(00)00047-1

Zonneveld, K.A.F., Bockelmann, F., Holzwarth, U., 2007. Selective preservation of organic-walled dinoflagellate cysts as a tool to quantify past net primary production and bottom water oxygen concentrations. Mar. Geol. 237, 109–126. doi:10.1016/j.margeo.2006.10.023

Zonneveld, K.A.F., Versteegh, G., Kodrans-Nsiah, M., 2008. Preservation and organic chemistry of Late Cenozoic organic-walled dinoflagellate cysts: A review. Mar. Micropaleontol. 68, 179–197. doi:10.1016/j.marmicro.2008.01.015

Zonneveld, K.A.F., Marret, F., Versteegh, G.J.M., Bogus, K., Bonnet, S., Bouimetarhan, I., Crouch, E., Vernal, A. De, Elshanawany, R., Edwards, L., Esper, O., Forke, S., Grøsfjeld, K., Henry, M., Holzwarth, U., Kielt, J., Kim, S., Ladouceur, S., Ledu, D., Chen, L., Limoges, A., Londeix, L., Lu, S., Mahmoud, M.S., Marino, G., Matsouka, K., Matthiessen, J., Mildenhal, D.C., Mudie, P., Neil, H.L., Pospelova, V., Qi, Y., Richerol, T., Rochon, A., Sangiorgi, F., Solignac, S., Turon, J., Verleye, T., Wang, Y., Wang, Z., Young, M., 2013. Atlas of modern dinoflagellate cyst distribution based on 2405 data points. Rev. Palaeobot. Palynol. 191, 1–197. doi:10.1016/j.revpalbo.2012.08.003

Appendix

Appendix 1: The relative abundances of the grouped taxa, including the average and standard deviation (Std. dev.) in all the samples of core P-10. Also shown is the H/A ratio.

Uvic ID (Year)	**Uvic ID**	Age (Corrected)	Cysts of *Alexandrium* spp.	Cysts of P*entapharsodinium dalei*	*Operculodinium centrocarpum*	*Spiniferites ramosus*	*Spiniferites* spp.	*Islandinium minutum*	*Islandinium*? *cesare*	*Brigantedinium* spp.	*Dubridinium* spp.	*Echinidinium aculeatum*	*Echininidinium cf. delicatum*	*Echinidinium cf. granulatum*	*Echinidinium* spp.	Cysts of *Protoperidinium americanum*	Cysts of *Protoperidinium fukuyoi*	*Quinquecuspis concreta*	Cysts of *Polykrikos* spp.	*Selenopemphix quanta*	*Selenopemphix nephroides/ undulata*	Spinny brown cysts	Unknown cysts	Heterotrophic/autotrophic ratio
2016	**66**	1999.7	5.0	2.3	20.8	0.7	0.3	0.3	1.0	45.0	0.7	11.1	3.4	0.3	2.7	1.0	0.3	0.3	1.3	2.0	0.7	0.7	0.0	2.4
2016	**67**	1998.6	3.3	0.7	21.3	0.7	1.0	1.0	1.3	48.2	0.3	5.3	2.3	1.0	2.3	0.3	0.0	2.3	0.7	4.3	1.3	2.3	0.0	2.7
2016	**68**	1997.5	4.3	2.7	19.6	1.3	2.7	0.7	1.3	48.8	1.7	1.7	2.3	1.7	2.3	0.7	0.7	0.7	0.7	3.3	0.7	2.3	0.0	2.3
2016	**69**	1996.4	4.7	0.0	17.1	4.0	1.7	1.3	1.0	42.6	0.7	7.7	3.4	2.0	4.4	1.3	1.0	1.0	0.7	2.0	1.0	1.3	1.0	2.6
2016	**70**	1995.3	4.0	0.3	21.6	2.7	1.3	1.0	0.3	46.5	1.0	3.7	2.7	0.7	5.3	1.7	0.0	3.3	0.7	1.7	0.0	1.3	0.3	2.3
2016	**71**	1994.2	2.7	0.7	22.3	3.3	1.7	0.0	1.7	49.2	1.0	1.3	5.0	0.7	0.7	1.0	0.0	1.3	2.7	1.7	1.0	2.0	0.3	2.3
2016	**72**	1993.1	2.3	0.3	19.6	3.0	1.3	1.0	1.0	48.8	1.0	3.7	5.3	1.3	4.7	2.0	0.7	0.3	0.7	0.0	1.0	1.7	0.3	2.8
2016	**73**	1991.9	2.8	2.5	26.6	2.8	1.9	1.9	2.2	38.6	1.3	1.9	2.2	0.9	6.6	1.9	0.9	0.6	0.3	1.3	0.9	0.9	0.6	1.7
2016	**74**	1990.8	6.2	1.3	17.9	2.6	0.3	0.3	0.3	54.1	2.3	2.9	1.3	1.3	2.6	1.0	0.3	0.3	0.7	1.0	1.0	2.3	0.0	2.5
2016	**75**	1989.7	2.3	1.0	36.8	5.2	1.0	0.3	1.0	30.9	2.6	2.3	1.6	1.3	6.8	0.7	0.3	1.6	0.3	1.6	0.3	2.0	0.0	1.2
2016	**76**	1988.6	3.0	2.0	32.2	6.6	1.7	1.0	0.7	33.9	1.0	1.3	1.0	0.7	4.7	1.3	0.3	1.7	0.0	1.0	2.0	3.3	0.7	1.2
2016	**77**	1987.5	2.9	1.0	36.0	6.4	0.3	1.6	1.6	24.4	2.3	3.5	1.9	0.3	9.0	1.6	0.0	1.3	0.0	0.3	1.9	2.9	0.6	1.1
2016	**78**	1986.4	3.7	3.7	36.6	4.7	0.7	1.4	0.3	29.5	0.3	1.7	1.7	1.4	5.1	1.4	0.0	0.7	1.4	0.7	1.7	3.4	0.0	1.0
		Average	3.6	1.4	25.3	3.4	1.2	0.9	1.1	41.6	1.2	3.7	2.6	1.0	4.4	1.2	0.4	1.2	0.8	1.6	1.0	2.0	0.3	2.0
		Std dev.	1.2	1.1	7.5	2.0	0.7	0.6	0.6	9.2	0.7	2.9	1.3	0.5	2.3	0.5	0.4	0.9	0.7	1.2	0.6	0.8	0.3	0.7

Appendix 2: The relative abundances of the grouped taxa, including the average and standard deviation (Std. dev.) in all he samples of core P-12. Also shown is the H/A ratio.

Uvic ID (Year)	**Uvic ID**	Age (Corrected)	Cysts of *Alexandrium* spp.	Cysts of P*entapharsodinium dalei*	*Operculodinium centrocarpum*	*Spiniferites ramosus*	*Spiniferites* spp.	*Islandinium minutum*	*Islandinium? cesare*	*Brigantedinium* spp.	*Dubridinium* spp.	*Echinidinium aculeatum*	*Echininidinium cf. delicatum*	*Echinidinium cf. granulatum*	*Echinidinium* spp.	Cysts of *Protoperidinium americanum*	Cysts of *Protoperidinium fukuyoi*	*Quinquecuspis concreta*	Cysts of *Polykrikos* spp.	*Selenopemphix quanta*	*Selenopemphix nephroides/ undulata*	Spinny brown cysts	Unknown cysts	Heterotrophic/autotrophic ratio
2016	**260**	1999.3	6.7	3.5	25.1	1.5	0.7	0.2	2.7	37.0	1.7	5.0	3.0	0.5	4.0	1.5	0.5	1.0	0.5	0.5	0.2	3.2	1.0	1.6
2016	**261**	1998.4	3.7	2.0	20.3	1.1	0.8	1.7	1.7	42.5	3.1	2.3	3.4	0.8	2.5	5.1	0.8	2.0	2.0	0.8	1.7	0.8	0.8	2.6
2016	**262**	1997.5	4.5	1.3	17.6	1.9	0.0	0.6	1.0	53.7	1.9	1.3	0.0	0.3	1.3	1.6	1.0	3.2	2.9	2.2	2.2	1.0	0.6	2.9
2016	**263**	1996.7	3.1	1.1	21.8	1.1	0.6	0.0	3.1	39.7	2.3	1.4	4.0	1.4	6.5	2.0	1.7	0.8	1.1	2.3	3.4	2.0	0.6	2.6
2016	**264**	1995.8	2.9	2.4	23.7	2.4	1.6	0.3	1.3	41.8	0.5	0.5	3.7	0.8	4.3	2.1	1.1	1.3	1.1	1.9	5.1	1.3	0.0	2.0
2016	**265**	1995.0	6.1	1.1	17.5	1.4	2.2	0.3	1.4	53.8	2.8	0.6	2.2	0.3	1.7	1.9	0.6	1.4	0.8	0.6	1.9	1.1	0.3	2.5
2016	**266**	1994.1	6.4	0.7	16.2	1.0	1.3	0.3	0.7	54.9	4.0	0.7	2.7	0.0	2.0	3.4	0.0	1.7	0.7	1.3	0.3	1.3	0.3	2.9
2016	**267**	1993.3	6.7	0.5	16.3	1.7	1.2	0.2	0.7	53.2	4.3	0.5	2.9	0.5	1.4	1.4	0.5	2.9	0.7	1.2	1.7	1.0	0.5	2.8
2016	**268**	1992.4	3.4	2.8	16.6	1.6	1.6	0.0	0.3	52.4	4.7	0.9	2.2	1.3	2.2	3.4	0.3	0.6	1.3	1.3	1.6	1.6	0.0	2.8
2016	**269**	1991.6	1.3	2.3	23.4	2.1	1.8	0.0	0.0	57.0	2.9	0.8	0.8	0.5	0.5	0.5	0.0	2.1	0.5	0.5	1.8	1.0	0.0	2.2
2016	**270**	1990.7	2.4	4.5	30.9	1.6	0.8	0.3	1.6	37.2	5.2	1.0	2.6	0.3	0.5	1.3	0.5	1.0	1.6	1.0	1.8	3.9	0.0	1.5
2016	**271**	1989.9	4.4	2.8	28.0	3.1	1.0	0.8	1.0	35.2	6.2	1.6	4.1	1.0	2.8	1.0	1.0	0.0	0.3	0.8	0.8	3.4	0.5	1.5
2016	**272**	1989.0	3.8	1.3	30.7	4.0	2.2	1.9	1.3	36.1	1.9	1.6	1.9	0.5	3.0	2.7	0.5	1.6	0.8	1.3	1.1	1.3	0.3	1.4
2016	**273**	1988.1	5.0	3.7	22.8	6.9	4.5	0.0	0.8	35.3	1.3	1.3	1.6	0.3	5.8	1.9	1.3	1.3	0.5	1.9	1.3	2.4	0.0	1.3
2016	**274**	1987.3	3.4	1.0	23.7	3.1	2.4	0.0	0.3	43.4	7.1	3.7	1.0	0.0	4.4	1.0	0.0	1.4	0.0	0.7	1.7	1.7	0.0	2.0
2016	**275**	1986.4	1.8	1.2	23.7	2.4	1.5	0.0	1.5	45.9	0.9	1.8	3.3	0.0	9.8	1.8	0.0	0.6	0.3	0.3	1.5	1.2	0.9	2.3
2016	**276**	1985.6	3.2	1.3	33.0	3.2	4.2	1.3	0.6	33.7	2.9	3.2	0.3	0.3	6.1	2.3	0.3	0.6	0.0	0.3	1.0	1.6	0.3	1.2
2016	**277**	1984.7	4.2	2.6	31.8	7.1	2.3	0.6	1.3	30.5	1.0	1.9	0.6	0.0	4.8	2.6	0.3	0.6	1.0	2.9	1.3	2.3	0.3	1.1
2016	**278**	1983.9	4.3	0.9	27.1	3.7	1.7	0.0	0.3	43.1	0.3	2.9	1.7	0.0	6.3	1.7	1.1	0.9	0.3	0.6	0.9	1.7	0.6	1.6
2016	**283**	1983.0	2.5	0.0	25.7	0.8	0.8	0.8	3.3	49.8	5.8	0.0	0.0	0.4	7.1	0.8	0.0	1.2	0.0	0.0	0.4	0.0	0.4	2.3
2016	**284**	1982.2	1.9	1.9	29.0	1.9	1.4	0.5	1.4	47.6	1.9	0.0	0.5	1.4	3.8	0.0	0.0	0.5	0.0	1.0	0.0	4.8	0.5	1.8
		Average	3.9	1.9	24.0	2.6	1.7	0.5	1.3	44.0	3.0	1.6	2.0	0.5	3.9	1.9	0.6	1.3	0.8	1.1	1.5	1.8	0.4	2.0
		Std dev.	1.6	1.2	5.3	1.7	1.1	0.6	0.9	8.1	2.0	1.3	1.3	0.5	2.4	1.1	0.5	0.8	0.7	0.8	1.1	1.1	0.3	0.6

Appendix 3: Dinoflagellate cyst analysis showing the cyst concentrations, the average and standard deviation (Std. dev.) for each grouped taxon in core P-10. Also shown is the total dinoflagellate cyst concentration, the average and standard deviation (Std. dev.).

Uvic ID (Year)	**Uvic ID**	Age (Corrected)	Total conc	Cysts of *Alexandrium* spp.	Cysts of *Pentapharsodinium dalei*	*Operculodinium centrocarpum*	*Spiniferites ramosus*	*Spiniferites* spp.	*Islandinium minutum*	*Islandinium? cesare*	*Brigantedinium* spp.	*Dubridinium* spp.	*Echinidinium aculeatum*	*Echininidinium cf. delicatum*	*Echinidinium cf. granulatum*	*Echinidinium* spp.	Cysts of *Protoperidinium americanum*	Cysts of *Protoperidinium fukuyoi*	*Quinquecuspis concreta*	Cysts of *Polykrikos* spp.	*Selenopemphix quanta*	*Selenopemphix nephroides/ undulata*	Spinny brown cysts	Unknown cysts
2016	**66**	1999.7	464	23	11	97	3	2	2	5	209	3	51	16	2	12	5	2	2	6	9	3	3	0
2016	**67**	1998.6	445	15	3	95	3	4	4	6	214	1	24	10	4	10	1	0	10	3	19	6	10	0
2016	**68**	1997.5	528	23	14	104	7	14	4	7	258	9	9	12	9	12	4	4	4	4	18	4	12	0
2016	**69**	1996.4	455	21	0	78	18	8	6	5	194	3	35	15	9	20	6	5	5	3	9	5	6	5
2016	**70**	1995.3	556	22	2	120	15	7	6	2	259	6	20	15	4	30	9	0	18	4	9	0	7	2
2016	**71**	1994.2	497	13	3	111	17	8	0	8	244	5	7	25	3	3	5	0	7	13	8	5	10	2
2016	**72**	1993.1	395	9	1	77	12	5	4	4	193	4	14	21	5	18	8	3	1	3	0	4	7	1
2016	**73**	1991.9	455	13	12	121	13	9	9	10	176	6	9	10	4	30	9	4	3	1	6	4	4	3
2016	**74**	1990.8	431	27	6	77	11	1	1	1	233	10	13	6	6	11	4	1	1	3	4	4	10	0
2016	**75**	1989.7	749	17	7	276	39	7	2	7	232	20	17	12	10	51	5	2	12	2	12	2	15	0
2016	**76**	1988.6	362	11	7	117	24	6	4	2	123	4	5	4	2	17	5	1	6	0	4	7	12	2
2016	**77**	1987.5	518	15	5	186	33	2	8	8	126	12	18	10	2	47	8	0	7	0	2	10	15	3
2016	**78**	1986.4	327	12	12	120	16	2	4	1	96	1	6	6	4	17	4	0	2	4	2	6	11	0
		Average	476	17	6	121	16	6	4	5	197	6	17	12	5	21	6	2	6	4	8	5	9	1
		Std. dev.	105	6	5	54	11	4	3	3	53	5	13	6	3	14	2	2	5	3	6	2	4	2

Appendix 4: Dinoflagellate cyst analysis showing the cyst concentrations, the average and standard deviation (Std. dev.) for each grouped taxon in core P-10. Also shown is the total dinoflagellate cyst concentration, the average and standard deviation (Std. dev.).

Uvic ID (Year)	**Uvic ID**	Age (Corrected)	Total conc	Cysts of *Alexandrium* spp.	Cysts of P*entapharsodinium dalei*	*Operculodinium centrocarpum*	*Spiniferites ramosus*	*Spiniferites* spp.	*Islandinium minutum*	*Islandinium*? *cesare*	*Brigantedinium* spp.	*Dubridinium* spp.	*Echinidinium aculeatum*	*Echinidinium cf. delicatum*	*Echinidinium cf. granulatum*	*Echinidinium* spp.	Cysts of *Protoperidinium americanum*	Cysts of *Protoperidinium fukuyoi*	*Quinquecuspis concreta*	Cysts of *Polykrikos* spp.	*Selenopemphix quanta*	*Selenopemphix nephroides/ undulata*	Spinny brown cysts	Unknown cysts
2016	**260**	1999.3	1341	90	47	336	20	10	3	37	496	23	67	40	7	53	20	7	13	7	7	3	43	13
2016	**261**	1998.4	1307	48	26	265	15	11	22	22	556	40	29	44	11	33	66	11	26	26	11	22	11	11
2016	**262**	1997.5	784	35	10	138	15	0	5	8	421	15	10	0	3	10	13	8	25	23	18	18	8	5
2016	**263**	1996.7	1060	33	12	231	12	6	0	33	421	24	15	42	15	69	21	18	9	12	24	36	21	6
2016	**264**	1995.8	1375	40	33	326	33	22	4	18	574	7	7	51	11	59	29	15	18	15	26	69	18	0
2016	**265**	1995.0	1404	86	16	246	20	31	4	20	755	39	8	31	4	23	27	8	20	12	8	27	16	4
2016	**266**	1994.1	1066	68	7	172	11	14	4	7	585	43	7	29	0	22	36	0	18	7	14	4	14	4
2016	**267**	1993.3	1414	95	7	231	24	17	3	10	753	61	7	41	7	20	20	7	41	10	17	24	14	7
2016	**268**	1992.4	848	29	24	141	13	13	0	3	444	40	8	19	11	19	29	3	5	11	11	13	13	0
2016	**269**	1991.6	1222	16	29	286	25	22	0	0	697	35	10	10	6	6	6	0	25	6	6	22	13	0
2016	**270**	1990.7	1520	36	68	470	24	12	4	24	565	80	16	40	4	8	20	8	16	24	16	28	60	0
2016	**271**	1989.9	1771	78	50	495	55	18	14	18	624	110	28	73	18	50	18	18	0	5	14	14	60	9
2016	**272**	1989.0	1357	51	18	417	55	29	26	18	490	26	22	26	7	40	37	7	22	11	18	15	18	4
2016	**273**	1988.1	1175	59	44	268	81	53	0	9	414	16	16	19	3	69	22	16	16	6	22	16	28	0
2016	**274**	1987.3	862	29	9	205	26	20	0	3	374	61	32	9	0	38	9	0	12	0	6	15	15	0
2016	**275**	1986.4	986	18	12	233	23	15	0	15	452	9	18	32	0	96	18	0	6	3	3	15	12	9
2016	**276**	1985.6	1310	42	17	432	42	55	17	8	441	38	42	4	4	81	30	4	8	0	4	13	21	4
2016	**277**	1984.7	1474	62	38	469	104	33	9	19	450	14	28	9	0	71	38	5	9	14	43	19	33	5
2016	**278**	1983.9	1492	64	13	405	55	26	0	4	644	4	43	26	0	94	26	17	13	4	9	13	26	9
2016	**283**	1983.0	638	16	0	164	5	5	5	21	318	37	0	0	3	45	5	0	8	0	0	3	0	3
2016	**284**	1982.2	1228	23	23	357	23	18	6	18	585	23	0	6	18	47	0	0	6	0	12	0	58	6
		Average	1221	49	24	299	33	21	6	15	527	36	20	26	6	45	23	7	15	9	14	18	24	5
		Std. dev.	281	25	17	114	25	14	7	10	122	26	16	19	6	27	14	6	9	8	10	15	17	4